

**NEW METAL BASED SATURABLE ABSORBER FOR
ULTRASHORT PULSE GENERATION**

MUHAMMAD TAUFIQ BIN AHMAD

**FACULTY OF ENGINEERING
UNIVERSITY OF MALAYA
KUALA LUMPUR**

2020

**NEW METAL BASED SATURABLE ABSORBER FOR
ULTRASHORT PULSE GENERATION**

MUHAMMAD TAUFIQ BIN AHMAD

**THESIS SUBMITTED IN FULFILMENT OF THE
REQUIREMENTS FOR THE DEGREE OF DOCTOR OF
PHILOSOPHY**

**FACULTY OF ENGINEERING
UNIVERSITY OF MALAYA
KUALA LUMPUR**

2020

UNIVERSITY OF MALAYA
ORIGINAL LITERARY WORK DECLARATION

Name of Candidate: MUHAMMAD TAUFIQ BIN AHMAD

Matric No: 17035898/1, KHA150089

Name of Degree: DOCTOR OF PHILOSOPHY

Title of Project Paper/Research Report/Dissertation/Thesis ("this Work"):

NEW METAL BASED SATURABLE ABSORBER FOR ULTRASHOR

T PULSE GENERATION

Field of Study: PHOTONICS

I do solemnly and sincerely declare that:

- (1) I am the sole author/writer of this Work;
- (2) This Work is original;
- (3) Any use of any work in which copyright exists was done by way of fair dealing and for permitted purposes and any excerpt or extract from, or reference to or reproduction of any copyright work has been disclosed expressly and sufficiently and the title of the Work and its authorship have been acknowledged in this Work;
- (4) I do not have any actual knowledge nor do I ought reasonably to know that the making of this work constitutes an infringement of any copyright work;
- (5) I hereby assign all and every rights in the copyright to this Work to the University of Malaya ("UM"), who henceforth shall be owner of the copyright in this Work and that any reproduction or use in any form or by any means whatsoever is prohibited without the written consent of UM having been first had and obtained;
- (6) I am fully aware that if in the course of making this Work I have infringed any copyright whether intentionally or otherwise, I may be subject to legal action or any other action as may be determined by UM.

Candidate's Signature

Date:

Subscribed and solemnly declared before,

Witness's Signature

Date:

Name:

Designation:

NEW METAL BASED SATURABLE ABSORBER FOR ULTRASHORT PULSE GENERATION

ABSTRACT

Cost-efficient, robust and flexible laser systems are vital for a wide-range of applications ranging from high-precision material processing to biomedicine. This thesis aims to explore pure silver and gold based saturable absorbers (SAs) as Q-switcher and mode-locker in various fibre laser cavities. The generations of Q-switched pulses in 1-, 1.55-, and 2-micron regions have been successfully demonstrated using a pure gold, which was deposited using electron beam deposition onto a PVA thin-film as SA. For instance, a stable Q-switched thulium-doped fibre laser (TDFL) operating at 1949 nm was successfully demonstrated with the gold SA. The proposed laser generates Q-switched pulses with the maximum repetition rate of 21.95 kHz, the thinnest pulse width of 2.60 μ s and the maximum pulse energy of 92.8 nJ. Passively Q-switched TDFL and erbium-doped fibre laser (EDFL) were also successfully demonstrated using a pure Ag thin-film, which was obtained using same technique and has 2% modulation depth. The silver-based Q-switched TDFL generates pulses at 28.33 kHz with pulse width of 4.82 μ s and energy of 161.7 nJ at pump power of 498 mW. Passively Q-switched and mode-locked EDFLs were also successfully achieved by utilizing D-shaped fibre deposited silver as SA. The generated Q-switched pulses exhibit maximum repetition rate of 66.74 kHz, the minimum pulse width of 6.12 μ s and maximum pulse energy of 139.08 nJ which is comparable to other passively Q-switched EDFL system. The mode locked EDFL operates at 1.0 MHz repetition rate with 455 ns pulse width and pulse energy of 10.73 nJ. These findings show that pure gold and silver material have a great potential for photonic applications.

Keywords: fibre laser; Q-switching; mode-locking; metal saturable absorber;

PENYERAP BOLEH TEPU BAHARU BEASASKAN LOGAM UNTUK

PENJANAAN DENYUT ULTRA PENDEK

ABSTRAK

Sistem laser fleksibel, lasak dan cekap kos adalah penting untuk pelbagai aplikasi dari pemprosesan bahan hingga ke bioperubatan. Tesis ini bertujuan untuk menerokai penyerap boleh tepu (SA) berasaskan perak dan emas tulen sebagai pensuis-Q dan pengunci-mod di dalam pelbagai kaviti laser gentian. Penghasilan denyut tersuis-Q pada lingkungan 1-, 1.55- dan 2-mikron berjaya ditunjukkan dengan menggunakan emas tulen yang didepositkan keatas filem nipis PVA melalui pemendapan pancaran elektron sebagai SA. Contohnya, laser gentian terdop thulium (TDFL) tersuis-Q beroperasi pada 1949 nm berjaya ditunjukkan dengan SA emas. Laser itu menghasilkan denyut tersuis-Q dengan kadar pengulangan maksima ialah 21.95 kHz, lebar denyut terpendek ialah 2.60 μ s dan tenaga denyut maksima ialah 92.8 nJ. TDFL dan laser gentian terdop erbium (EDFL) tersuis-Q pasif juga berjaya ditunjukkan dengan menggunakan filem perak tulen yang dihasilkan melalui teknik yang sama dan mempunyai kedalaman modulasi sebanyak 2%. TDFL tersuis-Q berasaskan perak ini menghasilkan denyutan pada 28.33 kHz dengan lebar denyut 4.82 μ s dan tenaga sebanyak 161.7 nJ dengan kuasa pengepaman 498 mW. EDFL tersuis-Q dan terkunci-mod pasif juga berjaya dicapai dengan menggunakan perak termendap pada gentian berbentuk-D sebagai SA. Denyut tersuis-Q yang terhasil menampilkan kadar pengulangan maksima 66.74 kHz, lebar denyut minimum 6.12 μ s dan tenaga denyut maksima 139.08 nJ, dimana ia setara dengan sistem EDFL tersuis-Q pasif yang lain. EDFL terkunci-mod juga beroperasi pada kadar pengulangan 1.0 MHz dengan lebar denyut 455 ns dan tenaga denyut 10.73 nJ. Penemuan ini menunjukkan bahawa bahan emas dan perak tulen mempunyai potensi yang baik dalam aplikasi fotonik.

Kata kunci: Laser gentian; Pensuisan-Q; Kekunci-mod; Penyerap boleh tepu logam;

ACKNOWLEDGEMENTS

Alhamdulillah, all praises be to Allah the almighty God who has put me in this beautiful life and has given me the strength to keep me in this journey of hard work until I achieve what I am aiming for. A special appreciation goes to Prof. Ir. Ts. Dr. Sulaiman Wadi Harun and Prof. Datuk Dr. Harith Ahmad for the guidance and continuous support, patiently guided me which were essential for the development of this study. I feel grateful to have an endless support from Ir. Dr. Anas Abdul Latiff, my mentor and supervisor during master's degree, who always helps me a lot in many ways in making sure that I can keep doing my research smoothly. I owe my profound gratitude to Assoc. Prof. Dr. Rozalina Zakaria, who sharing her research resources and believes in me to produce outcome from the resource. Not forgetting, my research mates, Dr. Ahmad Razif Muhammad, Dr. Hazlihan Haris, Dr. Arni Munira Markom, Dr. Hazli Rafis Abdul Rahim, Dr. Haziezol Helmi Mohd Yusof, Ir. Ts. Dr. Mohd Fauzi Ab Rahman, Dr. Muhammad Farid Mohd Rusdi, Dr. Ahmad Haziq Aiman Rosol and others who involve directly or indirectly, whose always lend a hand whenever I need their help either in my work or for moral support. I am thankful to and fortunate enough to get constant encouragement and moral support from my family especially my parents, Ahmad Salleh and Zubaidah Sarwan who always keep tabs on my research progress and give endless moral support throughout my work. Last but not least, I heartily thank my love of my life, Nurul Farahin Musa for the love she gave me, which had raised my spirit to do this research work more passionately

TABLE OF CONTENTS

Abstract	iii
Abstrak	iv
Acknowledgements	v
Table of Contents	vi
List of Figures	ix
List of Tables.....	xiv
List of Symbols and Abbreviations.....	xiv
CHAPTER 1: INTRODUCTION.....	1
1.1 Research Background	1
1.2 Research Motivation	5
1.3 Research Objectives.....	6
1.4 Thesis Outline.....	7
CHAPTER 2: LITERATURE REVIEW.....	9
2.1 Introduction.....	9
2.2 Laser Technology	9
2.3 Fibre Laser	12
2.3.1 Ytterbium-doped Fibre Laser	13
2.3.2 Erbium-doped Fibre Laser.....	14
2.3.3 Thulium-doped Fibre Laser	16
2.4 Pulsed Laser Generation	18
2.4.1 Q-switching Technique	18
2.4.2 Mode-locking Technique	19
2.5 Surface Plasmon Resonance (SPR)	20

2.6	Noble Metals.....	23
2.7	Laser Performance Analysis.....	25

CHAPTER 3: PURE GOLD THIN-FILM SATURABLE ABSORBER AS Q-SWITCHER 32

3.1	Introduction.....	32
3.2	Preparation of Pure Gold Thin-Film.....	34
3.3	Material and Optical Characterization of Gold Thin-Film.....	37
3.4	Q-switched Fibre Laser operating at 1-micron Region	41
3.5	Q-switched Fibre Laser operating at 1.55-micron Region	48
3.6	Q-switched Fibre Laser operating at 2-micron Region	54
3.7	Summary.....	61

CHAPTER 4: ELECTRON BEAM DEPOSITED SILVER SATURABLE ABSORBER AS PASSIVE Q-SWITCHER IN 1.55- AND 2-MICRON FIBRE LASERS 63

4.1	Introduction.....	63
4.2	Fabrication and Characterization Process of Silver Thin-Film	64
4.3	Q-switched Thulium-doped Fibre Laser operating at 2-micron Region	69
4.3.1	Laser Configuration.....	69
4.3.2	Q-switching Performance.....	70
4.4	Q-switched Erbium-doped Fibre Laser operating at 1.55-micron Region	74
4.5	Q-switched Erbium-doped Fibre Laser with 1480 nm Pumping Regime	80
4.6	Summary.....	86

CHAPTER 5 : Q-SWITCHED AND MODE-LOCKED FIBRE LASERS USING SILVER DEPOSITED ONTO D-SHAPED FIBRE AS SATURABLE ABSORBER

.....87

5.1 Introduction..... 87

5.2 Fabrication and Characterization of SA Device Based on Silver Deposited onto D-shape Fibre..... 89

5.3 Q-switched EDFL using Silver Deposited onto D-shaped Fibre as SA 94

5.4 Mode-locked EDFL using Silver Deposited onto D-shaped Fibre as SA 105

5.5 Summary..... 109

CHAPTER 6: CONCLUSION AND FUTURE WORKS 111

6.1 Conclusion 111

6.2 Future Research Direction 113

References 115

List of Publications and Papers Presented 121

LIST OF FIGURES

Figure 1.1: Optical characteristic of silica glass	2
Figure 2.1: Ruby laser, the first working laser in the world	10
Figure 2.2: Simple gas laser generator	11
Figure 2.3: Simple semiconductor laser diode.....	12
Figure 2.4: Absorption and emission cross-sections of ytterbium ions	14
Figure 2.5: Energy level diagram of ytterbium ions	14
Figure 2.6: Optical characteristic of silica fibre at various wavelength.....	16
Figure 2.7: Energy level diagram of erbium ions	16
Figure 2.8: Energy level diagram of thulium ions	17
Figure 2.9: Fundamental pulse generation process	19
Figure 2.10: Phase locking phenomenon in mode-locked generation	20
Figure 2.11: A basic model plasmon quantisation	21
Figure 2.12: Electron behaviour inside the metal particles during localised SPR.....	22
Figure 2.13: Output spectrum for a typical laser.....	25
Figure 2.14: A typical Q-switching pulse train.....	27
Figure 2.15: A pulse representation in frequency-domain.....	29
Figure 3.1: Fabrication process of PVA film.....	34
Figure 3.2: Dried PVA film from petri dish after 3 days.....	35
Figure 3.3: Placement of PVA film and gold inside the vacuum chamber.....	36
Figure 3.4: Illustration on thickness of the gold thin-film (Inset) Real image of the gold thin-film	37
Figure 3.5: FESEM image of the gold thin-film.....	38
Figure 3.6: EDX analysis on the gold thin-film.....	38

Figure 3.7: Linear absorption spectra of the gold thin-film in spectrum ranging from 950 nm to 2100 nm wavelength.....	40
Figure 3.8: Nonlinear transmission measurement of the gold thin-film using balance twin-detector technique	40
Figure 3.9: Balance twin-detector configuration for nonlinear transmission measurement	41
Figure 3.10: Ring laser configuration for 1- μ m operation with pure gold SA	42
Figure 3.11: Optical spectra of the Q-switched and CW laser at pump power of 61.1 mW	43
Figure 3.12: Typical pulse train of the Q-switched laser at threshold, median, and maximum pump power	45
Figure 3.13: Frequency plot of the Q-switched laser at maximum pump power.....	46
Figure 3.14: Power and energy analysis of the Q-switched laser at various pump power	47
Figure 3.15: Repetition rate and pulse width analysis of the Q-switched laser at various pump power.....	47
Figure 3.16: Ring laser configuration for 1.55- μ m with pure gold SA	49
Figure 3.17: Optical spectra of the Q-switched and CW laser at pump power 17.3 mW	50
Figure 3.18: Typical pulse train of the Q-switched laser at threshold and maximum pump power.....	51
Figure 3.19: Repetition rate and pulse width analysis of the Q-switched laser at various pump power.....	52
Figure 3.20: Output power and pulse energy analysis of the Q-switched laser at various pump power.....	53
Figure 3.21: Frequency plot of the Q-switched laser at maximum pump power.....	54
Figure 3.22: Ring laser configuration for 2- μ m operation with pure gold SA	55
Figure 3.23: Optical spectra of the Q-switched and CW laser at pump power of 343.13 mW	56
Figure 3.24: Repetition rate and pulse width analysis of the Q-switched laser at various pump power.....	57

Figure 3.25: Typical pulse train of the Q-switched laser at threshold, median, and maximum pump power	58
Figure 3.26: Power and energy analysis of the Q-switched laser at various pump power	60
Figure 3.27: Frequency plot of the Q-switched laser at maximum pump power.....	61
Figure 4.1: (a) PVA thin-film fabrication process (b) Depositing of silver onto PVA thin-film using E-beam deposition method. Inset shows the real image of the fabricate SA film	65
Figure 4.2: (a) EDX analysis and (b) FESEM image of the silver SA	67
Figure 4.3: (a) Linear and (b) nonlinear absorption characteristics of the silver SA.....	68
Figure 4.4: Configuration of the Q-switched TDFL with pure silver thin-film as SA ...	69
Figure 4.5: Temporal characteristics of a typical TDFL pulse train and single pulse envelope at (a) threshold and (b) maximum pump power.	71
Figure 4.6: RF analysis of the pulse at maximum pump power.....	71
Figure 4.7: Laser spectrum for Q-switched and CW laser operation.....	73
Figure 4.8: TDFL characteristics in variation of pump power (a) power and energy (b) Q-switching phenomenon on changing of pulse width and repetition rate.....	73
Figure 4.9: Configuration for Q-switched EDFL with silver thin-film	75
Figure 4.10: Output spectra of the EDFL configured with Q-switching and CW operation	76
Figure 4.11: Typical pulse train and corresponding single pulse enveloped of the EDFL at (a) threshold and (b) maximum pump power.....	77
Figure 4.12: Repetition rate and pulse width analysis of the Q-switched laser at various pump power.....	78
Figure 4.13: Output power and pulse energy analysis of the Q-switched laser at various pump power.....	79
Figure 4.14: RF spectrum analysis of the Q-switched EDFL at maximum pump power	79
Figure 4.15: Configuration for the silver SA based Q-switched EDFL with 1480 nm pumping	81

Figure 4.16: Typical pulse train at different pump powers (a) 45.8 mW (b) 89.6 mW, and (c) 133.5 mW	82
Figure 4.17: Output spectra of the Q-switched EDFL with and without SA device	83
Figure 4.18: RF spectrum of the Q-switched laser	84
Figure 4.19: Pulse repetition rate and pulse width versus pump power.....	85
Figure 4.20: Average power, peak power and pulse energy versus pump power.....	85
Figure 5.1: D-shaped fibre preparation setup.....	90
Figure 5.2: Comparison in dimension of a standard SMF to the polished fibre with loss of 2 dB. Inset shows a cross-section view of the fibre.....	91
Figure 5.3: Cross-section microscopic view of the fibre at different insertion loss	91
Figure 5.4: Coating process using E-beam evaporation method on substrates, such as D-shaped fibre	92
Figure 5.5: Energy dispersive spectroscopy (EDS) analysis on the surface of the D-shaped area	93
Figure 5.6: Linear absorption of the silver at different wavelength ranging from 1300 to 2100 nm.....	93
Figure 5.7 : Nonlinear absorption curve of the silver layer showing modulation depth of 2%.	94
Figure 5.8: Experimental setup for Q-switched EDFL using D-shaped fibre with pure silver as SA	95
Figure 5.9: Spectral overview of the Q-switched EDFL at the threshold pump power of 35.2 mW.....	96
Figure 5.10: The performance of the Q-switched EDFL against pump power; (a) Repetition rate, (b) Pulse width, (c) Output power, (d) Pulse energy and (e) Peak power	99
Figure 5.11: Oscilloscope trace for all samples at pump power of 65.7 mW	102
Figure 5.12: RF spectra for various samples at 65.7 mW pump power.....	104
Figure 5.13: Optical spectra of the mode-locked and CW laser at pump power of 68 and 70.8 mW, respectively.....	107
Figure 5.14: Typical pulse train of the mode-locked laser at maximum pump power .	107

Figure 5.15: Frequency plot of the mode-locked laser at maximum pump power of 101.3 mW 108

Figure 5.16: Average power, peak power and pulse energy analysis of the mode-locked laser at various pump power 109

University of Malaya

LIST OF TABLES

Table 1.1 Work package based on research objectives.....	7
Table 2.1: Performance of the current laser utilizing gold (Au) and silver (Ag) as the saturable absorber.....	31
Table 4.1: Comparison with recent reports on Q-switched laser at 2-micron wavelength	74
Table 4.2: Comparison with recent reports on Q-switched laser at 1.55-micron wavelength	80
Table 5.1: The D-shaped fibre characteristics of four samples with different polishing depth.....	91
Table 5.2 : Measured lasing performance of four different samples of D-shaped fibre with different insertion loss.....	97
Table 5.3: Comparison of silver-based saturable absorber lasing performance	105
Table 6.1: Summary of pulsed fibre laser generated by fabricated SAs.....	113

LIST OF SYMBOLS AND ABBREVIATIONS

Ag	:	Argentum (silver)
ASE	:	Amplified spontaneous emission
Au	:	Aurum (gold)
CW	:	Continuous wave
dBm	:	Decibel per milliwatt
DI	:	Deionized
E-beam	:	Electron beam
EDFL	:	Erbium-doped fibre laser
EDX	:	Energy-dispersive x-ray spectroscopy
Er	:	Erbium
FESEM	:	Field emission scanning electron microscopy
FWHM	:	Full width at half-maximum
GVD	:	Group velocity dispersion
InGaAs	:	Indium gallium arsenide
LD	:	Laser diode
mbar	:	millibar
NA	:	Numerical aperture
Nd:YAG	:	Neodymium-doped yttrium aluminium garnet
NIR	:	Near infrared
OSA	:	Optical Spectrum Analyser
OSC	:	Oscilloscope
OSNR	:	Optical signal-to-noise ratio
PD	:	Photodetector
Pd	:	Palladium

Pt	:	Platinum
PVA	:	Polyvinyl alcohol
RFSA	:	Radio frequency spectrum analyser
SA	:	Saturable absorber
SMF	:	Single mode fibre
SPM	:	Self-phase modulation
SPR	:	Surface plasmon resonance
TDFL	:	Thulium-doped fibre laser
Tm	:	Thulium
UV	:	Ultraviolet
WDM	:	Wavelength division multiplexer
wt.%	:	Weight percentage
Yb	:	Ytterbium
YDF	:	Ytterbium-doped fibre
YDFL	:	Ytterbium-doped fibre laser
ϵ	:	Dielectric constant
Ω	:	Ohm
h	:	Plank's constant
η	:	Power conversion efficiency
λ	:	Wavelength

CHAPTER 1: INTRODUCTION

1.1 Research Background

Lasers have become so universal nowadays and it is kind of hard to imagine that the first one ever was built less than 60 years ago (Maiman, 1960). Laser, which is an abbreviation for “light amplification by stimulated emission of radiation”, is a technology ordinarily used in our everyday lives. While the science of light itself has not changed, laser technology advanced rapidly and today, countless of laser types available that would not have been thought possible 60 years ago. Some of the latest advancement of the laser technology including the generation of short and ultra-short pulse in fibre laser cavity.

Usage of fibre lasers technology throughout scientific, medical and industrial application has become necessity every single day. Unlike conventional bulk lasers, fibre lasers do not require any mechanical alignment (Nishizawa, 2014), thus it is more reliable for end-users. In addition, the compactness and flexibility of fibre lasers empower them to outclass bulk lasers in many areas (Du et al., 2014; S. Huang et al., 2014). Various wavelength operation can be realized using fibre laser technology ranging from 1-, 1.55- to 2-micron region which all covered in this research. The 1-micron fibre laser can be realised using ytterbium-based gain medium pumped with 980 nm laser source and it possesses low quantum defect (Yao et al., 2014), hence suitable for high-power pulsed fibre laser. The 1.55-micron fibre laser is the most common laser used in our surrounding especially in fibre optic telecommunication system. This is due to lowest attenuation generated naturally by silica fibre at that specific wavelength, see Figure 1.1 (Nagayama et al., 2002). The laser can be realized using erbium-doped fibre (EDF) as a gain medium in conjunction with two pumping options, either 980 nm or 1480 nm laser source. The latest among all is 2-micron fibre laser, which utilised thulium-based gain medium pumped by 800 nm or 1550 nm laser source. The unique water absorption characteristic

of 2-micron laser allowing it to reduce the penetration depth on human tissues (Ichikawa et al., 2013; Sakata et al., 2012), therefore reducing risk in medical surgery.

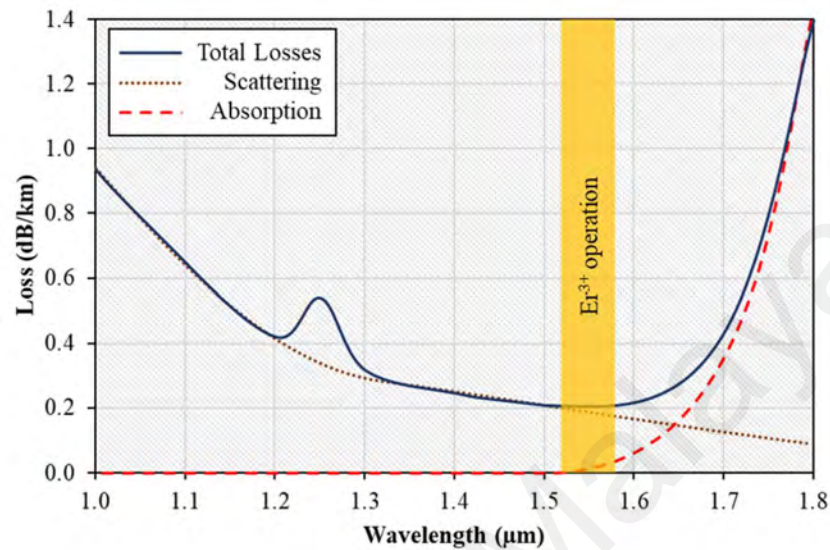


Figure 1.1: Optical characteristic of silica glass

The introduction of pulsed fibre laser on top of continuous wave (CW) fibre laser has its own importance in real world application, such as for cutting, engraving, and cleaning (Chen et al., 1996; Leone et al., 2009; Perry et al., 1999). Normally, the pulsed laser is very narrow in duration, up to femtoseconds. In some cases, the pulse width can be wider due to laser cavity specification such as cavity length and insertion losses. Several approaches have been proposed by researchers to generate pulsed laser, one of is by incorporating a saturable absorber (SA) device in the laser cavity as mode-locker or Q-switcher. This approach has been favoured among researchers due to high possibilities of self-starting mode-locking or Q-switching. This allow extensive access of pulse parameters without using expensive and sophisticated modulators that eventually reduce the achievable pulse performance directly from the laser source (Keller, 2003).

SA can be divided into two types; real and artificial. The real SA utilises the saturable absorption properties of the material to increase the light intensity for a short time, while the artificial mimicking the real one by manipulating the nonlinear effect in reducing optical losses for higher intensities photon, without any absorption happen (Ismail et al., 2012). This research will fully employ real SA in generating pulsed laser, through either its mode-locking or Q-switching operation. In this work, pure metal-based SAs are proposed as Q-switcher and mode-locker. These new SAs utilise the unique plasmonic features of metal which benefits application in various operating wavelength.

Metal can be described in two conditions; pure and oxide. Raw metal obtained from earth are normally in oxide form, except for noble metal which are resistance to oxidation in normal condition. To date, the metal-based pulsed laser generation are usually explored in oxide form. The latest, titanium oxide (TiO_2), tin oxide (SnO_2), and iron oxide (Fe_2O_3) were incorporated into erbium-doped fibre laser (EDFL) to generate Q-switched pulse in 1.55-micron operating wavelength (Ahmad, Reduan, et al., 2018; Mao et al., 2018; N. Siddiq et al., 2018). An EDFLs has also demonstrated in generating mode-locked pulse laser in that similar region, for instance by implementing zinc oxide into a polymer film using seeding solution technique (Alani et al., 2018). Metal performed quite well in pulse generation at different operating wavelength such as 1- and 2-micron. A SA made out from nickel oxide (NiO) was proved to produce Q-switched pulsed using ytterbium-doped fibre (YDF) as passive gain medium (Jannifar et al., 2018). Another 1-micron Q-switched pulsed laser was realised by employing iron oxide (Fe_2O_3) fabricated using magnetic deposition technique (Al-Hayali et al., 2018). Another iron oxide (Fe_2O_3) SA has been shown to function as Q-switcher in 2-micron region as proposed in thulium holmium co-doped fibre laser (Koo et al., 2018). Subsequently, metal-based SA has potential to generate soliton, a condition where the linear and nonlinear effect is balance.

It was also shown that cobalt oxide (Co_3O_4) SA capable to produce soliton output, even though the SA is not the only reason of it to occurs (Ahmad, Samion, et al., 2018).

Noble metals are another form of metal, which is not naturally or chemically oxide by any other substance. Most metal are exposed to natural oxidation with different resistance between each other. Oxidation takes time to occurs and it can be prevented or reduced to minimum by not exposing the metal to air or water. There is some noble metal SA that has been demonstrated in fibre laser application at various operating wavelength. Lately, silver has been tested to generate Q-switched pulsed laser in 1.55-micron region, utilising EDFL as a gain medium (Lokman et al., 2018). In 2-micron region, Q-switched pulsed laser was realised using chemical synthesis method on gold in bulk mirror configuration (X. Zhang et al., 2018). All-fibre YDF laser (YDFL) was also incorporated with metal-based copper SA to activate a self-starting pulse operating in Q-switching mode at 1-micron region (Muhammad et al., 2018). In this thesis, new pure metal based SAs are proposed and investigated for pulse generation in 1.0, 1.55 and 2.0 μm region.

In this thesis, the generation of laser were induced by gold (Au) and silver (Ag) as a passive saturable absorber. It was fabricated using an electron beam deposition technique onto a host material. There are two types of host material used in this work; polyvinyl alcohol (PVA) and D-shaped fibre. The saturable absorbers were analysed physically and optically using Field-emission Scanning Electron Microscope (FESEM), Energy-Dispersive X-ray Spectroscopy (EDX), linear absorption configuration and balanced twin-detector configuration. The saturable absorbers were later, incorporated into three different laser cavities, each with different gain media. The gain media used are Ytterbium, Erbium and Thulium; covering different operating wavelengths. With that, the outcome of the laser can be observed to produce an ultrashort pulse laser.

1.2 Research Motivation

The high demand of pulse laser has encouraged researchers to produce a cost-efficient, robust and simple laser system. The laser, a fibre laser system was used. The reason is because its simplicity, compactness and robustness. Simplicity came from the alignment-free system, due to light is contains inside the fibre. Without alignment, it is easy to manage a fibre in a tight space, just by making sure the bending loss is minimal, hence a compact-size system was created. A fibre laser is also are strong with all the coatings around it. Although it was made by glass or silica, its fragility is very low compared to a normal type of glass lens. With all these qualities, the system will be reasonable in cost.

As known, there two techniques of producing pulse laser; Q-switching and mode-locking. These techniques are widely applied in not just industry, but also in medical and research (Dausinger et al., 2004; Lei et al., 1999). To introduce flexibility in the laser, the fibre laser resonator was used. All-fibre laser resonator consists of fibre-based devices of gain medium, laser source and other passive components. Other than flexibility, fibre laser also provides an alignment-free system.

Material processing is one of the examples of the laser application in industry, allowing cutting, welding, soldering, and even changing the crystallite properties of the material by using lasers. These non-contact applications are important in machining especially in processing difficult material such as ceramic (bristle), rubber (elastic), and diamond (hardness). Laser was also known to be used in surgery, cancer treatment, and kidney stone destruction. In medical, laser provides great flexibility and precision in the operation. All these laser technologies were valued to nearly 11.1 billion US dollar in 2017 global sales, with roughly 6.6% increase from 10.4 billion dollar in previous year. This shows huge marketability of laser in the world and it will continue to increase in upcoming years.

The passive pulsing technique in laser system requires a device named saturable absorber (SA). Through years, new SA emerges into the market consisting different material ranging from graphene, transition metal dichalcogenide (TMD), to MXene. Metal is also one of the new materials used in fabricating the SA. Metal-based SA has unique optical features including broad saturable absorption, large third-order nonlinearity, and ultrafast response time (Gao et al., 2005; Yu et al., 2019). The surface plasmon resonance (SPR) from the metal enhance the saturable absorption capabilities throughout various wavelength region. Furthermore, the high third-order nonlinearity of metal-based SA ease the formation of pulse.

1.3 Research Objectives

This work aims to explore pure silver and gold based SAs as Q-switcher and mode-locker in various fibre laser cavities. Based on preliminary study on this topic, a few objectives have been highlighted to guide this research to achieve the target. The research objectives embark as following:

- i. To fabricate the passive saturable absorber using silver (Ag) and gold (Au), through electron beam deposition technique.
- ii. To characterise the physical and optical properties of silver and gold saturable absorber.
- iii. To demonstrate pulsed fibre laser at various region using these saturable absorbers.

Therefore, three work packages, one for each objective are implemented to ensure all research objectives are meet. The list of work packages is described in Table 1.1.

Table 1.1 Work package based on research objectives

Work Package	Task
WP 1	Fabrication of the saturable absorber
	<ul style="list-style-type: none">• Preparation of host medium from polyvinyl alcohol (PVA) and D-shaped fibre• Coating the host material with silver and gold using electron beam deposition technique
WP 2	Characterisation of the metal saturable absorber
	<ul style="list-style-type: none">• Physical characterisation using energy-dispersive X-ray spectroscopy (EDX) and field emission scanning electron microscopy (FESEM)• Optical characterisation using balanced twin-detector measurement technique
WP 3	Demonstration of the pulsed fibre laser
	<ul style="list-style-type: none">• Pulsed laser generation using ring cavity configuration in 1.55- and 2-micron operating region• Spectral and temporal characterisation of the laser

1.4 Thesis Outline

This thesis containing six chapters, including this introductory chapter. The background, motivation and objective of the research have been described in this chapter. **Chapter 2** presents a thorough literature review on related research topics including basic

laser development, fibre laser technology, pulse laser techniques, fundamental of pulsing mechanism, saturable absorber materials, and analysis methods on laser performance.

Next three chapters will discuss the actual works for the proposed study. **Chapter 3** reports on the development various Q-switched fibre laser by using gold (Au) thin-film as a passive SA. The fabrication and characterisation of the gold thin-film was discussed in this chapter, along with the analysis of the laser performance. The gold thin-film SA capabilities were tested into three laser cavities with different operating wavelengths of 1-, 1.5- and 2- μm and each of these cavities consist of different gain media of Ytterbium (Yb), Erbium (Er), and Thulium (Tm), respectively.

Chapter 4 proposes and demonstrates other Q-switched fibre laser based on silver (Ag) thin-film SA. As before, the fabrication, characterisation and analysis were reported in this chapter. The Ag thin-film SA is able to operate in two wavelength regions; 1.5- and 2-micron. The ability of these gold and silver thin-film in resonating pulse are promising and further studies are reported in the next chapter.

Chapter 5 demonstrate the generation of Q-switched and mode-locked pulses using another Ag based SA. This Ag was not fabricated on a thin-film form, rather a side-polished fibre coating was used. A normal silica fibre was side-polished until a small part of the core exposed. Then, the Ag was coated the exposed area, enabling light in the fibre to reach the SA. The process was explained in this chapter, alongside the analysis of the laser performance. Finally, the finding of this study is concluded in **Chapter 6**. Several suggestions on future works were also highlighted in this chapter. These suggestions can be done to improvise the proposed laser system.

CHAPTER 2: LITERATURE REVIEW

2.1 Introduction

This chapter presents a thorough literature review related to the study to assist readers to understand a basic concept of fibre laser and saturable absorber technology. It is important to understand that there are different types of laser available right now, one of it is fibre laser. The fibre laser utilizing rare-earth elements doped in a silica fibre to generate laser in specific wavelength. To increase the performance of the laser, Q-switching and mode-locking techniques were needed to convert a continuous wave laser into a pulsed laser. These techniques exploiting the optical properties of a device, called saturable absorber (SA). Nowadays, there are a lot of SA comprise on different element and composition, and one of it is metal. The surface plasmon resonance (SPR) plays important role in the operation of metal-based SA. Metal-based material such as gold (Au) and silver (Ag) rely on the SPR to introduce pulse into the cavity. The pulsed laser performance is analysed by their spectral and temporal characteristics, which will be introduced in this chapter.

2.2 Laser Technology

The laser commonly classifies into four major types, based on the medium used to excite the photons and introduced the stimulated emission. The types are solid-state, gas, liquid and semiconductor laser. All these types have common in the operation which utilizing the active ion from the element, except for semiconductor.

A solid-state laser means by its name itself, a laser which is form by a medium in a solid form. This medium need to be in a condition where photons can travel inside it and hence, glass and crystalline materials are the suitable host material for solid-state laser. This diaphaneity material is added with another substance to introduce impurities which

normally called doping. Rare-earth elements such as erbium (Er), ytterbium (Yb), neodymium (Nd) are the example of element used as a dopant. Ruby laser is the first laser in the world (Maiman, 1960), and it is considered as a solid-state laser. This laser produces a laser in visible light region of 694 nm wavelength. This deep-red colour laser is still used in some applications nowadays. As illustrated in Figure 2.1, a solid-state laser used another source of light energy as a pumping source. Particularly, the ruby laser applied xenon flashtube to pump the ruby. Today, laser diodes are the most common of light source used for pumping.

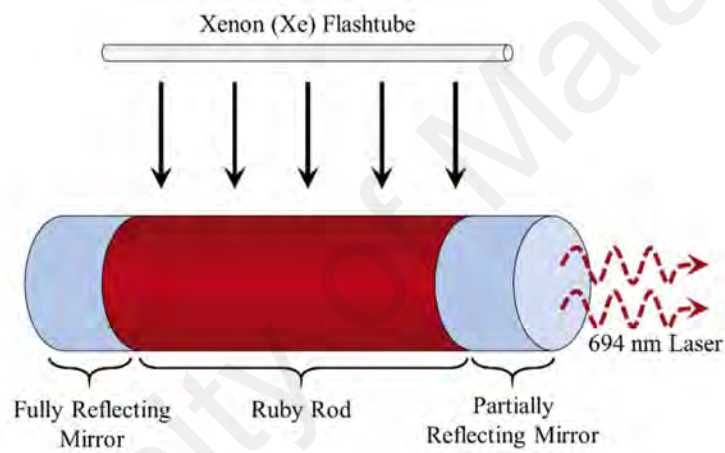


Figure 2.1: Ruby laser, the first working laser in the world

For a gas type laser, the high intensity light was produced by discharging an electrical current through a gas, which act as a medium for the laser. Compare to solid-state, this type of laser uses the active medium while the element is in gaseous state. Gas lasers is often to be seen in application where it requires high quality laser beam with long coherency (Rundquist et al., 1998). The gas can be a single element or multiple element mixture of gases. The gas then seals into a silica tube, containing it from the environment. The silica tube consists of mirrors at both end, which is quite similar to the solid-state principle. Then, the gas will be charged by electron through a pair of anode-cathode

terminal, as shown in Figure 2.2. A gas laser is working on principal of converting an electrical energy into light energy. The first ever gas laser generates a light beam in infrared region of $1.15 \mu\text{m}$ wavelength. There are several types of gas laser, such as neon (Ne), carbon dioxide (CO_2) and excimer laser, whereas the gas type determines the operating wavelength and the efficiency of the laser.

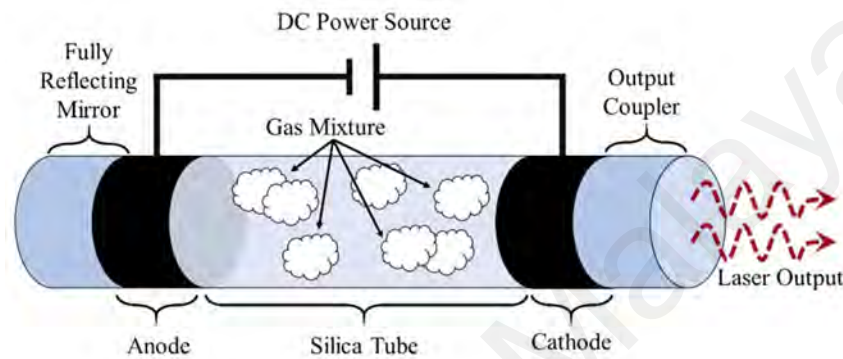


Figure 2.2: Simple gas laser generator

A liquid laser, on the other hand, shares the same principle as solid-state laser. Alike the name, the medium for generating this laser must be in a liquid form, energised by a light source. An example of liquid laser is a dye laser. In dye laser, the liquid medium used is organic-based solution. The organic dye mixture is dissolved by a solvent, such as water, ethanol, or cyclohexane. Typically, liquid laser was used to generate laser beam in the near ultraviolet (UV) region up to near infrared (NIR) region of the spectrum.

The most modern, efficient laser is generated by a semiconductor laser. This laser is crucial to our society as it was used widely in our everyday life. This type of laser consumes low power to operate, small and compact design, robust and long-lasting, and the most important is cost-efficient. Semiconductor laser are well-known as laser diode. Although semiconductor is in a solid form, it not considered as solid-state laser due to their different working principle. Specifically, a semiconductor laser used electrical

energy as a pumping mechanism. As shown in Figure 2.3, a semiconductor laser consists of a p-n junction of semiconductor material, act as a medium. The electrical energy drives the electrons to move through the junction and left a hole. As electron falls back into the hole, photons are released. As more electrical energy provided to the diode, more photon is produced, hence generating a high-intensity laser beam.

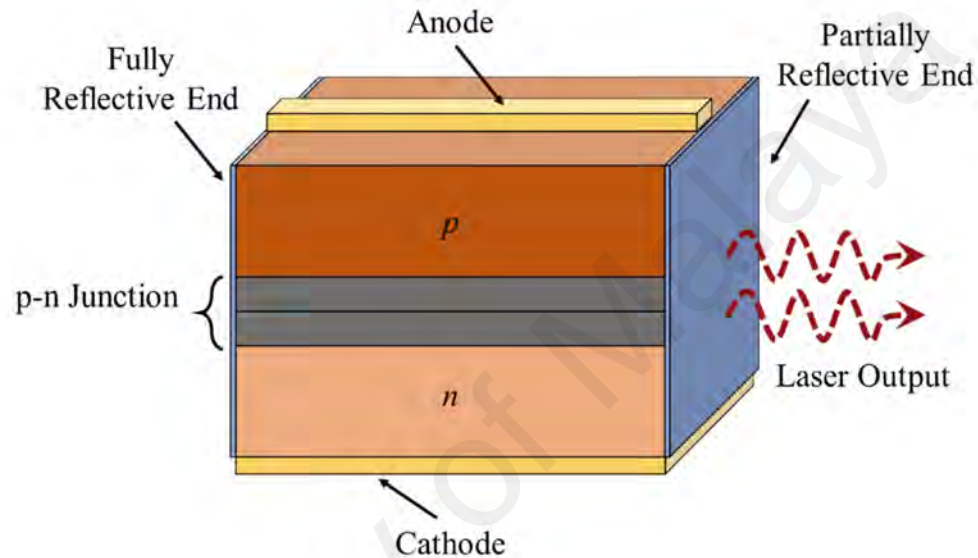


Figure 2.3: Simple semiconductor laser diode

2.3 Fibre Laser

Fibre laser is a special kind of solid-state laser. It uses an optical fibre that has been doped in rare-earth ions; typically, ytterbium, erbium, thulium, neodymium, praseodymium and holmium as the active medium. It has a high potential to generate laser with high average output power, high beam quality, high power efficiency and broad wavelength tunability. This section discusses about the working principle of several fibre lasers used in this study.

2.3.1 Ytterbium-doped Fibre Laser

The development of rare-earth element doped fibres has been beneficial in generating high quality, narrow-linewidth infrared beam laser with high optical efficiency. This research uses ytterbium-doped fibre (YDF) as one of the gain media, in producing laser operating in 1-micron wavelength region pumped with 980 nm source. The pumping wavelength is chosen based on YDF behaviour that possess effective absorption and emission cross-section at that wavelength, as shown in Figure 2.4. Ytterbium ions (Yb^{3+}) have a very simple electronic level structure as illustrated in Figure 2.5, consists of only one excited state ($^2F_{5/2}$) within reach from the ground-state ($^2F_{7/2}$). The quantum defect is very minimal due to small gap between the absorption and emission wavelength region, hence allowing high optical efficiency especially in high-power lasers (Dupriez et al., 2006). By pumping the YDF with 980 nm diode-laser, an efficient laser can be generated at around 1050 nm region.

YDF laser (YDFL) operates at around 1-micron wavelength region, which is considered as a normal dispersion region for the gain medium. Most of the SA fabricated operates in normal dispersion region, giving YDF a massive advantage compared to erbium-doped and thulium-doped fibre, which operates in anomalous dispersion region (Haris et al., 2014). Thus, no external element needed to compensate the dispersion of the medium. However, there are another aspect that should be considered in designing YDFL, especially on the nonlinear effect. The nonlinear effect for instance, group velocity dispersion (GVD) and self-phase modulation (SPM) influencing the broadness and stability of the pulse. These two phenomena need to balance each other so that the cavity could generate stable, high-efficiency pulse.

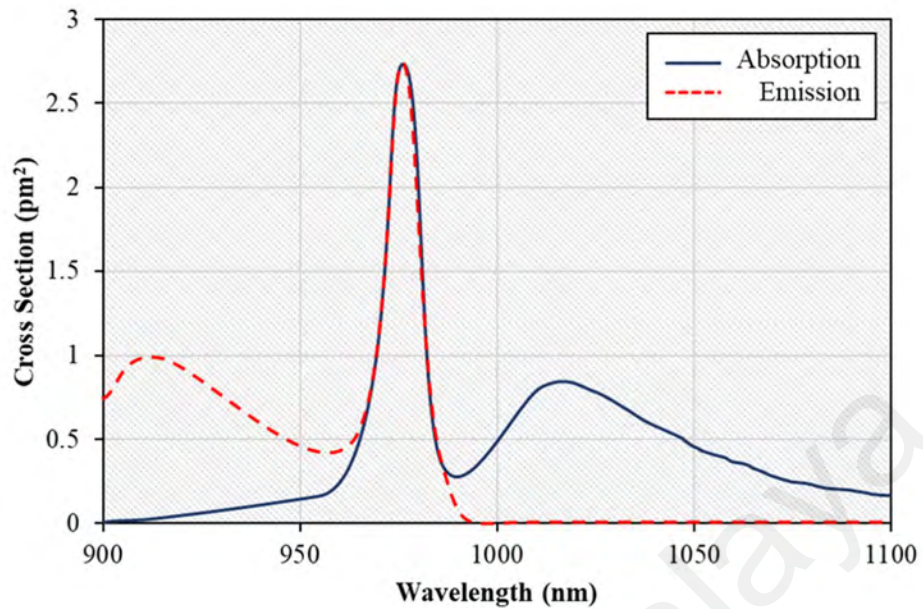


Figure 2.4: Absorption and emission cross-sections of ytterbium ions

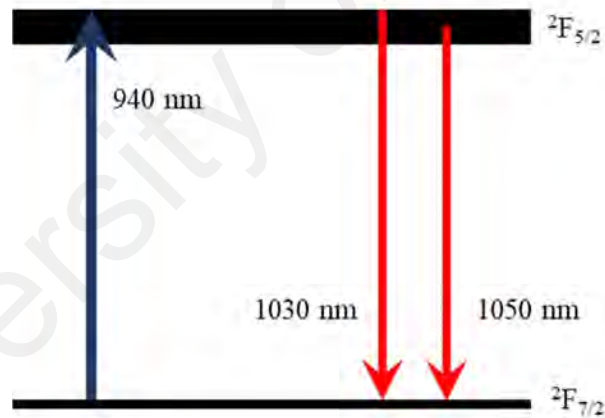


Figure 2.5: Energy level diagram of ytterbium ions

2.3.2 Erbium-doped Fibre Laser

Rare-earth doped fibres such as YDF and Erbium-doped fibre (EDF) are important for application in developing new active devices such as ultrashort pulse laser and optical amplifier devices. These rare-earth ions are normally doped in the core of silica fibre.

This allows doped fibre to absorb light, typically at shorter wavelength and emit them at longer wavelength. Silica fibre has a wide wavelength range with high optical transparency as shown in Figure 2.6. The figure indicates that in 1.55-micron wavelength region, silica can have extremely low linear absorption and scattering losses, as low as 0.2 dB/km. Erbium ions (Er^{3+}) operates effectively in that low loss region, make it suitable to use in optical communication system. The EDF can be used in both amplifier and laser system, which function in similar mechanism. The EDF was used in this research as a gain medium for ultrashort pulse generation due to its wide-ranging gain spectrum and anomalous dispersion at 1.55-micron region. This dispersion reacts simultaneously with the nonlinearity originated in silica fibre, promising a stable, self-starting pulse generation that are suitable for various practical application, especially in telecommunication window.

EDF has emerged as an effective gain medium for various photonics applications, including laser and amplifier operating in 1.55-micron region. The most common pump scheme used in those applications are 980 nm, based on transition of ${}^4\text{I}_{15/2}$ to ${}^4\text{I}_{11/2}$. In this research, 980 nm pump regime was used to excite Er^{3+} from ground level of ${}^4\text{I}_{15/2}$ to second level of ${}^4\text{I}_{11/2}$. A non-radiative decay occurs, forcing the ions down to first level of ${}^4\text{I}_{13/2}$, where the upper-state lifetime is up to approximately 10 ms, longer than normal period of phonon decay. This allow Er^{3+} to stay longer in excited state, reducing amount of power needed for amplification, hence improving the quantum efficient. In-band pumping of 1480 nm is also suitable for erbium, exploiting the first energy level into 1.55-micron emission. Both pump regime, 980 nm and 1480 nm will generate stimulated emission at same energy band and wavelength. Figure 2.7 shows erbium energy level diagram and mechanism of energy transition between levels.

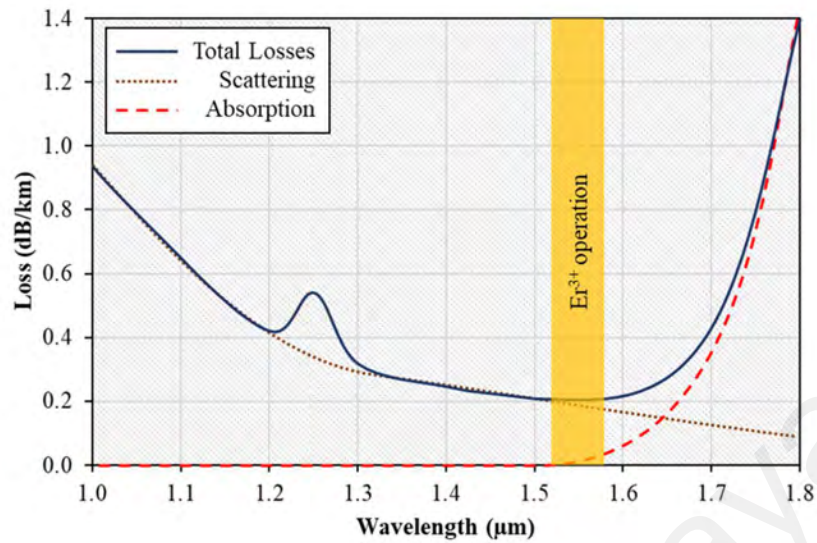


Figure 2.6: Optical characteristic of silica fibre at various wavelength

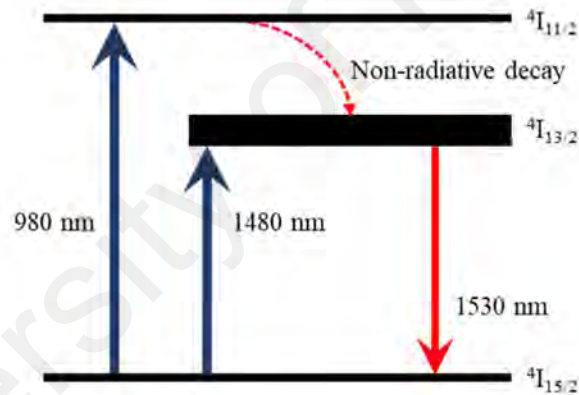


Figure 2.7: Energy level diagram of erbium ions

2.3.3 Thulium-doped Fibre Laser

The growing interest on exploring new wavelength region has attracted the development of thulium-doped fibre (TDF), new rare-earth doped fibre for use as gain medium in generating laser in 2-micron wavelength region. Market demands for these new fibres are increasing due to the global development which primarily focus on design

efficiency. Thulium, along with another rare-earth element are capable to generate high-efficiency emission at various wavelength. These rare-earth are doped into the core of high-quality silica fibre to form a gain medium, which are beneficial to laser and amplifier application. The main energy transition of thulium ions (Tm^{3+}) are located at energy level of 3F_4 to 3H_6 . At this energy transition, 2-micron emission occurs with two pumping scheme possibilities, which are 800 nm and 1550 nm. For this research, 1550 nm pump scheme was used, covering excitation to the first energy level and stimulated emission at 2-micron wavelength region as shown in Figure 2.8. However, this pumping scheme requires high energy excitation due to lower quantum efficiency compared to 800 nm scheme.

In 800 nm pump scheme, Tm^{3+} are excited into energy level of 3H_4 , allowing cross-relaxation to occur. This allow non-radiative decay of multiple Tm^{3+} to lower energy level of 3F_4 and attracting any neighbouring ground-state ion to this level, thus increases the quantum efficiency tremendously. Nevertheless, power limitation from single-mode 800 nm pump preventing this pump scheme to be use widely. Generally, both pumping schemes will produce emission in the similar wavelength output and energy band.

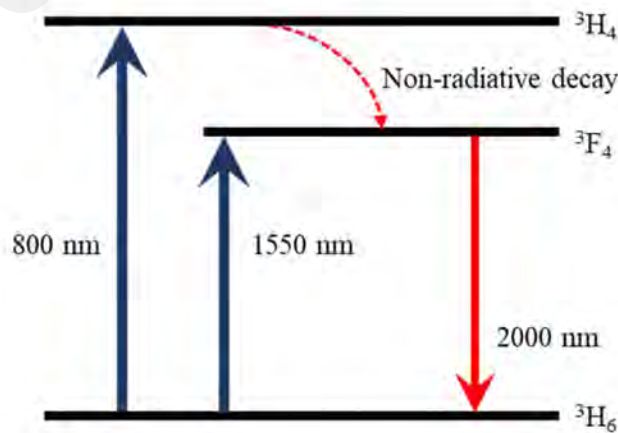


Figure 2.8: Energy level diagram of thulium ions

2.4 Pulsed Laser Generation

Pulsed lasers are lasers which emit light not in a continuous mode, but rather in the form of light flashes or optical pulses of some duration at some repetition rate. They can be achieved by either Q-switching or mode-locking techniques. Both techniques are discussed in this section.

2.4.1 Q-switching Technique

The basic Q-switched pulse is formed by saturable and non-saturable absorption introduced by SA in the laser cavity. Figure 2.9 shows the mechanism of the Q-switched pulse generation. As shown in the figure, loss, gain and pulse curves represent the absorption, population inversion and the output laser intensity, respectively. When input pump photons are continuously supplies to SA, the population inversion accumulate in it until at certain level will surpass the loss. At this point, the SA is saturated, and the loss severely decreases, allowing the photons to pass through. The combination of pass-through photons combines with accumulated photons generates an intense light which form laser with narrow-size pulse. The released photons reduced the population inversion in the SA, while the loss back to its original level and starts absorbing photons again. This process is repeated continuously if enough photons energy is supplied. The repeating process will eventually form a pulse train with constant repetition rate.

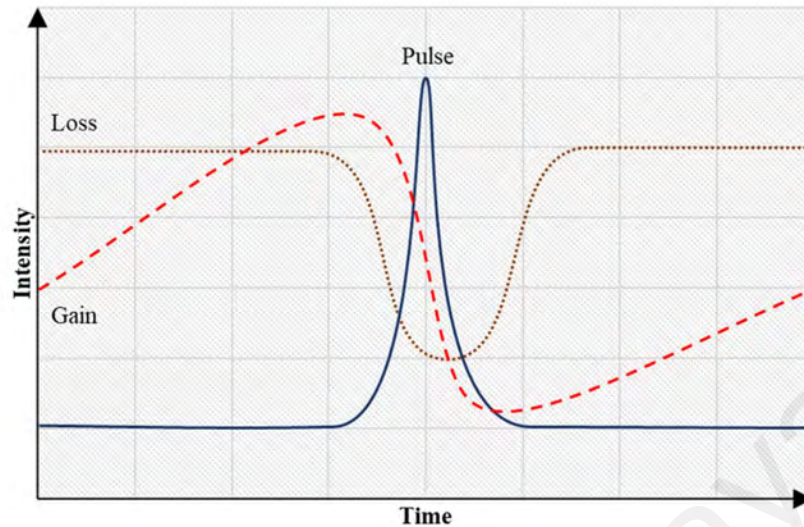


Figure 2.9: Fundamental pulse generation process

2.4.2 Mode-locking Technique

The word “mode-locking” referring to the fixed phase mechanism of multiple pulse with different frequency modes inside a laser cavity. Mode-locking process will generate very narrow pulse width, ranging from nanosecond up to femtosecond pulse. The fundamental of mode-locked generation is quite like Q-switched, with additional pulse phases are required in generating mode-locked pulse. The discreet coherent phasing occurs inside mode-locked laser is important since the number of phasing will determine the pulse width. Passive mode-locking is popular than active, since it does not require any external devices to control the pulse generation. Active mode-locking uses acousto-optic modulator to manipulate the amplitude modulation of the light. In fibre laser, many non-coherent longitudinal modes occur, with typical continuous wave may have minimum number of coherent phases, thus generating very weak mode-locked pulse. To obtain better mode-locked pulse, several coherent phases are required to be locked as shown in Figure 2.10. The pulse is produced based on the time taken by photon to make a round-

trip inside the cavity. This proves that a single round-trip of photon is equivalent to time taken for the SA to complete the absorption process. It is also worth to know that a mode-locked laser with soliton pulse shaping can generate more stable and ultrashort pulse. The presence of soliton pulse required a balance laser operation of two factors: self-phase modulation (SPM) and group velocity dispersion (GVD) (Bao et al., 2009).

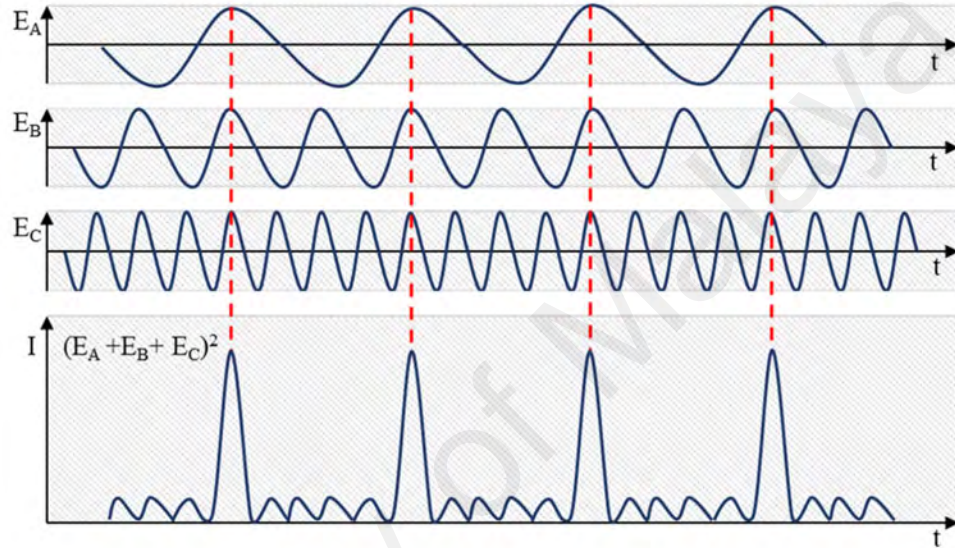


Figure 2.10: Phase locking phenomenon in mode-locked generation

2.5 Surface Plasmon Resonance (SPR)

Originated from a Latin word, plasmon in metal is a quantisation by the oscillation of electrons at plasma frequency. This longitudinal oscillation is caused by the Coulomb force, whereas led the long-range correlation of the electrons. Figure 2.11 illustrates the phenomenon of the oscillation. An external source of electric field is exposed to a metal plate, forcing the electron to move against the direction of the field. At this point, the electron will expose the proton on the other side, where in common situation there are interacted between each other, just like a magnet. When the electric field is removed, the

electron will rapidly move back to proton. In conductive material, the density of electron is very high, causing the electron to repel each other, also like a magnet. Here, the electron will continue to oscillate at plasma frequency until the energy is depleted by the other external factor. This model has been demonstrated and known as volume or bulk plasmon (Langmuir, 1928).

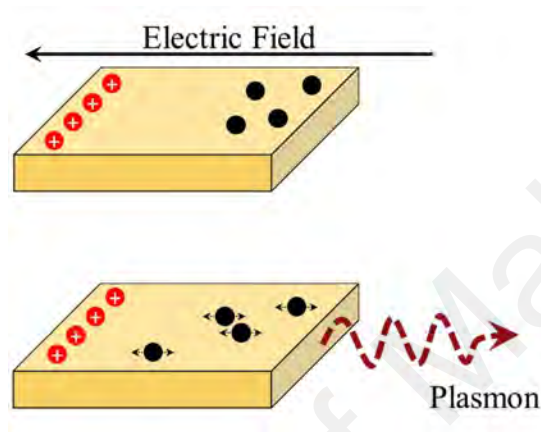


Figure 2.11: A basic model plasmon quantisation

This phenomenon is essential in determining the optical characteristics of a metal. The functionality of the plasmon can be related to the plasma frequency, where the light is transmitted or reflected. Any light with a frequency below the plasma frequency will be reflected, while light above the plasma frequency will be transmitted. This is happening because the electron cannot respond fast enough to block the electric field of the high frequency light (Maier, 2007).

Any metallic particle which are smaller or similar in size to the wavelength may create strong interaction between the electron and the electromagnetic radiation. The strong interaction often known as localised surface plasmon resonance (SPR). Localised SPR can be observed when the frequency of the incident light and the oscillating electron are matching, where the structure size is in nanometre (Murray et al., 2007). This forces the

electron to oscillate without external electrical charge and the behaviour is shown in Figure 2.12

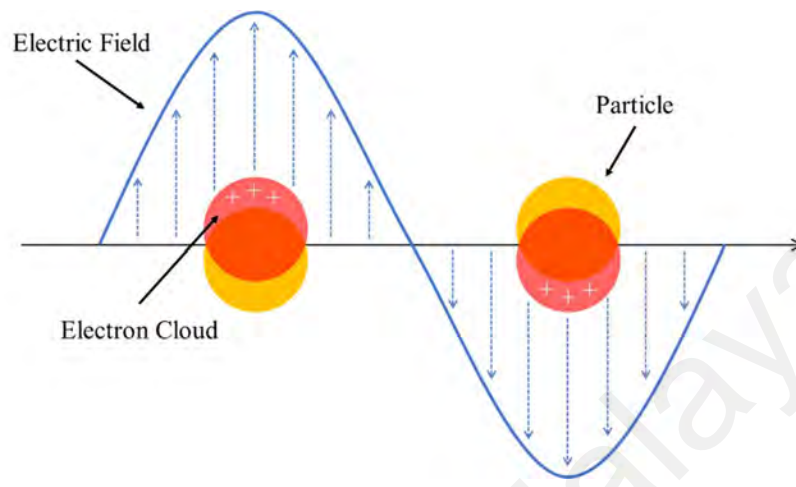


Figure 2.12: Electron behaviour inside the metal particles during localised SPR

The localised SPR characteristic is influenced by several factors such as size, shape and distribution of the particles. Modification or alteration of at least one of these factors can change the effect of the localised SPR modes. There are a lot of particle shapes ranging from a basic spherical, to a complex star-shaped can be used as the modifier. Plus, the inter-particle arrangement and distance between particles are also associated with the modes changing. There are also possible to increase the size of the particles to attract more absorption and scattering towards the material. It is important to highlight that the scattering will be high if the particle size is too big, hence will ignored the absorption and reduce the optical performance of the material (Fernando et al., 2012). It was demonstrated in 1998, where by increasing the particle size from 10 nm to 90 nm, the resonance peak shifted from 400 nm to 800 nm (Bohren et al., 2008).

The SPR effect shows the possibility of the metallic particle to be used as a SA in non-linear optical configuration. Noble metal such as gold and silver are good candidates to

be implemented into a pulse laser generation, in addition with their unique optical properties. The SPR effect that leads to pulse generation is referred as ground-state plasmon band bleaching, where the incident light creates an excitation inside the SPR frequency and causing the metallic particles to behave as a SA.

In general, when incident light is exposed to the metallic, it is also possible but rarely, a condition where the particles change into a behaviour of reverse saturable absorber due to free carrier absorption. In this rare situation, the absorption occurs at high intensity, reversing the common application of SA (Elim et al., 2006; Qu et al., 2006). These types of absorption allow metal to be used as SA without relying on typical mechanism of bandgap size, which is the energy difference of conduction and valance band in the material.

2.6 Noble Metals

Since the earliest day when man first discovered copper (Cu), the study towards the properties of many kind of metal has been changing the way of our living. Metal comprising 25% of Earth's crust. Copper, gold (Au), silver (Ag), tin (Sn), lead (Pb), and iron (Fe) are considered as prehistoric metal because it was known to be used by prehistoric man in their living (Reardon, 2011). Each of this metal have their distinct properties, for instance, gold and silver are used for decoration and trading, due to their softness and shiny surface. Alloy, a combination of at least one metallic substance with non-metallic substance have introduced human being to bronze, which consist of copper and tin. Bronze known by its toughness compared to a pure copper, but able to be cast into different shapes and hardened by forging process.

Metal has been classed in many categories, one of it is noble metal. Noble metal has slightly different meaning in different field of studies. For example, in atomic physics, the metal was classed based on their atomic properties (Novaro, 2005), while in the chemistry, it was based on their resistance to oxidation or corrosion in moist air. Even with this simple oxidation properties have attracted different opinion among researchers, either it considered noble metal or not. There are eight metals that are agreed by most of researcher as a noble metal, including gold and silver (Brooks, 1992). There are also other elements that are very resistant to corrosion but not make it into the list, such as titanium (Ti). Due to their resistance, noble metal can only be dissolved by acidic reaction, using nitric acid.

Despite of options available for noble metal, gold (Au) and silver (Ag) have their own unique optical properties that worth to be explored. The exploration of these metal has attracted wide attention among researchers. One of the most important features is broad saturable absorption band induced by the localised SPR. The SPR enhances the absorption ability of the material in various wavelength region, depending on several parameter including particles size (Qu et al., 2006). Besides the SPR, metal also exhibits a large third-order nonlinearity coefficient and ultrafast response time. The third-order nonlinearity is a crucial aspect in implying metal as a SA. As a reference, the coefficient value of graphene and carbon nanotubes are $\sim 10^{-7}$ and $\sim 10^{-8}$, respectively. The generation of self-starting pulse will become easier with the large coefficient value of the third-order nonlinearity (D. Wu et al., 2015). The third-order nonlinearity coefficient for gold was measured to be $\sim 10^{-6}$, one order higher than graphene (Liao et al., 1997), while silver was measured to be comparable to carbon nanotubes. The last feature that is equally necessary in possibility of generating ultrashort pulse is the response time. The response time is depending on the material itself, how fast they interact with photon (H. Zhang et al., 2014).

2.7 Laser Performance Analysis

Laser is operating at specific wavelength and it can be a multiwavelength operation. Multiwavelength operation means that the laser has more than one specific peak in a same wavelength region. These wavelengths can be observed through an optical spectrum, where the operating peak is significantly higher as compare to others. The highest peak along the x-axis is considered as the main operating wavelength. Figure 2.13 shows an example of low-resolution spectrum, where the operating wavelength is determined. Different application requires different operating wavelength because of the light interact differently at specific wavelength. For instance, the lasers are in safe-eye mode if it is operating in 2-micron wavelength, due to high water absorbance (Theodosiou et al., 2019). From the peak, the optical signal-to-noise ratio (OSNR) is obtained. It is measured in y-axis and represented in decibel (dB). The OSNR represent the difference between the laser emission with amplified spontaneous emission (ASE), which leads for better detection. Low OSNR will cause the ASE to be mistakenly detected as a part of the laser. This problem might reduce the possibility of detecting the pulse inside the laser (Paschotta, 2008).

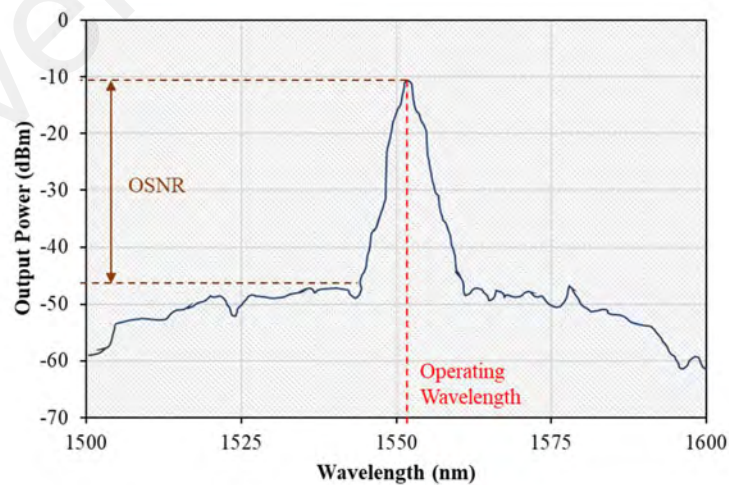


Figure 2.13: Output spectrum for a typical laser

For a passive Q-switching laser, the energy and width of the pulse are theoretically independent against the pump power. Instead, the pulse width is directly proportional to the cavity round-trip time, which time taken for a photon to make complete cycle inside the cavity (Spühler et al., 1999). In other hand, it also stated that the pulse width is inversely proportional to the saturable losses of the cavity. However, a typical Q-switched laser shows that the pulse width decreases as the pump power rises (Herda et al., 2008). This phenomenon happens from the SA inside the cavity, which react against the pump power and reduce the saturable losses inside the cavity. The pulse width is also known as full width at half-maximum (FWHM), can be expressed as:

$$\tau_w = \frac{S_p \tau_{rt}}{\gamma_0} \left[\frac{\delta(1 + \delta)\eta}{\delta - \ln(1 + \delta)} \right] \quad (2.1)$$

where the S_p is the factor of the pulse shaping, τ_{rt} is the round-trip time, γ_0 is the constant of the saturable loss in a round-trip, δ is the losses ratio of saturable and non-saturable, and η is the energy extraction efficiency (Zayhowski et al., 1994).

Figure 2.14 shows the illustration of a typical Q-switching pulse train. The temporal characteristic of the pulse train is analysed to obtain the repetition rate and the pulse width. Pulse duration was measured first by the period for each cycle. From the duration, repetition rate can be realised using the frequency equivalent to one over period equation. The repetition rate can be defined as number of emitted pulses per second. For Q-switching, it is common to observe the repetition rate as linearly dependent to pump power (Jackson, 2007). In other hand, pulse width is the period at half of the pulse maximum amplitude. As seen in the figure, the pulse become thinner as the pump power increases due to the reaction time of the SA against the pump power. This causing the

pulse to increase in repetition rate as more pulse generated at the same period, at the same time shrunken the pulse width to allow space for more pulse.

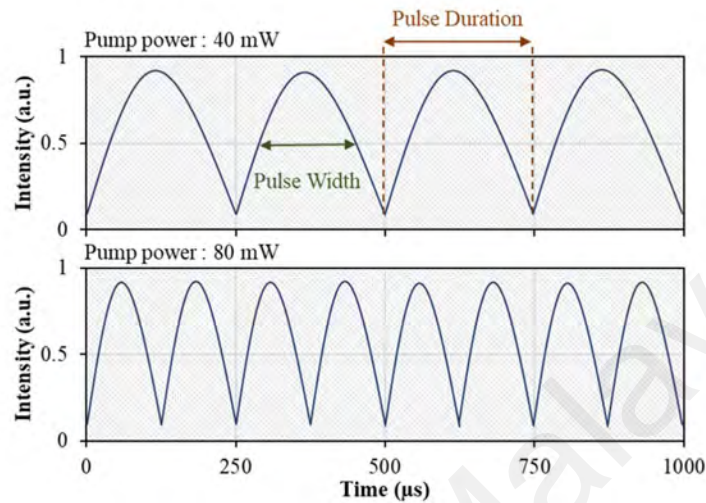


Figure 2.14: A typical Q-switching pulse train

For mode-locking, the repetition rate is fixed, depending on the cavity length. This technique allows an ultrashort pulse to form inside the cavity. The repetition rate is expressed by:

$$F = \frac{C}{nL} \quad (2.2)$$

where n is the refractive index, L is the total cavity length, and C is the constant velocity of light in vacuum condition.

The pulse generated contains an energy inside each envelope. While an average power can be measured directly through a power metre, pulse energy requires additional step to be obtained. Pulse energy can be defined as equal distribution of stored energy through the amount of pulses in a single period. Pulse energy can be represented as:

$$E_p = \frac{P_{avg}}{F} \quad (2.3)$$

where P_{avg} is the average output power, and F is the repetition rate of the pulse. The lifetime of the gain medium is a crucial part in generating high pulse laser alongside with the saturable loss generated by the SA. This is because of the accumulated energy in the cavity are stored in the gain medium (S.-L. Huang et al., 1999). On the other side, there is a peak power, a maximum occurring optical power of a single pulse and expressed by this following equation:

$$P_p = \frac{E_p}{\tau_p} \quad (2.4)$$

as E_p is the pulse energy and τ_w is the pulse width. Both these values can be obtained using equation (2.1) and (2.3). For nanosecond and longer pulse, the peak energy is obtained directly from the oscilloscope via a photodetector, but this method cannot be used for picosecond and shorter pulse. This is because the photodetector not fast enough to measure the peak power, hence the usage of equation (2.4) is necessary.

The stability of the generated pulse can be determined using radio frequency spectrum analyser (RFSA) and the spectrum shows as Figure 2.15. The first peak, known as the fundamental peak, must be equal to the repetition rate of corresponding pulse. For example, the pulse repetition rate is 110 kHz and the fundamental peak must be located at approximately 110 kHz in the spectrum. The difference between the apex of the first peak to the pedestal floor determined the signal-to-noise ratio (SNR), indicating the stability of the pulse, which higher SNR contributing in higher stability of the pulse. Other peaks in spectrum are harmonics frequencies, which are the value of positive integer

multiple the frequency of the fundamental peak. These harmonics must be periodic equal to fundamental frequency. The amplitude of these harmonics will continue to drop until its levels with pedestal floor.

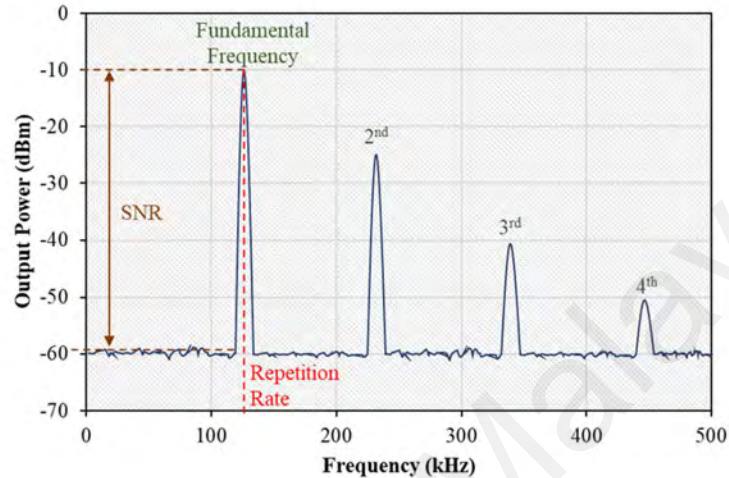


Figure 2.15: A pulse representation in frequency-domain

All these laser performances are important aspect in characterizing a pulse laser. Despite on discovering new method and material, it is necessary to review reported works that has been published. There are several reports on metal-based SA available, but due to the material is newly used in SA, the number of reports is still low. In 2014, an erbium-doped fibre laser was reported to produce Q-switched pulse by using gold as SA (Fan et al., 2014). The gold solution was prepared through a chemical synthesising process before it was deposited on a microfibre. The microfibre was fabricated using a standard flame brushing technique and was placed on a glass slide for deposition process. The next year, another report shows a Q-switched pulse was generated in a visible region using gold SA (D. Wu et al., 2015). In the report, the gold solution was prepared using the similar chemical synthesising process as before. The solution was then mixed with polyvinyl alcohol (PVA) to turn the solution into more practical thin-film form. The film was cut

into small piece and sandwiched in between two fibre ferrules. This sandwiched technique is one of the most common method for implementing film into a laser cavity.

In the same year, another Q-switched erbium-doped fibre laser was reported, but this are using silver as the SA (Guo et al., 2015). The silver was prepared through a solvothermal reduction process, with three samples in different amount of alcohol mixture. The alcohol composition was reported to affect the size of particles of the silver. The prepared silver was embedded onto the fibre ferrule by using photo-deposition technique. This technique utilises the phonon interaction of red-light laser with the prepared silver. Later in 2017, a neodymium-doped yttrium aluminium garnet (Nd:YAG) laser was able to produced pulse at 1-micron region through a Q-switching technique (Y. Wu et al., 2017). The pulse originated from a silver film SA, synthesised through a seed-mediated growth method. The silver was transferred to quartz carrier substrate with spin coating and drying method afterwards to produce the silver film. The film was observed to sustain in high-power operation without suffer any optical damage. Table 2.1 shows the comparison on these works. These comparisons signify the potential usage of metal-based material, especially gold and silver in generating pulse laser. The SA can be fabricated and implemented into the cavity using various method. The ability of the SPR effect from metal can be utilised to produce a SA that can operate in various wavelength.

Table 2.1: Performance of the current laser utilizing gold (Au) and silver (Ag) as the saturable absorber

Authors	SA Type*	Wavelength (nm)	Rep. Rate (kHz)	Pulse Width (μs)	Pulse Energy (nJ)	Peak Power (mW)
(Fan et al., 2014)	Gold	1562	58.1	1.78	133	74.72
(D. Wu et al., 2015)	Gold	635	546.4	0.24	27.7	74
(Guo et al., 2015)	Silver	1565	58.5	2.40	132	55
(H Ahmad, NE Ruslan, MA Ismail, et al., 2016)	Silver	1559	74.1	3.20	8.17	3
(Harith Ahmad et al., 2016)	Silver	1962	56.2	4.2	67.3	16.0
(Y. Wu et al., 2017)	Silver	1064	223.7	0.20	510	2550
(Fu et al., 2017)	Silver	1068	65.7	1.84	53.1	29
(Lokman et al., 2018)	Silver	1560	65.4	6.70	146.4	21
(Rosdin et al., 2018)	Silver	1565	55.7	8.16	34.7	2

*SA = saturable absorber

CHAPTER 3: PURE GOLD THIN-FILM SATURABLE ABSORBER AS Q-SWITCHER

3.1 Introduction

The pulsed laser technology has evolved significantly, and it was driven by the demands in current medical and optoelectronics industries. Evolution of this technology begins in the 80s, when the first laser was generated using a dye gain medium and only a decade later, a solid-state gain medium was used for laser generation (Grudin, 2013). High-cost and bulky physical of solid-state lasers has pushed into a swift development of fibre lasers as an alternative in producing high-performance laser. The lasers have wide potential to be implemented into various applications from biomedical, machining, sensing, to communication. In general, there are two types of high-performance laser; Q-switched and mode-locked lasers. Q-switched can be realized by manipulating Q-factor of the laser and the operation is dependent on input power and repetition rate. On the other side, mode-locked repetition rate is only depending on cavity length, with light dispersion and non-linearity affecting the process. Both operations have their uniqueness and specific application where it is suitable to be used. For instance, Q-switched was widely used in cosmetic and data storage industry, thanks to their high peak power feature.

From the last decades, many studies on passively Q-switched fibre laser have been carried out due to their advantages in terms of compactness, robustness, and simplicity. Together with these advantages, the potential to be implemented into various end-user applications such as optical sensing, laser therapy, and high-speed internet attract more attention to this emerging technology. Adding to the value, the usage of noble metals of gold (Au), silver (Ag) and copper (Cu) as passive Q-switcher have been impressive, thanks to their unique optical features. These features include their large third-order

nonlinearity, fast response times of a few picoseconds, and broad absorption from localized surface plasmon resonance (SPR).

Up to date, combinations of diverse material and method have been reported, all aim to deliver the best saturable absorber (SA) for pulsed laser application. Various SAs have been proposed on Q-switching generation based on different 2D nanomaterials, ranging back from graphene, transition metal dichalcogenides (TMDs), topological insulator (TIs), to black phosphorus (BP). Lately, MXene and Bismuthene come into the scene of ultrashort pulse application. All these 2D materials utilize the bandgap size of material to determine the suitable operating wavelength based on their absorption profile. On the other hand, metal-based SAs have also gained interest in the recent years to take advantage of broad saturable absorption introduced by SPR effect at wide wavelength region, from visible to infrared. By this, the metal-based SAs able to operate alike 2D nanomaterial with an additional function of operating in wider wavelength region. Adding to that, third-order nonlinearity of metal-based is much larger contrasted to other 2D nanomaterials, especially for gold and silver. The nonlinearity was projected to suppress the gain medium from any mode competition, which will improve the performance of Q-switched laser. These SPR and nonlinear characteristics play an important role in pulsed generation, which influencing the absorption profile of the light propagation through metal SA.

In this chapter, the use of pure gold SA as Q-switcher for pulse generation is investigated and demonstrated. This chapter discusses on the pure gold SA preparation and characterization and fibre laser configuration, and then presents analysis data for the spectral and temporal laser performances of Q-switching operation at 1-, 1.55-, and 2-micron region.

3.2 Preparation of Pure Gold Thin-Film

Gold (Au) element is the main component for the proposed SA. It was obtained by depositing gold onto a polyvinyl alcohol (PVA) film by using electron beam (E-beam) deposition technique. The PVA film was used as a host polymer owing to its low optical absorption at the laser operating wavelength. In addition, it is robust, flexible and can be simply integrated in between fibre ferrules. In preparing the film, 1 gram of PVA powder was mixed into 120 ml of de-ionized (DI) water as illustrated in Figure 3.1. The mixture was stirred at temperature of 145 °C until the powder dissolve completely. Subsequently, 5 ml of PVA solution was poured and left dry in a petri dish under room temperature for 3 days, to produce a film as Figure 3.2 with approximately 30 μm of thickness.

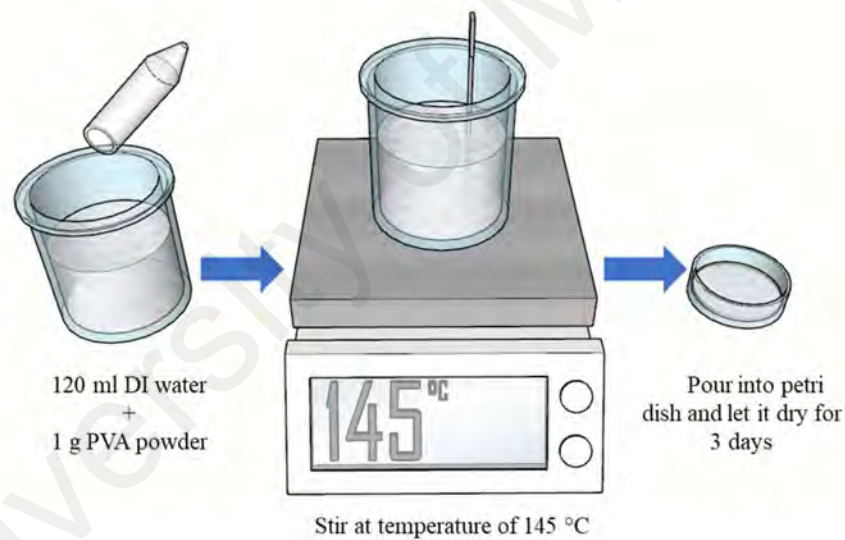


Figure 3.1: Fabrication process of PVA film

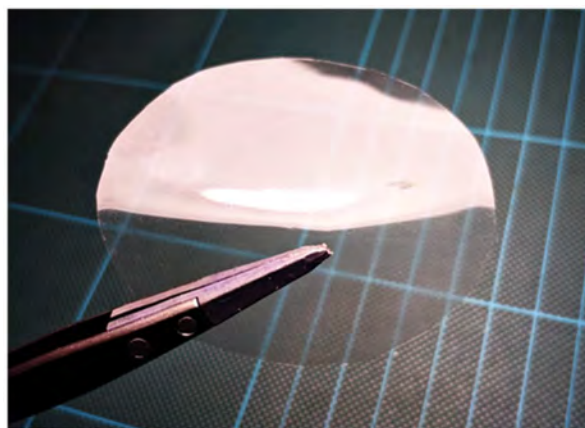


Figure 3.2: Dried PVA film from petri dish after 3 days

Both PVA film and gold was then placed inside a vacuum chamber for E-beam deposition process as shown in Figure 3.3. E-beam deposition is considered as a “top-down” fabrication method along with other method that are categorized under physical deposition, for instance, E-beam lithography, sputter coating, and thermal evaporator. In this work, a Korean-made electron beam evaporation machine assembled by Korea Coating Materials and Components (KCMC), model number EB43-T was used.

This process has two steps; vacuuming and coating. Vacuuming is the preliminary step of generating pressure inside a chamber to form a full vacuum condition. At this condition, electrons may freely propagate inside the chamber, allowing it to collide with gold palettes placed at the bottom of the chamber. When the chamber reaches the pressure of 1×10^{-4} mbar or lower, coating begins. Coating step starts by supplying extremely high current to tungsten filament and electron is generated. Tungsten was used due to high melting point and the resistance at extreme temperature. Multiple negative-charged deflecting magnets inside the chamber were used to aim the electron path towards the gold. The gold was placed in a crucible, a container that can withstand high temperature generated from the electron.

High intensity electron causes atoms from the gold to transform into a gaseous state at a very short time. It changes back to solid form and coating everything inside the chamber, except for the PVA film located on top of the chamber which covered by a mechanism called “shutter”. Shutter is located in between the gold and the PVA film, controlling the thickness of the coating. Shutter is open for a duration of time and exposing the PVA film to the gaseous atoms of gold, cumulating a pure gold layer on top of the PVA film. The thickness is measured to be approximately 16 nm, monitored through a microscopic camera located at the same eye-level with PVA film. The details thickness is shown in Figure 3.4. The amount of time taken to achieve the desired thickness is based on the deposition rate, which is equivalent to thickness (Å) over time (second). Deposition rate can be modified by simply tuning the current flow through the tungsten filament. Basically, the parameters setting in the machine is based on the metal itself, whereas different metal have different setting to transform into the gaseous state. The gold thin-film, hence known as pure gold SA was sealed in a vacuum container to prevent oxidation. This implementation process is considerable as simple and relatively low. Besides, utilizing this process to produce a capable SA film device is part of the novelty in this work.

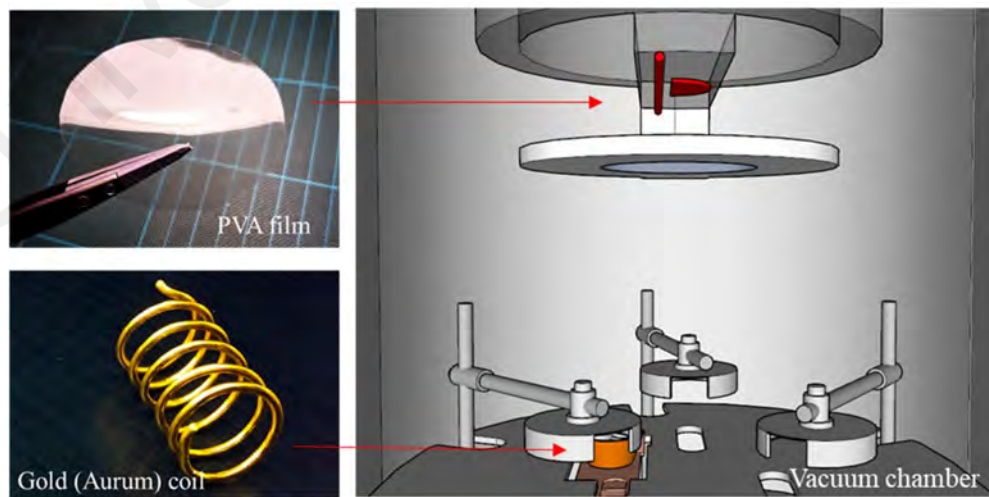


Figure 3.3: Placement of PVA film and gold inside the vacuum chamber



Figure 3.4: Illustration on thickness of the gold thin-film (Inset) Real image of the gold thin-film

3.3 Material and Optical Characterization of Gold Thin-Film

The presence of gold in the sample of SA was verified through various measurements including field emission scanning electron microscopy (FESEM), and energy-dispersive X-ray spectroscopy (EDX) analysis. Figure 3.5 shows the FESEM image of the prepared gold thin-film, which indicates the existence of the homogeneous and uniform thin gold layers on the film. A homogenous distribution of gold on the film surface was observed through this high-resolution image. This image also confirms the absence of >200 nm aggregates or voids on the film, which otherwise results in non-saturable scattering losses. The material composition of the gold was confirmed by the EDX analysis on the FESEM image, as shown in Figure 3.6. The result shows that the gold thin-film consists of 41.97 wt.% of Au and 58.03 wt.% of PVA (C_2H_4O)_x film. This indicates that almost half of the thin-film surface was covered with gold. For pure metal, Raman spectroscopy analysis could not be performed due to no polarizability change during molecular vibration, which are essential requirement to obtain the Raman spectrum.

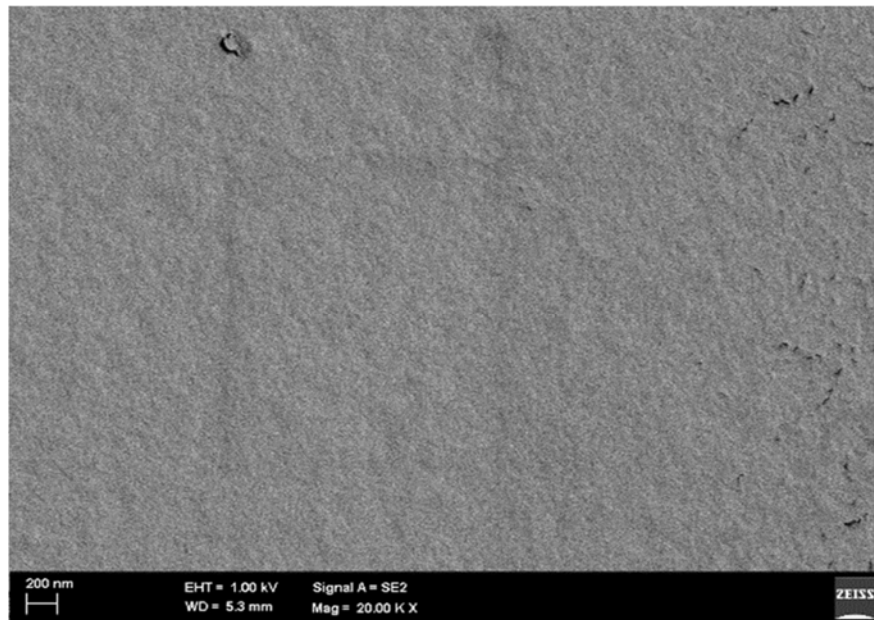


Figure 3.5: FESEM image of the gold thin-film

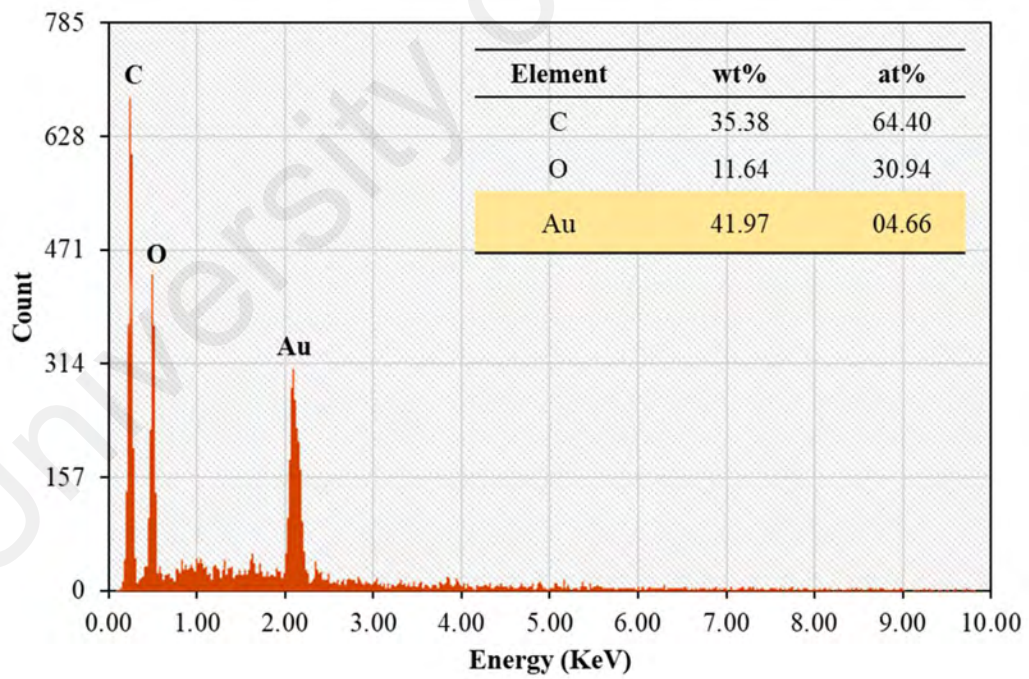


Figure 3.6: EDX analysis on the gold thin-film

Another important parameter for SA is the linear and nonlinear optical response. The investigation towards the linear optical response of pure gold SA was performed by launching a white light source, which covered broader wavelength, towards the gold thin-film and the measurement result is depicted in Figure 3.7. It shows that the linear absorption spectrum within range of 950 to 2100 nm with an absorption loss presence at 1- μm , 1.55- μm , and 2- μm is 4.5 dB, 4.1 dB, and 3.45 dB, respectively. Next, the nonlinear transmission measurement was performed by launching a mode-locked laser into the SA to confirm its saturable absorption ability. The mode-locked laser used operated in 1560 nm region, pulsing at 1 MHz repetition rate and width of 3 ps. Through a balance twin-detector measurement, the modulation depth of the gold thin-film is measured to be around 4 % as shown in Figure 3.8. The measurement data was fitted according to a simple two-level saturable absorber model (Lecourt et al., 2006), which is given by

$$T(I) = \frac{\alpha_{sat}}{1 + \left(\frac{I}{I_{sat}}\right)} + \alpha_{ns} \quad (3.1)$$

where $T(I)$ is the transmission coefficient, α_{sat} is the saturable absorption or modulation depth, α_{ns} is the non-saturable absorption, I is the input intensity, and I_{sat} is the saturation intensity. The I_{sat} is defined as the optical intensity required in a steady state to reduce the absorption to half of its unbleached value. The configuration for this measurement technique is presented in Figure 3.9.

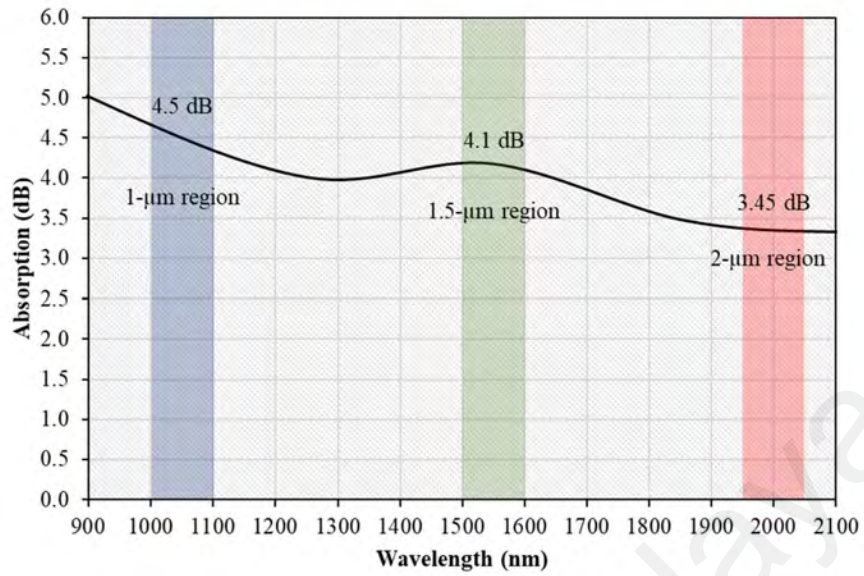


Figure 3.7: Linear absorption spectra of the gold thin-film in spectrum ranging from 900 nm to 2100 nm wavelength

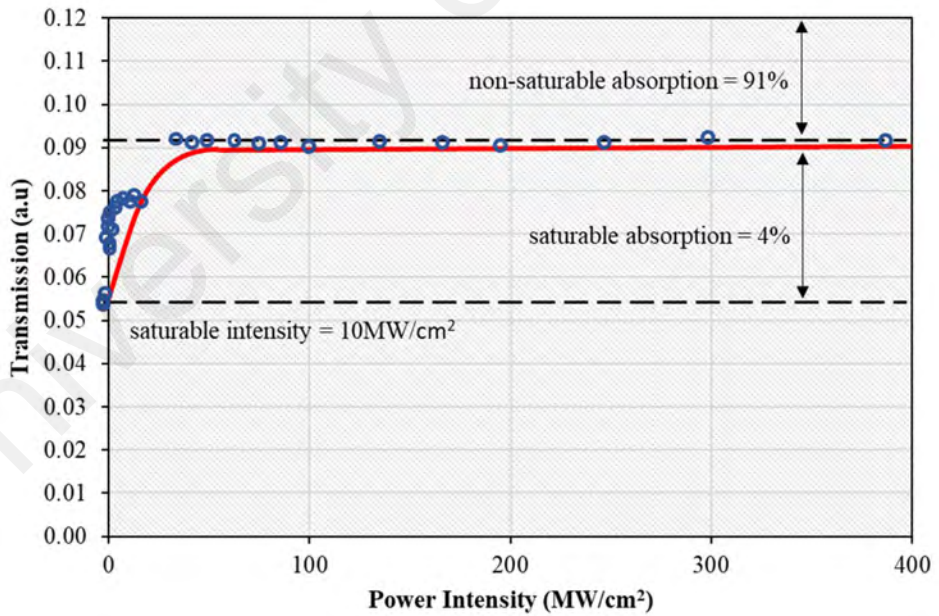


Figure 3.8: Nonlinear transmission measurement of the gold thin-film using balance twin-detector technique

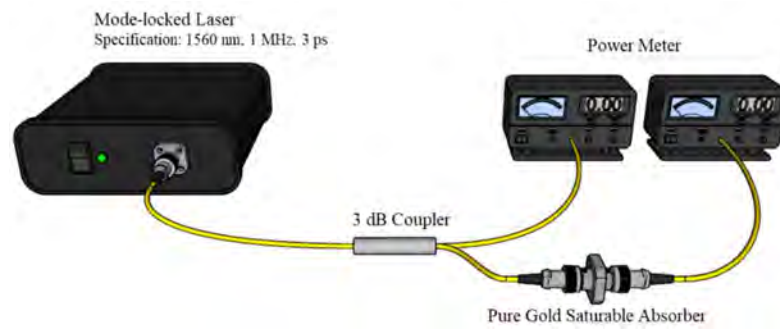


Figure 3.9: Balance twin-detector configuration for nonlinear transmission measurement

3.4 Q-switched Fibre Laser operating at 1-micron Region

A Q-switched ytterbium-doped fibre laser (YDFL) operating in 1- μm region is demonstrated using the fabricated gold thin-film as a passive SA. Figure 3.10 shows the configuration of the ring laser used which employs an ytterbium-doped fibre (YDF) as a gain medium. The cavity employs a 2-meter-long YDF as an active gain medium, which was forward pumped by a 980 nm single-mode laser source via a 980/1064 nm wavelength division multiplexer (WDM). The YDF has an ions absorption of 23 dB/m at 1020 nm with core diameter of 4 μm . A polarization independent optical isolator was included to ensure unidirectional light propagation inside the cavity. A 10-dB optical coupler taps 10% of the laser output for data collection, while remaining 90% left oscillating inside the cavity. The gold thin-film was employed by sandwiching a tiny piece of it between two fibre ferrules to form a fibre compatible device. The insertion loss of the gold thin-film was measured to be 4.5 dB. An optical spectrum analyser (OSA: Yokogawa AQ6370B) was used to display the optical laser spectrum. A broadband power meter with power detector measures the laser output power. The 350 MHz digital oscilloscope (OSC: GW Instek, GDS-3352) analyses the temporal performance of the pulse, while the 7.8 GHz radio frequency spectrum analyser (RFSA: Anritsu MS2683A) measures the pulses train in frequency domain. A 1.2 GHz photodetector (PD, Thorlabs

DET101CFC) with rise/fall time of 60 ps was pre-integrated with the oscilloscope and RFSA to interpret the frequency spectrum of the output pulses for the laser.

Figure 3.11 illustrates the optical spectra through the OSA by comparing the spectral performance of the Q-switched laser with continuous wave (CW) laser at threshold pump power of 61.1 mW. As shown, the laser spectrum of the CW laser originated at 1069.5 nm. Due to cavity loss generated by the incorporated gold thin-film in the cavity, the laser shifts to shorter wavelength of 1063.5 nm, where higher gain is accumulated. The optical signal-to-noise ratio (OSNR) of the Q-switched laser is approximately 19.78 dB, with full-width at half-maximum (FWHM) of 0.525 nm. It is observed that the spectral width becomes narrower in Q-switching operation. This is attributed to the high nonlinear effect inside the cavity.

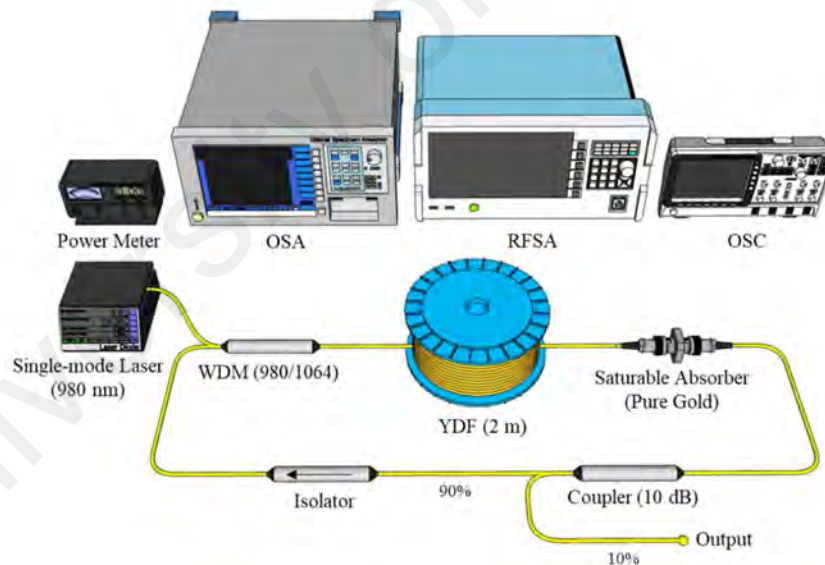


Figure 3.10: Ring laser configuration for 1- μ m operation with pure gold SA

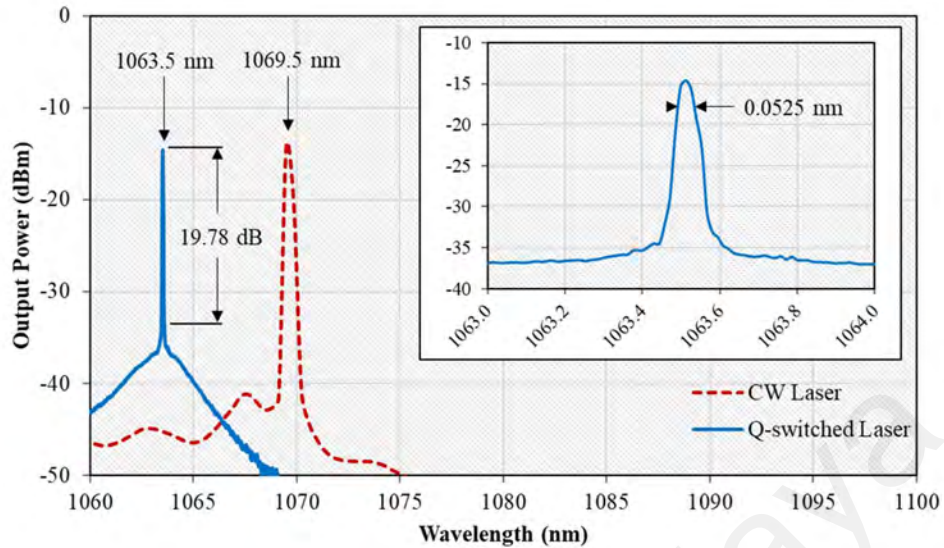


Figure 3.11: Optical spectra of the Q-switched and CW laser at pump power of 61.1 mW

A stable Q-switched pulse is observed as the pump power reach 61.1 mW. It maintains the operation even the pump power is increase to 87.4 mW. When the pump power was further increased beyond 87.4 mW, an unstable Q-switched state was observed due to over-saturated SA at high incident intensity. The pump power is increased up to the pump limit of 200 mW, but the Q-switched pulses has been completely diminished. As it reduced back to below 87.4 mW, the pulses are recovered, thus shows that gold thin-film can withstand laser intensity up to 200 mW. In absence of the gold thin-film, no pulse is generated, and only a typical CW laser can be observed. The Q-switching occurs when the energy inside the cavity reaches a certain saturable value, determined by the saturation time of the material used in the SA. The SA absorb photons and excite electrons up to conduction state. When all the conduction state space is occupied by the electrons excited by those photons, the SA will reach it saturable condition, allowing formation of the pulsed laser.

Figure 3.12 illustrate the temporal performances of the Q-switched laser taken at three different pump powers of 61.1 mW, 74.3 mW, and 87.4 mW for threshold, median, and

maximum, respectively. As shown, the pulse train has become narrower in increment of pump power. At maximum accessible pump power, the pulse train has a narrowest pulse width of 4.23 μs . The pulse duration is measured to be around 16.16 μs , consistent to the repetition rate of 61.88 kHz. As seen, the pulse train has a stable amplitude over 600 μs , indicating the stability of the generated Q-switched laser. The stability of the pulse can further observe in frequency domain as presented in Figure 3.13. As shown, there are 10 harmonics lining up over the 700 kHz span and the frequency of the fundamental peak is 61.88 kHz, proving the repetition rate shown before in Figure 3.12. The signal-to-noise ratio (SNR) is measured to be approximately 56.31 dB from the peak to the pedestal, revealing the pulse stability. It is also worth to notice that the proposed laser operated stably in the laboratory condition for at least 48 hours without any noticeable degradation of performance.

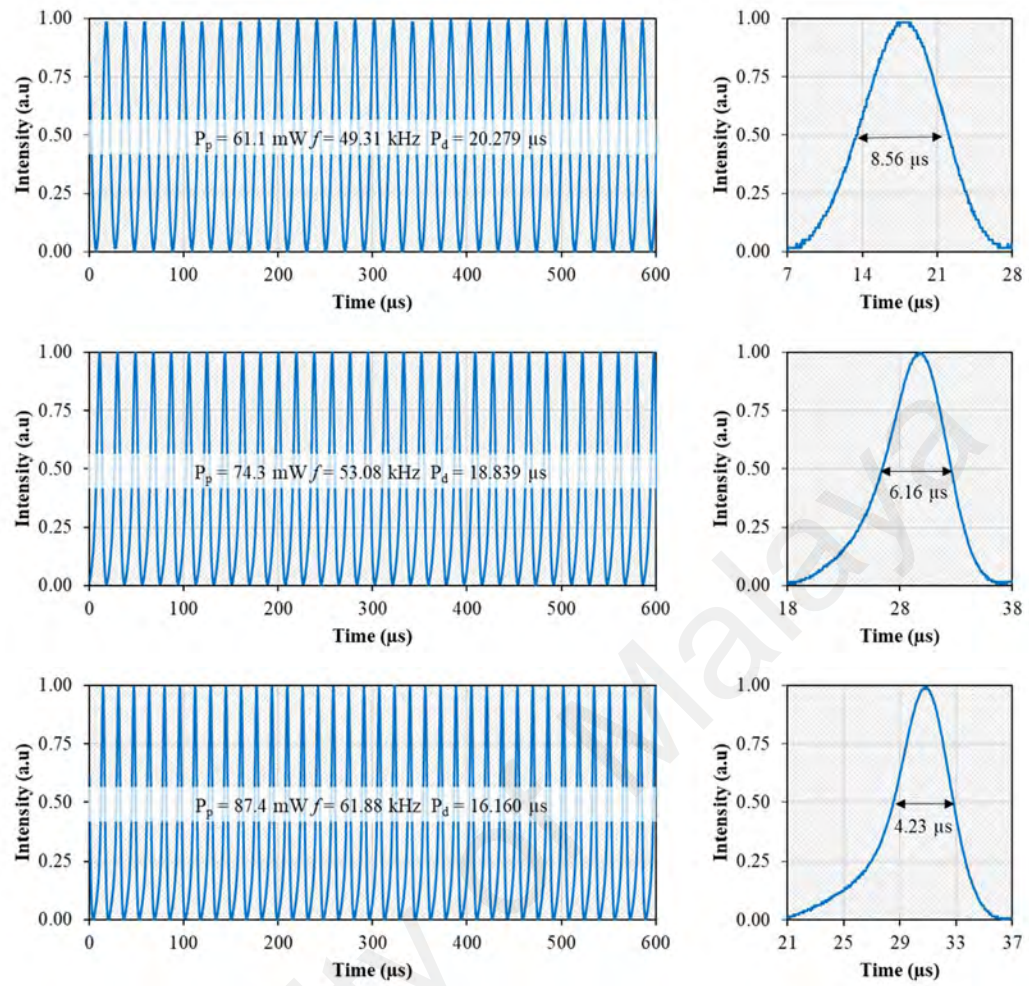


Figure 3.12: Typical pulse train of the Q-switched laser at threshold, median, and maximum pump power

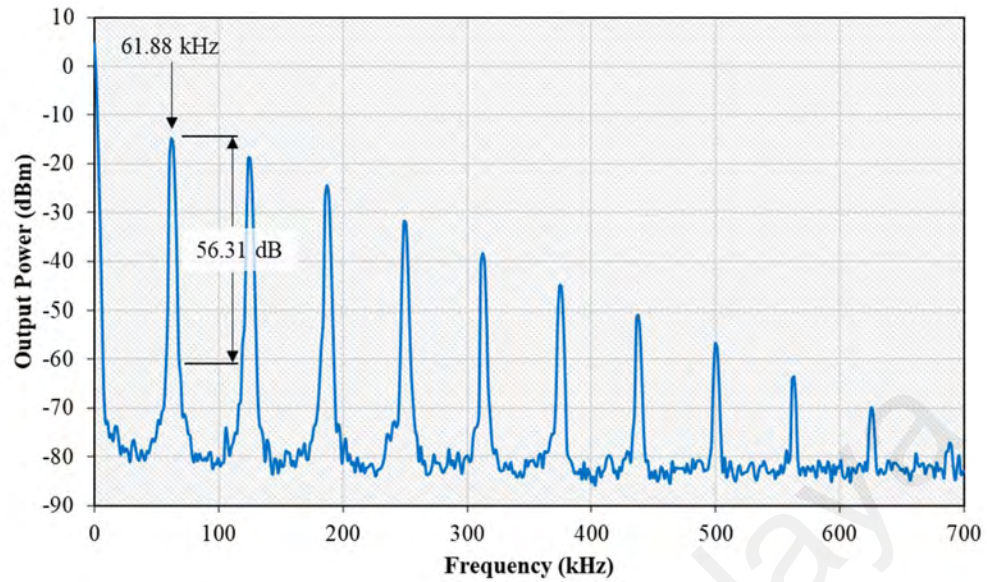


Figure 3.13: Frequency plot of the Q-switched laser at maximum pump power

The Q-switched laser performances were also analysed under various pump power as presented in Figures 3.14 and 3.15. As illustrated in Figure 3.14, the output power of the laser linearly escalates starting from 0.52 mW to 3.14 mW, accommodating a slope efficiency of 9.58 %. The efficiency is directly related to intra-cavity loss, which can be further improved through cavity optimization. At the same time, the peak power inclines rapidly compare to output power. This happen from the combination of shorten pulse duration and shrunken pulse width of the Q-switching operation. Thus, the peak power escalates from 1.23 mW to 12 mW as the pulse width shrinks from 8.56 μ s to 4.23 μ s. The pulse energy reading increases from 10.55 nJ to 50.74 nJ and it signified by a total energy contains in a single pulse. Therefore, pulse energy is affected by variation of either one or both the output power and pulse width. As can be observed in Figure 3.15, the pulse energy increment with pump power is small at pump power region from 74.3 mW to 78.7 mW. This is attributed to a sudden increase in the repetition rate and a minor drop of the output power.

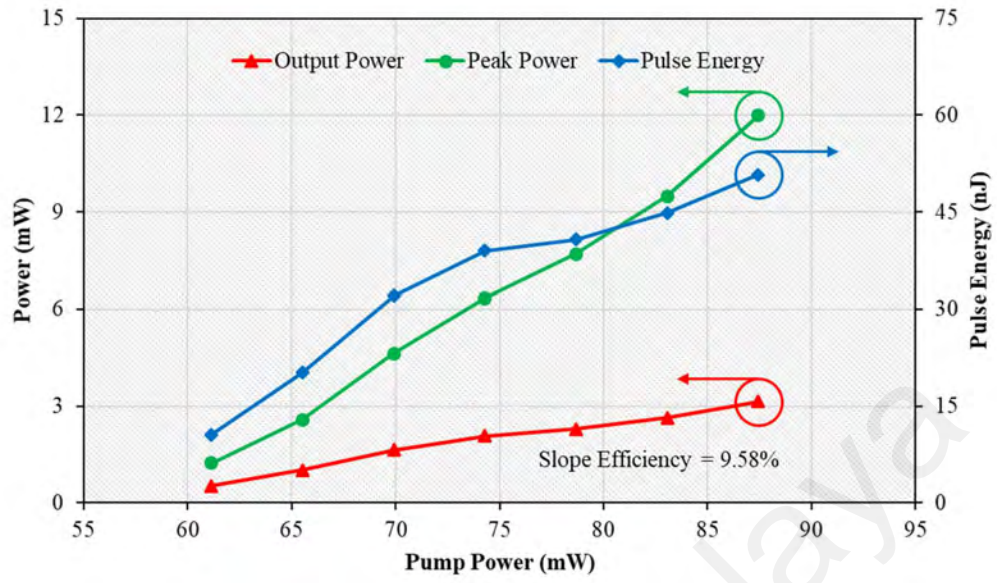


Figure 3.14: Power and energy analysis of the Q-switched laser at various pump power

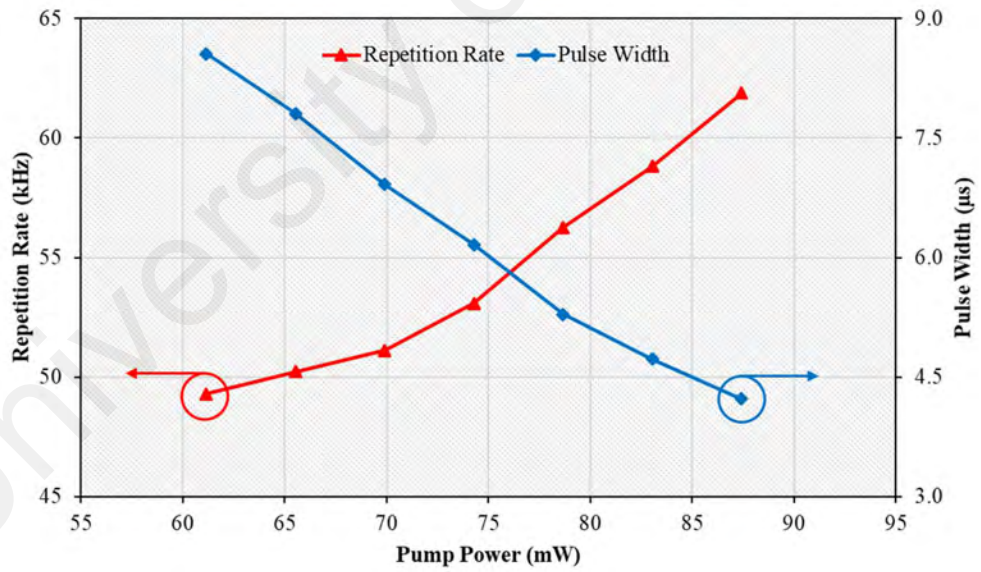


Figure 3.15: Repetition rate and pulse width analysis of the Q-switched laser at various pump power

The experimental results show that the incorporation of gold thin-film can initiate self-started Q-switched pulses in YDFL cavity. This indicates that the saturable absorption characteristic of the gold film has a great potential to be applied in various laser applications. Furthermore, the use of pure gold SA offers simplicity in integration and fabrication, compactness, and flexibility. This possibly will benefit users in actual laser applications. The performance of Q-switched pulse is expected to be further improved by optimizing the SA and the laser cavity. The scattering loss of the gold thin-film can be improved by reducing the thickness of PVA film and gold layer.

3.5 Q-switched Fibre Laser operating at 1.55-micron Region

The configuration for the proposed gold thin-film based SA for Q-switched erbium-doped fibre laser (EDFL) is shown in Figure 3.16. This ring laser consists of a 2.4-meter erbium-doped fibre (EDF) as the gain medium and a 10-dB output coupler to tap 10% of the output for observation, retaining the rest to oscillate in the cavity. The EDF used had an erbium ion concentration of 2000 ppm with a numerical aperture (NA) of 0.24. The gain medium was forward pumped by a 980 nm laser diode via a 980/1550 nm wavelength division multiplexer (WDM). An isolator was used in the cavity to only allow unidirectional propagation of the laser resonator and preventing any detrimental effects. The gold thin-film was sandwiched in between two fibre ferrules to form a fibre compatible SA device.

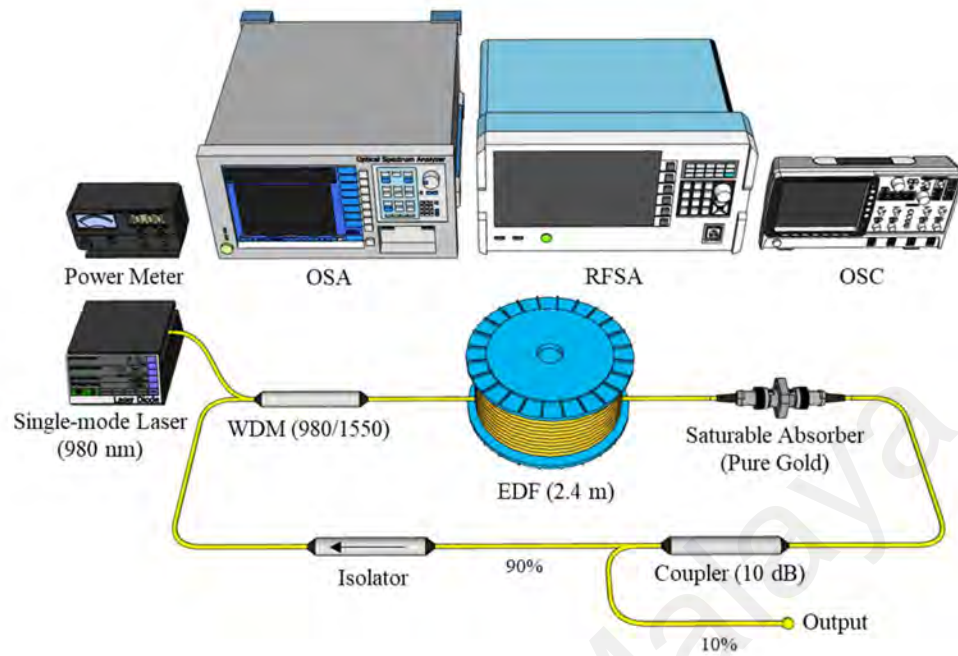


Figure 3.16: Ring laser configuration for 1.55- μm with pure gold SA

At first, only CW laser is observed when the cavity is fed with input threshold pump power of 7.7 mW. As the pure gold SA was inserted into the cavity, a stable and self-starting Q-switching pulse was obtained by tuning the input pump power to slightly above threshold of 17.3 mW. Figure 3.17 compares the output spectrum of the laser at the threshold pump power, with and without the presence of the saturable absorber. In absence of the SA, the laser basically operates at 1563 nm with an OSNR of approximately 21 dB. The operating wavelength is later shifted to 1560 nm after the SA is incorporated into the cavity due to loss introduced by it. To compensate the loss, the laser operates at a shorter wavelength, where higher gain is accumulated. Hence, increasing the OSNR reading slightly to 24 dB.

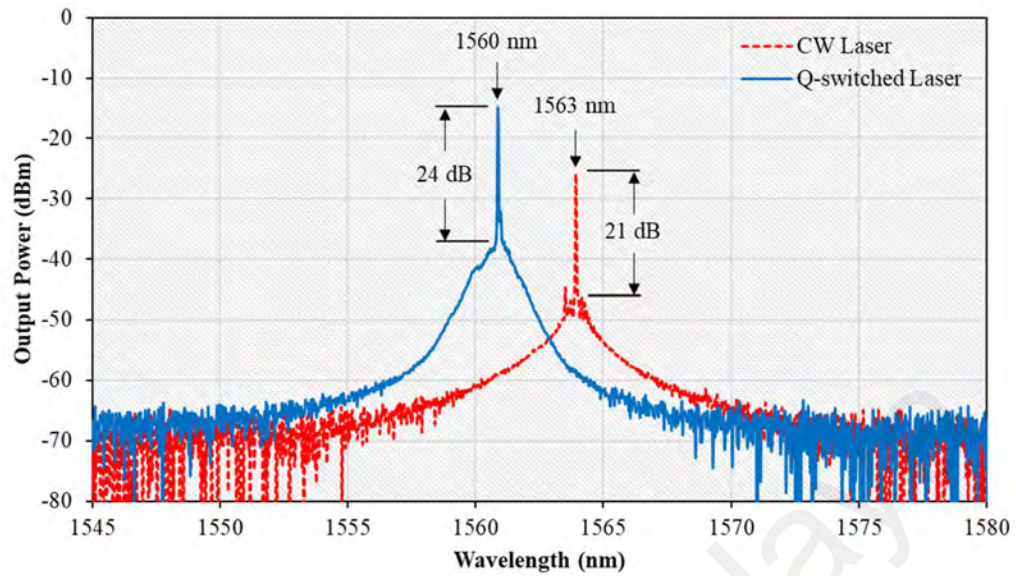


Figure 3.17: Optical spectra of the Q-switched and CW laser at pump power 17.3 mW

The Q-switched laser was later analysed by using digital oscilloscope. Figure 3.18 shows the typical oscilloscope trace at two different pump powers when the pure gold SA was introduced into the cavity. Measured repetition rates for both stable Q-switched laser are 24.34 kHz and 88.11 kHz, for pump power of 17.3 mW and 179.5 mW respectively. It was observed that more pulses with narrower width in the same period of time (120 μ s) were obtained as the input power increased. This is due to the higher power that forces the SA to saturate faster, and hence generating more pulses in a period of time while narrowing the pulse width. No distinct amplitude modulation was seen in any envelope of the spectrum, which indicates that the self-mode locking effect is weak. This phenomenon is a typical feature of passive Q-switching. The pulse is observed to be sinusoid-like because of its natural breadth; causing the process of the pulse “falling time” to touch the next adjacent pulse “rising time” in cyclical repetition. It can be confirmed by harmonics RF spectrum that this is directly related to the pulse width size.

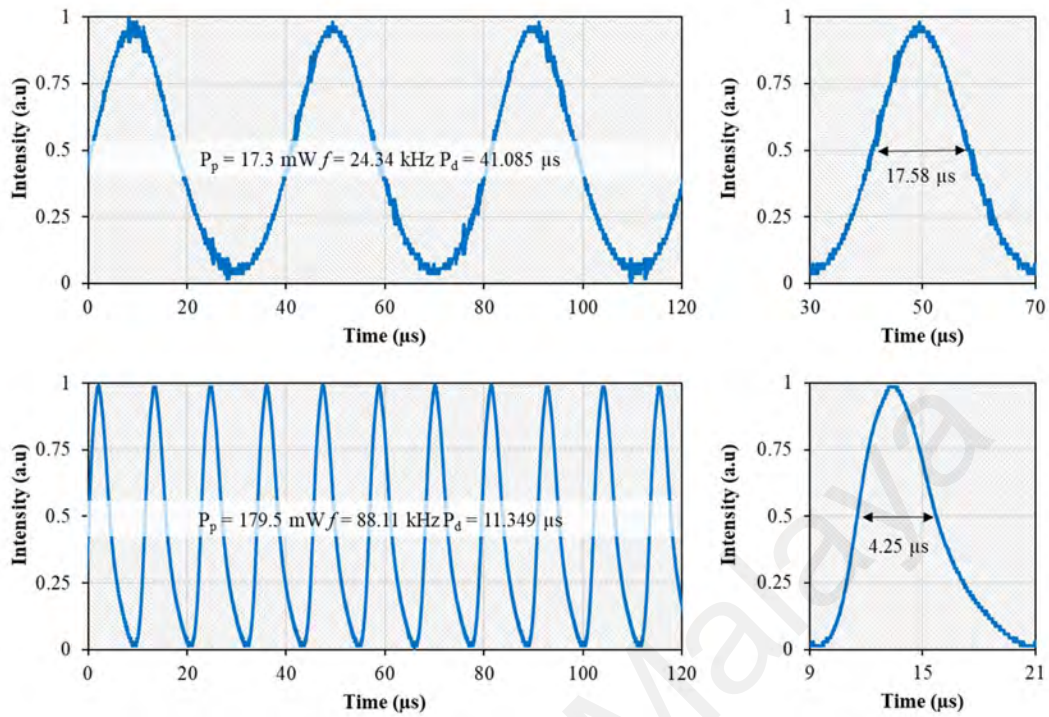


Figure 3.18: Typical pulse train of the Q-switched laser at threshold and maximum pump power

Distribution of the pulse analysis against the increment of pump power was charted accordingly. Figure 3.19 shows the relationship between repetition rate and pulse width with different pump power. A stable pulse duration in output pulse trains was observed, together with a monotonic increment of the repetition rate due to the linear increase of pump power. The Q-switched laser depends on the light intensity created by the SA. Photons from low-intensity light are absorbed into the SA and excite the electrons up to conduction state. In high-intensity light, the number of photons is increased; hence, some of the photons are not absorbed. This is due to the electrons in the conduction state being fully occupied by other electrons excited by some of the absorbed photons. The pulse is generated when the cavity energy reaches a certain saturable value, determined by the recovery time of the material used in the saturable absorber. The repetition rate of the pulse depends on the stored energy, which varies according to the pump power. It can be

tuned to more than 60 kHz by adjusting the input pump power from 17.3 mW to 179.5 mW, with a frequency range varied from 24.34 kHz to 88.11 kHz. The corresponding pulse width reduces from 17.58 μs to 4.25 μs . Figure 3.20 shows the relationship between average output power and pulse energy as a function of pump power. The output power as well as the pulse energy increase from 0.19 mW to 2.90 mW and from 8.0 nJ to 32.9 nJ respectively as the pump power increases linearly from 17.3 mW to 179.5 mW. The pulse energy is expected to be further improved by increasing the pump power. The pulse energy will slightly increase, even though Figure 3.20 shows that the pulse energy is near saturation point. Furthermore, the overall performance of the laser can be improved by optimizing cavity loss, especially in terms of pulse energy.

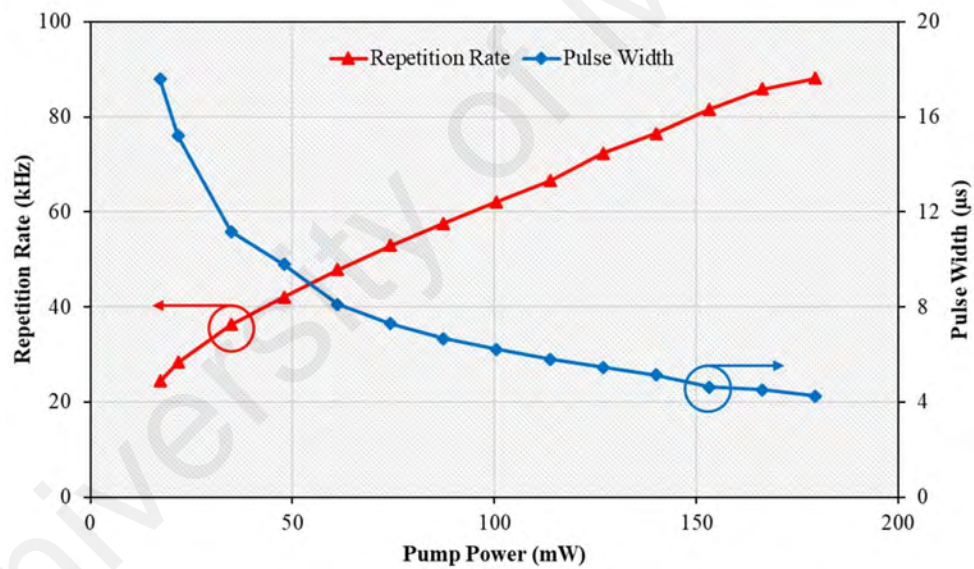


Figure 3.19: Repetition rate and pulse width analysis of the Q-switched laser at various pump power

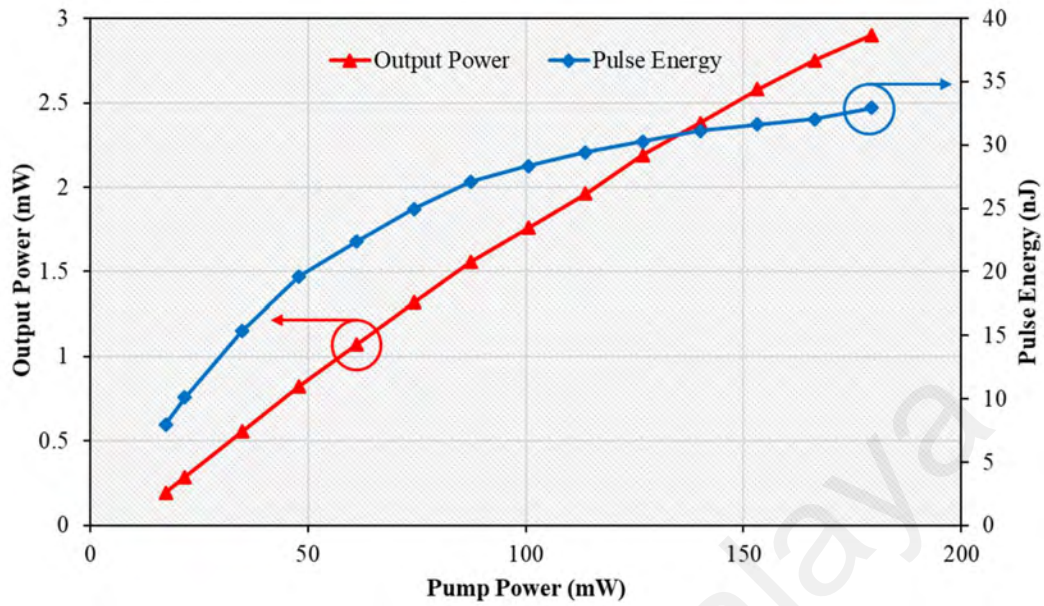


Figure 3.20: Output power and pulse energy analysis of the Q-switched laser at various pump power

The RF spectrum of the Q-switched pulse train was investigated, and the result is shown in Figure 3.21 at a pump power of 179.5 mW. The fundamental RF peaked at 88.11 kHz, corresponding to a width of 4.25 μ s with SNR of 57.42 dB. The inset figure shows the RF spectrum at a wider frequency range, which indicates the stability of the pulse. These results indicate the potentiality of gold thin-film in pulse generation and saturable absorption in appropriate laser application. The fabrication cost of pure gold SA is low, due to the simplicity of the fabrication process, hence reducing the cost of the laser itself. The simple and low-cost laser is applicable in applications such as environmental sensing and biomedical diagnostics.

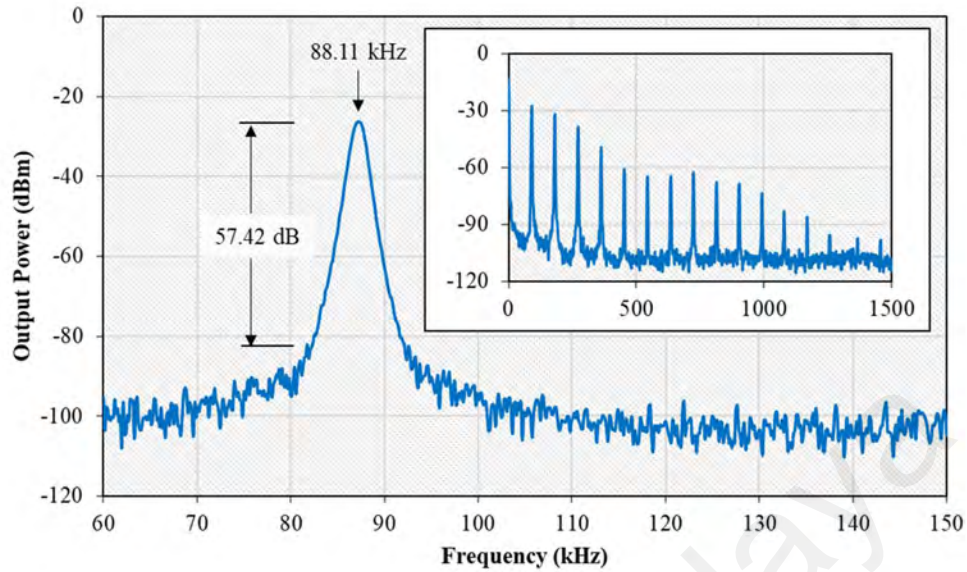


Figure 3.21: Frequency plot of the Q-switched laser at maximum pump power

3.6 Q-switched Fibre Laser operating at 2-micron Region

In this work, the fabricated pure gold SA was also incorporated into a laser cavity with thulium-doped fibre (TDF) as a gain medium. Figure 3.22 illustrates a ring cavity laser configuration, which employed a fibre laser operating at 1552 nm as a pump power source. The pump source is a homemade erbium/ytterbium co-doped fibre laser with the maximum output power of 1W, which was fabricated based on a cladding-pumping method. The cavity also consists of 1550/2000 nm wavelength division multiplexer (WDM), 5-meter-long TDF and 10 dB optical coupler. The TDF used has a numerical aperture (NA) of 0.15 with core and cladding diameter of 9 μm and 125 μm respectively. The peak core absorption of the fibre was around 9.3 dB/m at 1180 nm and 27 dB/m at 793 nm. The 10-dB optical coupler was used to split out 90% and 10% of laser to the cavity and output port respectively. The 7 GHz bandwidth InGaAs photodetector (PD: EOT ET-5010F) with rise and fall time of 28 ps was used to convert the laser output into an electrical signal via 10% output coupler. The PD was used with 500 MHz digital

oscilloscope (OSC: LeCroy Wavejey 352A) to record the laser output temporal behaviour. The 7.8 GHz RF spectrum analyser (RFSA) was used to display the output pulses in frequency domain.

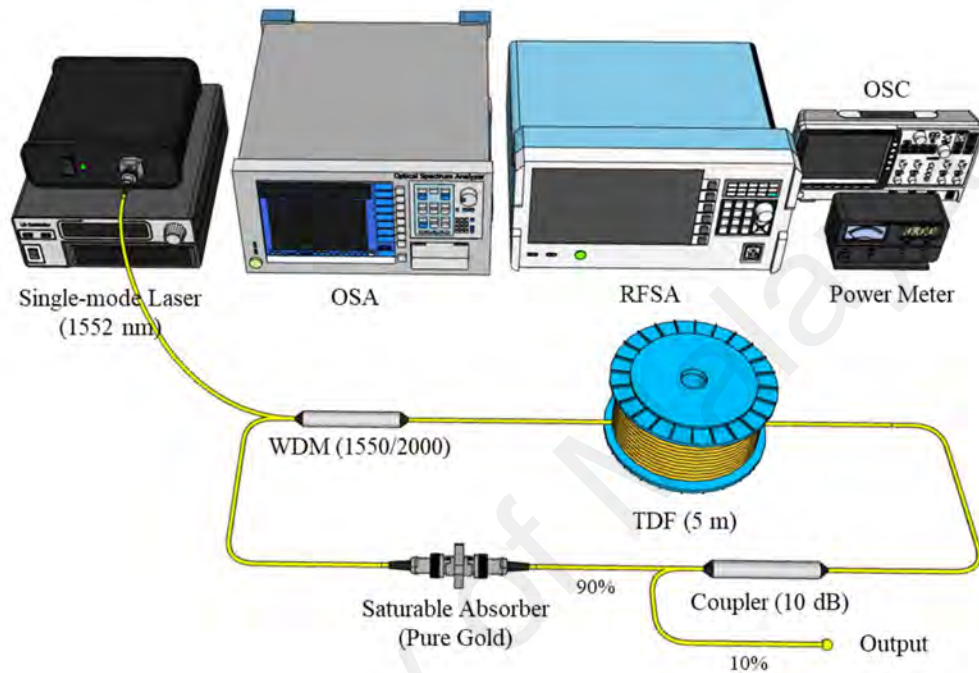


Figure 3.22: Ring laser configuration for 2- μm operation with pure gold SA

The output laser spectrum was recorded in absence of pure gold SA inside the cavity by using the optical spectrum analyser (OSA: Yokogawa AQ6375) with a resolution of 0.05 nm and the result is shown in Figure 3.23. The laser operated at centre wavelength of 1969 nm with spectral bandwidth of 1.52 nm which confirms the cavity works accordingly. As the sample of gold thin-film approximately 1 mm x 1 mm was sandwiched between two fibre ferrules and incorporated into the cavity, laser spectrum shifted to slightly shorter wavelength to operate at centre wavelength of 1949 nm as depicted in the figure. This blue shift phenomenon occurs due to the insertion loss introduced by the pure gold SA. To compensate for this loss, laser wavelength tends to

operate at a slightly higher gain as in this case towards the 1949 nm wavelength as the pump power raised to the Q-switching threshold 343.13 mW. Inset of the figure showed the enlarge peak lasing centred at 1949 nm having an optical signal-to-noise ratio (OSNR) and 3-dB bandwidth of 33.95 dB and 4.44 nm respectively. Broaden linewidth from 1.52 nm in continuous wave to 4.44 nm in Q-switching mode was observed mainly due to the self-phase modulation (SPM) effect in the laser cavity.

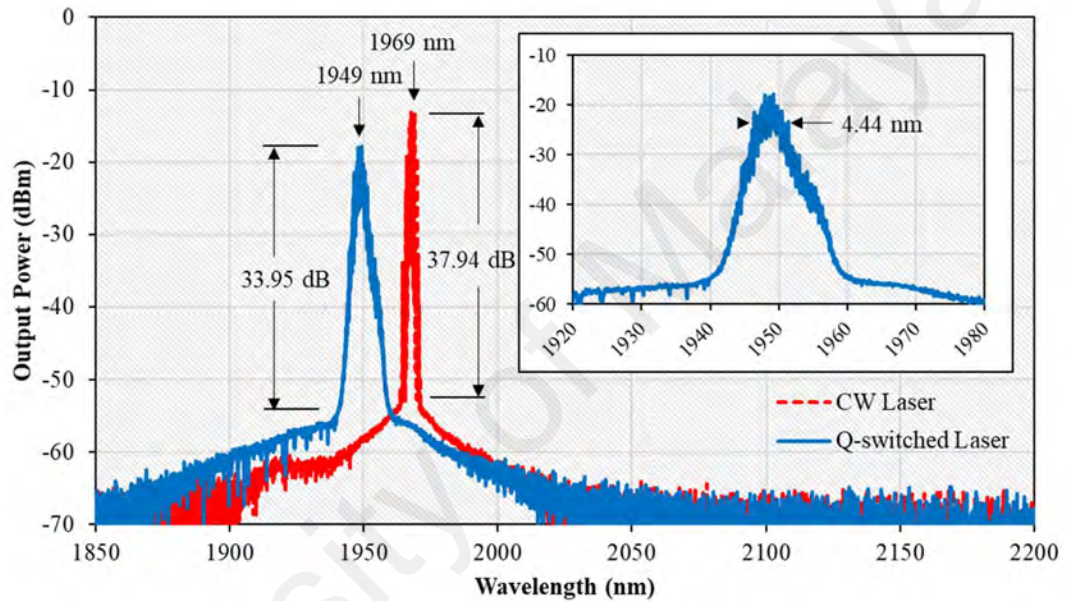


Figure 3.23: Optical spectra of the Q-switched and CW laser at pump power of 343.13 mW

The observation on the temporal performances of the Q-switching regime were conducted in time- and frequency-domain. Figure 3.24 shows the relation of repetition rate and pulse width as a function of pump power, which were obtained from the oscilloscope train of Q-switched laser incorporating pure gold SA as a Q-switcher device. Repetition rate of the pulse depends on the stored energy, which varies by the pump power. The pulse train were observed ranged from 11.70 kHz to 21.95 kHz as the pump

power varied from 343.1 mW to 467.3 mW. The pulse width, on the other hand, shrunk from 4.96 μs to 2.60 μs with the variation of pump power within the same range.

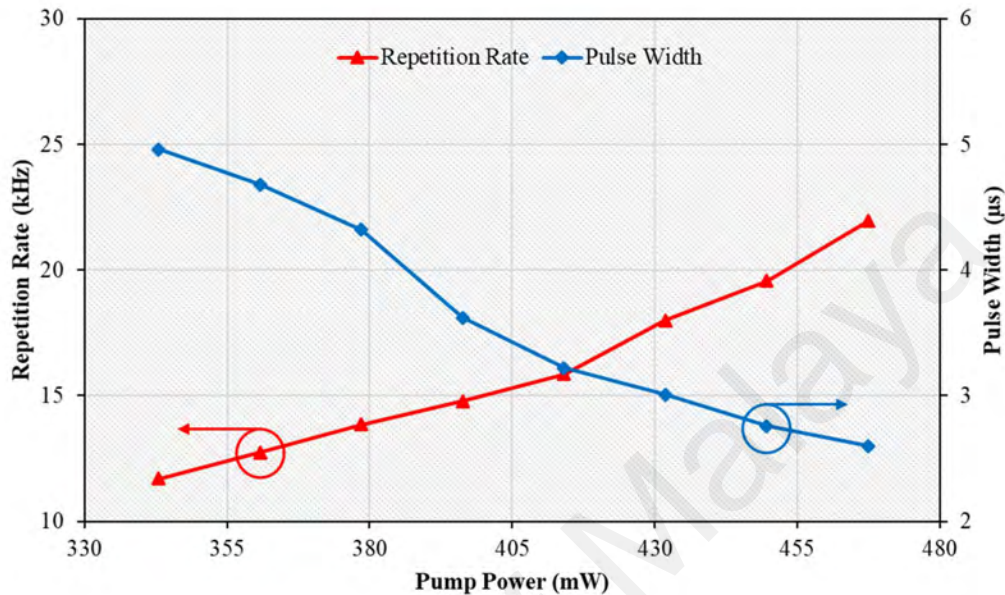


Figure 3.24: Repetition rate and pulse width analysis of the Q-switched laser at various pump power

The typical pulse trains of the pure gold SA Q-switched laser at the pump powers of 343.1 mW, 414.1mW and 467.3 mW are illustrated in Figure 3.25. They indicate the durations of 87.47 μs , 63.05 μs , and 45.56 μs , which correspond to a pulse repetition rate of 11.7 kHz, 15.9 kHz and 21.95 kHz respectively, without noticeable timing jitter. The corresponding pulse widths were approximately 4.95 μs , 3.22 μs and 2.60 μs at the pump powers of 343.1 mW, 414.1mW and 467.3 mW respectively. These values are comparable to the values obtained by other SAs. The maximum operation limit of 21.95 kHz at 467.3 mW pump specifies that the fabricated gold thin-film saturates at higher power illumination. This makes the pulses unstable and diminished beyond 467.3 mW pump power. However, it is worth to mention that when the pump power is decreased after the pulse disappearance, the stable Q-switched could be obtained again. This

indicates that the optical damage threshold of gold thin-film is higher than the maximum available pump power of 1W. The stability of the Q-switched laser was also monitored over 20 hours with little fluctuations in laser performance.

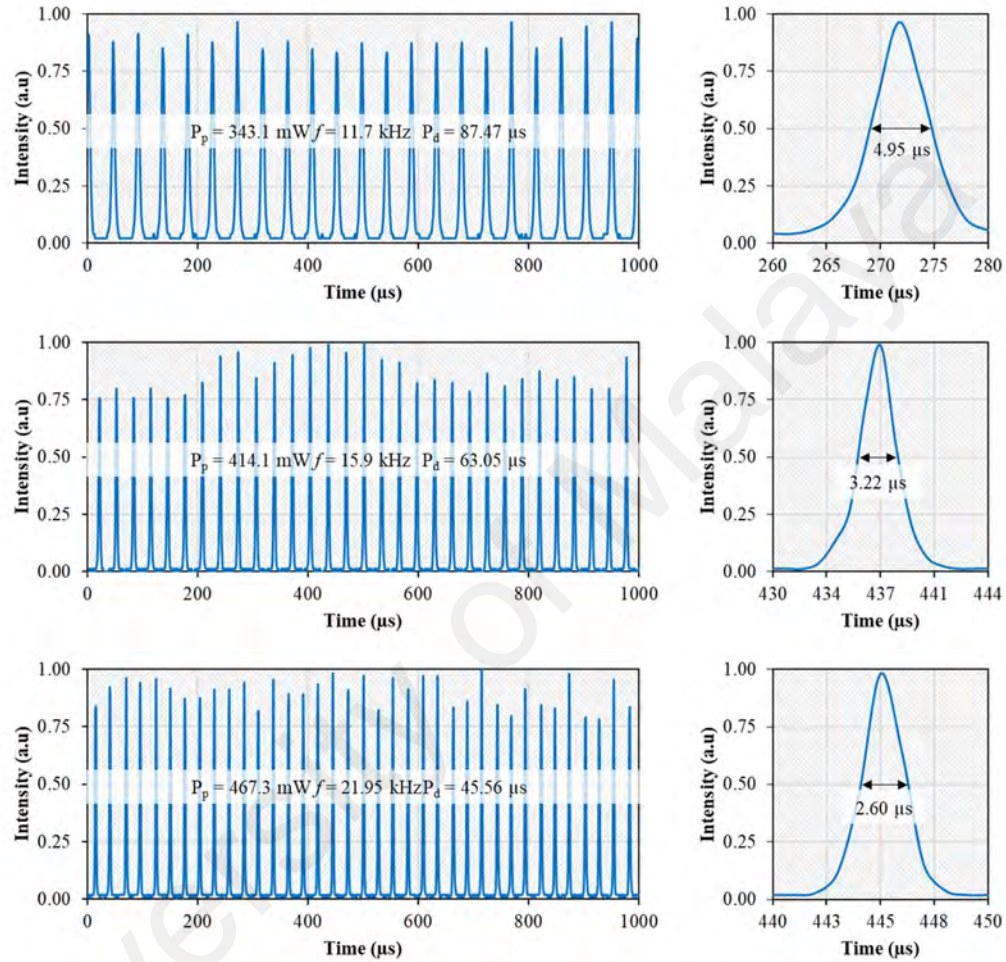


Figure 3.25: Typical pulse train of the Q-switched laser at threshold, median, and maximum pump power

The temporal characteristics of the Q-switched laser shows amplitude instabilities as can also be seen in the Figure 3.25. This pulse-to-pulse amplitude fluctuation of the self-Q-switched pulse train is found to be about 40%. The fluctuation is due to the slight variation of pump power. However, the pure gold SA manages to work on this 2-micron region. To verify that the gold film was responsible for the Q-switched pulse generation,

the film was removed from the cavity. In this case, no Q-switched pulses was visible on the oscilloscope at any pump powers. The laser operation was also tested with non-coated PVA film in the cavity instead of gold film SA, as a result, no trace of pulsing behaviour was present within the pump power range. This confirms that the Q-switched operation was attributed to the SA. The pulse width is expected to be further narrowed by optimizing the laser cavity length, reducing the intra-cavity loss such as improving the splicing point, and enhancing the pump power. Since only a thin layer of gold was employed as the SA, it is expected that the polarization dependent absorption effect is very small and negligible.

The relation of the power and pulse energy of the Q-switched laser with the variation of pump power were also investigated. The results are plotted in Figure 3.26, where both average output power and pulse energy increased with the input pump increment. Output power varied from 0.845 mW to 1.971 mW with 0.91% slope efficiency as the 1552 nm pump power increased from 343.1 to 467.3 mW. On the other hand, the pulse energy increased from 72.2 nJ to 92.8 nJ as the input pump power increases from 343.1 to 431.8 mW. Beyond the input power of 431.8 mW, pulse energy dropped from maximum achievable value of 92.8 nJ to 89.8 nJ. This related to the slightly higher repetition rate increment compared to the average output power leads to a more energy distribution. Since the pulse energy is determined by the gain fibre and pumping strength, under higher pumping strength, pulse train became unstable and amplitude fluctuation appeared before it completely diminished. Therefore, material with high magnitude of saturation intensity is required to allow the SA bleaching at very high energy level, thus produce higher pulse energy. Along in the figure, the peak power against the pump power is plotted. It indicates that peak power varied from 14.56 mW to 34.536 mW as pump power varied from 343.1 to 467.3 mW.

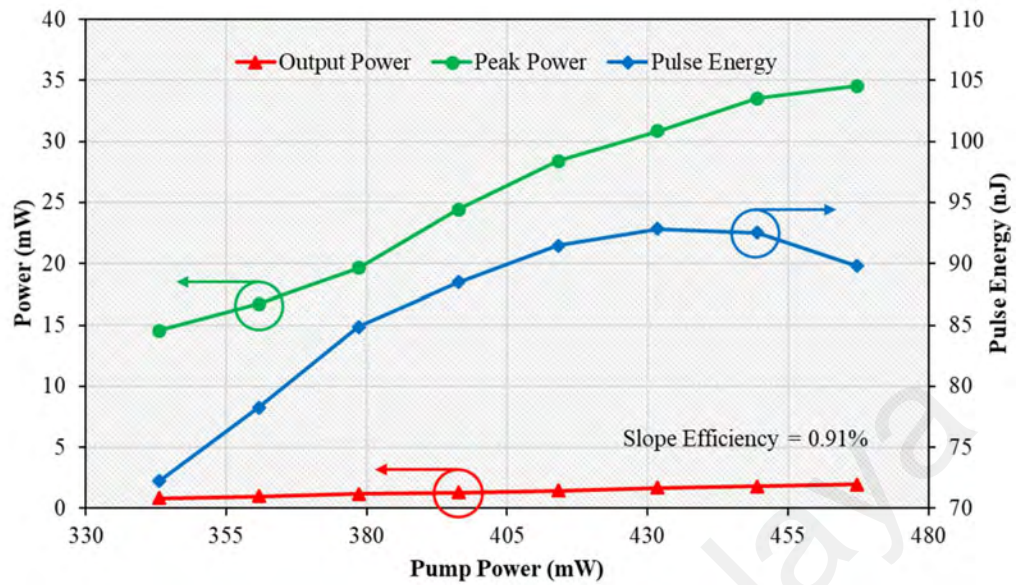


Figure 3.26: Power and energy analysis of the Q-switched laser at various pump power

Figure 3.27 shows the corresponding RF spectrum at the maximum pump power of 467.3 mW, which was obtained within 600 kHz span. As illustrated in the figure, the fundamental repetition rate of the laser is 21.95 kHz which agrees with the pulse duration of 45.56 μ s measured in Figure 3.25. The SNR of the fundamental mode in RF spectrum was obtained at 28.9 dB while the harmonic peaks were observed to gradually decrease until more than 15th harmonic, before it was disappeared. This indicates that the Q-switching operation has a broad pulse width (micro-seconds) and the frequency domain transformation is corresponded to its time-domain. This SNR value was below than 30 dB, which clearly indicates the less stability of the Q-switching pulses generation and this result agreed well with the oscilloscope trace.

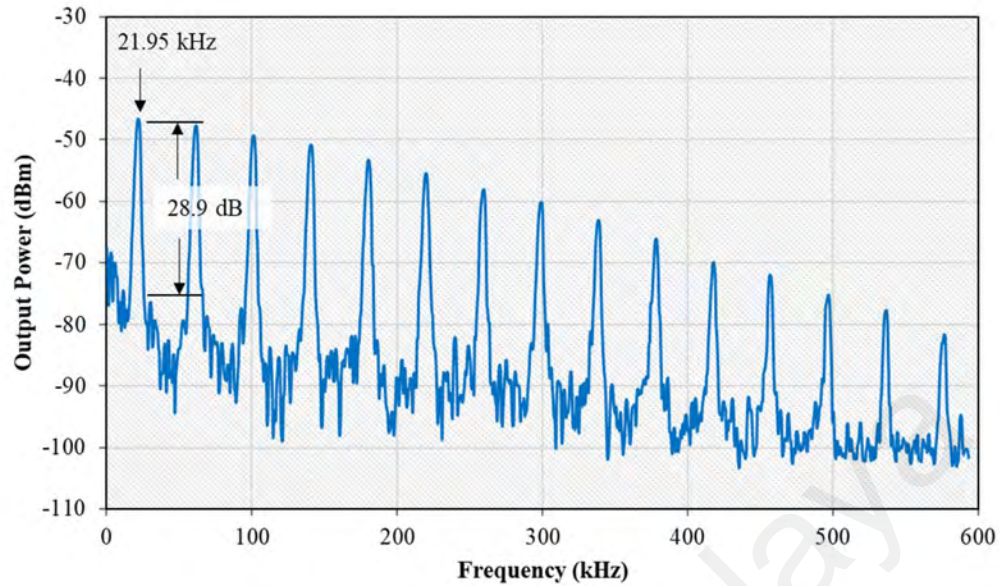


Figure 3.27: Frequency plot of the Q-switched laser at maximum pump power

3.7 Summary

The generations of Q-switching pulses train in 1-, 1.55-, and 2-micron regions have been successfully demonstrated using a pure gold thin-film as SA. The gold SA was fabricated using electron beam deposition technique onto a PVA thin film. Then, the thin-film was cut into 1×1 mm piece and inserted between two fibre ferrules so that it can be integrated into various ring laser cavities. At first, the SA device is incorporated into the YDFL cavity. The YDFL generates Q-switching pulses train as the pump power is increased beyond 61.1 mW. The laser operates at 1063.5 nm with the maximum repetition rate of 61.88 kHz and the thinnest pulse width of 4.23 μ s are recorded at the 87.4 mW pump power. The output power increases linearly up to 3.14 mW, while the pulse energy varies from 10.55 nJ to 50.74 nJ as a pump power increased. Meanwhile, the maximum peak power of 12 mW is obtained at the pump power of 87.4 mW. In an EDFL cavity, the laser generates a Q-switching pulse at 1560.0 nm with a tuneable repetition rate from 24.34 kHz to 88.11 kHz. The pulse tuned to a maximum input pump power of 179.5 mW

produced a pulse width and pulse energy of 4.25 μs and 32.91 nJ, respectively. A stable Q-switched TDFL has also been successfully demonstrated based on ring cavity by incorporating the pure gold SA. The proposed laser generates Q-switching pulses train as the pump power is increased beyond 343.1 mW. The laser operates at 1949 nm with the maximum repetition rate of 21.95 kHz and the thinnest pulse width of 2.60 μs are recorded at the 467.3 mW pump power. The output power increases linearly up to 1.971 mW, while the pulse energy varies from 7.2 nJ to 92.8 nJ as a pump power increased. This finding shows that pure gold shows promising performance in generating Q-switching pulse in a wide wavelength region ranging from 1 to 2 μm .

CHAPTER 4: ELECTRON BEAM DEPOSITED SILVER SATURABLE ABSORBER AS PASSIVE Q-SWITCHER IN 1.55- AND 2-MICRON FIBRE LASERS

4.1 Introduction

As discussed in the previous chapters, the passively Q-switched pulsed lasers have been widely studied and demonstrated due to their advantages in terms of compactness, simplicity, and easy implementation. In addition, they have potential applications in many areas ranging from medical, material processing, communication to sensing. On the other hand, noble metals, such as gold (Au), copper (Cu), and platinum (Pt) have also drawn great attentions for various photonics applications, due to their fascinating optical features, especially in nanoparticles form. The most highlighted features are a large third-order nonlinearity, broad absorption governed by localized surface plasmon resonance (SPR), and fast response times of a few picoseconds.

In the previous chapter, the Q-switched pulse generations were demonstrated using a pure gold as saturable absorber (SA) in three different laser cavities; ytterbium-, erbium- and thulium-doped fibre laser, which operates in 1-, 1.55-, and 2-micron region, respectively. Several works have been reported on the pulses generation in erbium-doped fibre laser (EDFL) cavity using pure silver as SA. For instance, Guo et al. demonstrated a self-started Q-switched laser operating at wavelength of 1564.5 nm. The SA was prepared using solvothermal reduction method and the laser has produced Q-switched pulses with repetition rate of 58.5 kHz, pulse width of 2.4 μ s and pulse energy of 132 nJ at the pump power of 139 mW. The modulation depth of 18.5% was recorded, indicates that silver has potential to perform as SA.

In this chapter, various Q-switched fibre lasers operating in 2.0- and 1.55-micron wavelength region are demonstrated using a pure silver thin-film as SA. The silver SA

broad absorption was governed by localized surface plasmon resonance (SPR) effect. The silver SA was produced by electron beam deposition method with polymer as the host material. This technique able to produce an accurate and homogenous distribution of silver layer throughout the surface of the SA. The SA is integrated into two different ring fibre laser configurations operating at eye-safe, 2-micron region and 1.55-micron region, widely known as C-band. The 2-micron spectral region has attracted interest among researchers in recent year especially in application of light detection and ranging (LiDAR), medical surgery, defence technology, and free-space communication. The laser in this region can be achieved by utilizing the ion transition of thulium. The thulium-doped fibre (TDF) used in this chapter is forward pumped by 1550 nm laser source to excite ions from 3F_4 state to 3H_6 . The energy released from ions emits high intensity photon with wavelength of 2-micron. The 2-micron laser is also transmissive in air and absorbable in organic tissues. On the other hand, the 1.55-micron laser can be achieved by pumping an erbium-doped fibre (EDF) with 980 nm pump. This EDF lasers has widely known from its performance in telecommunication application.

4.2 Fabrication and Characterization Process of Silver Thin-Film

The pristine polyvinyl alcohol (PVA) thin-film was used as a host polymer owing to its low optical absorption at the laser operating wavelength. In addition, it is robust, flexible and can be simply integrated in between fibre ferrules. In preparing PVA film, 1 gram of PVA powder was mixed into 120 ml of de-ionized (DI) water. The mixture was stirred at temperature of 145 °C until the powder dissolve completely. Subsequently, 5 ml of PVA solution was poured and left dry in a petri dish under room temperature for 3 days. The PVA thin-film with a thickness of about 30 μm was then coated with silver using electron beam (E-beam) deposition technique as illustrated in Figure 4.1 (a).

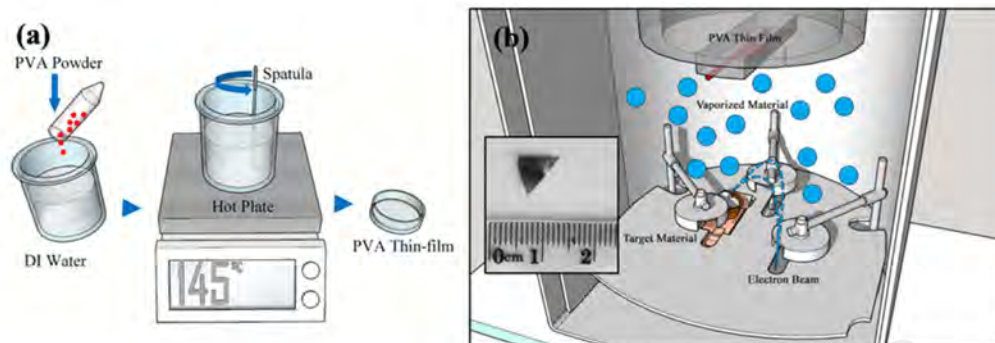


Figure 4.1: (a) PVA thin-film fabrication process (b) Depositing of silver onto PVA thin-film using E-beam deposition method. Inset shows the real image of the fabricate SA film

The depositing process is started by placing the prepared PVA thin-film in the upper part of the vacuum chamber as shown in Figure 4.1(b). This silver coating involves two main processes; vacuum and deposition process. Vacuum process works as preliminary process, to generate pressure inside the deposition chamber to form a full vacuum condition. At this condition, electrons can freely propagate in the chamber, allowing it to strike the target material. When the chamber reaches the pressure level of 1×10^{-4} mbar or lower, deposition process starts. It begins by supplying the tungsten filament with current flow to generate electrons. These electrons hit the target material and transforms the atoms from the target material into a vapor state. At desired deposition rate (thickness / time), the shutter is open to achieve an approximately 16 nm thickness of silver coating. Inset of Figure 4.1(b) shows the transparent PVA thin-film, which was turned into silver colour film after the completion of the process. The fabricated SA was then sealed in a vacuum bag to prevent silver oxidation.

The silver SA was analysed using energy-dispersive x-ray (EDX) as shown in Figure 4.2 (a). The substance composition of silver (Ag) was peak at approximately 3

KeV, with additional substance of carbon (C) and oxygen (O) presence in the analysis. The dominant combination of C and O substances are originated from PVA thin-film $(C_2H_4O)_n$, with Ag consists of 32.06 Wt% in total composition. It is also shown in Figure 4.2(b), field emission scanning electron microscope (FESEM) image of homogenous distribution of Ag throughout the PVA thin-film surface.

Figure 4.3 (a) shows a linear absorption spectrum of the silver SA which indicates the absorption loss of about 2.2 dB at 1550 nm and 1.6 dB at 2000 nm. The linear spectrum achieved by analysing absorption properties of silver SA using a broadband white light source. Due to the surface plasmonic resonance, silver provides a broadband linear absorption band covering both 1.5 and 2.0 μm wavelength regions. Based on the linear absorption range of the silver thin-film, the SA is expected to work in both 1.5- and 2-micron wavelength regions. The SA also been tested using balanced twin-detector measurement technique to analyse the nonlinear absorption properties as seen in Figure 4.3 (b). This technique was completed by directing a picosecond mode locked EDFL on the SA and the absorption of silver is decreasing when intensity increases. This is due to reflectivity of the silver itself, which is the highest among all other materials. The saturable absorption and saturable intensity obtained are 2% and 700 kW/cm^2 at 1.5-micron, respectively. The low modulation depth is due to low thickness of silver coating. This allow more photon transmission through the saturable absorber, reducing the scattering loss generated by it. The fundamental of localized surface plasmon resonance (SPR) able the pulsing to produce inside the cavity. The nonlinear analysis for 2-micron was unable to complete due to limitation of equipment availability. The value was stated to show that even low modulation depth able to produce pulse in pure metals.

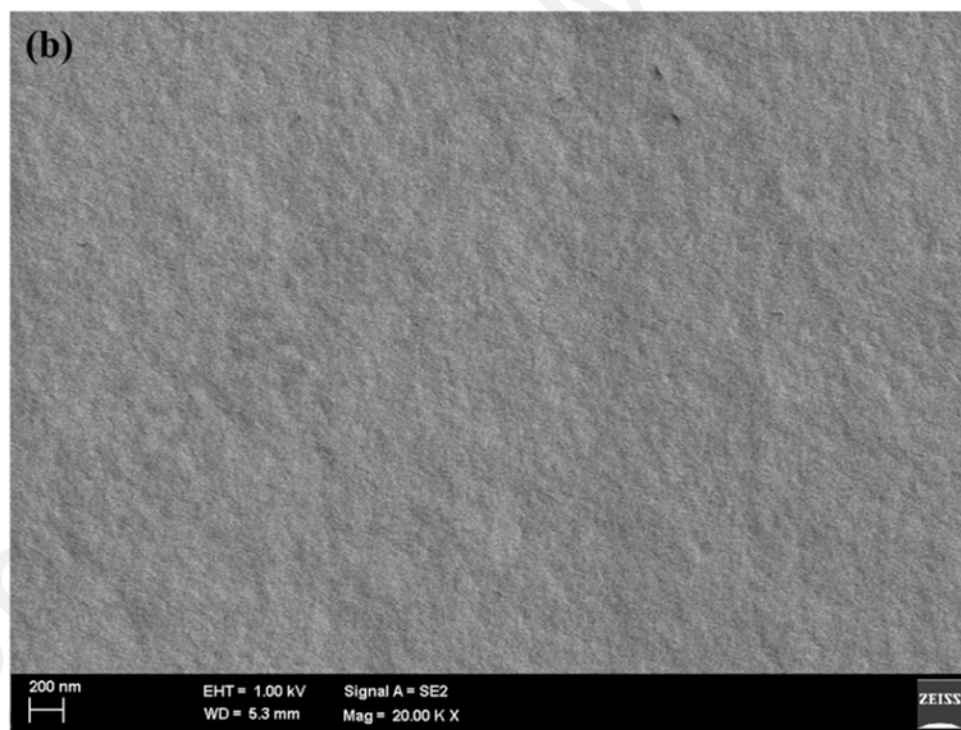
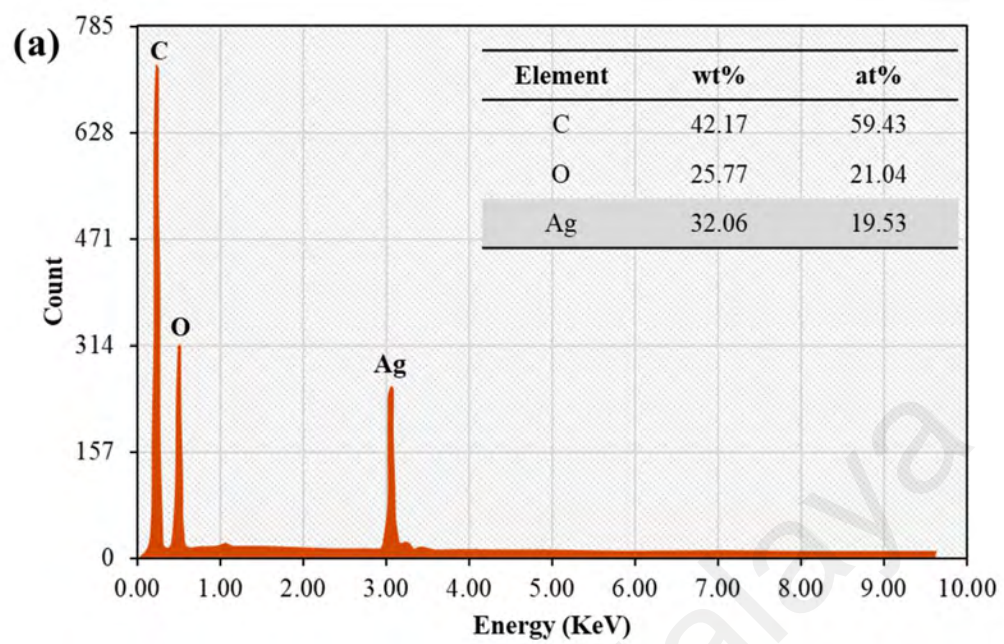


Figure 4.2: (a) EDX analysis and (b) FESEM image of the silver SA

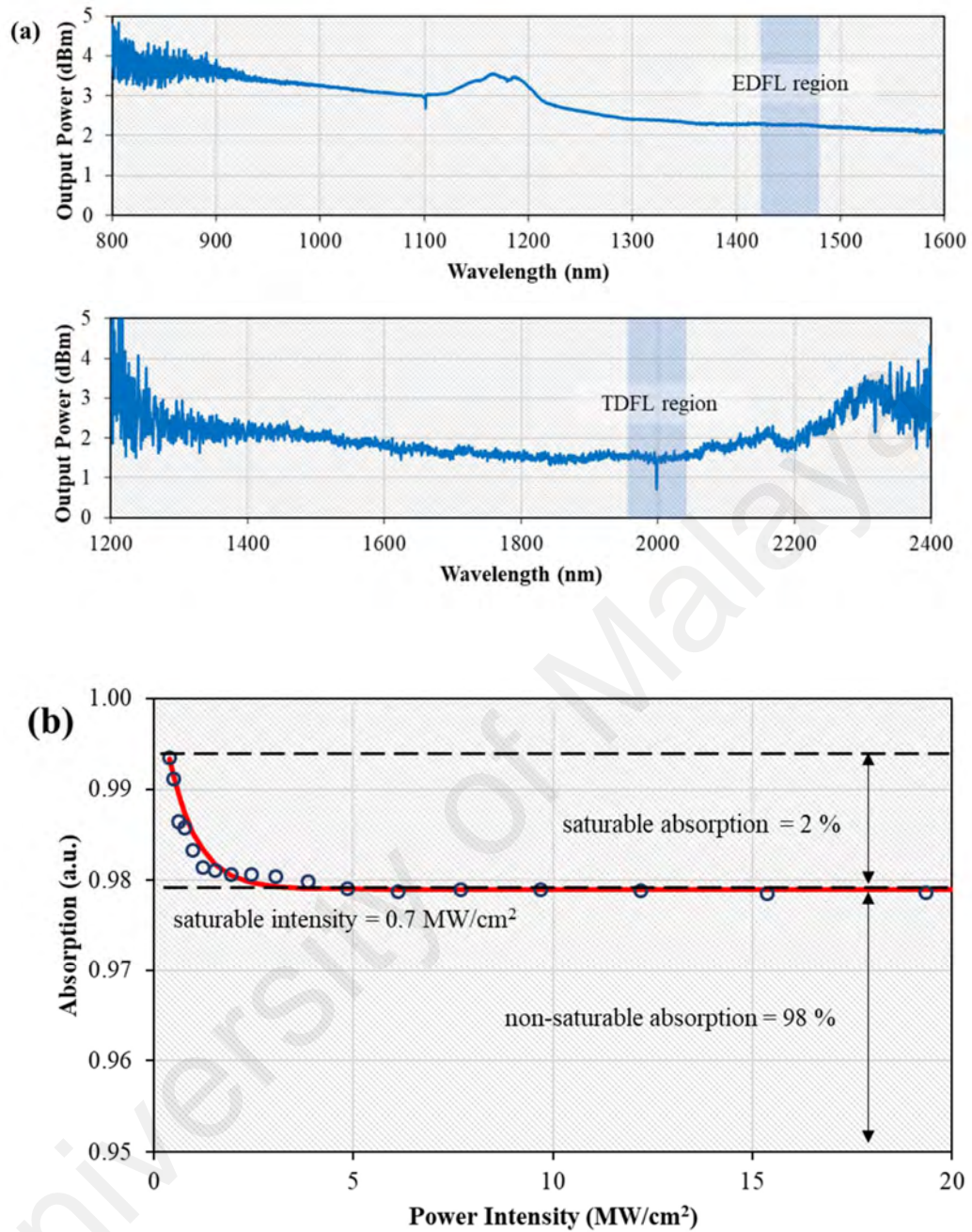


Figure 4.3: (a) Linear and (b) nonlinear absorption characteristics of the silver SA

4.3 Q-switched Thulium-doped Fibre Laser operating at 2-micron Region

4.3.1 Laser Configuration

Firstly, the fabricated silver SA was incorporated into a ring configuration of thulium doped fibre laser (TDFL) as shown in Figure 4.4. The proposed laser cavity utilizing a 5-metre long of thulium-doped fibre (TDF) as an active gain medium. The TDF was forward pumped by a single-mode, 1550 nm laser source via a 1550/2000 nm wavelength division multiplexer (WDM). The TDF has a numerical aperture (NA) of 0.15, with peak core absorption of the fibre was around 9.3 dB/m at 1180 nm and 27 dB/m at 793 nm. The core and cladding diameter of the fibre are 9 μm and 125 μm respectively. The silver SA thin-film approximately 1×1 mm in size was employed by sandwiching it between two fibre ferrules. The insertion loss generated by the SA was measured to be around 4.5 dB. A 10-dB coupler was used to extract 10 % output while keeping the rest inside the laser cavity. The temporal characteristic was realized by using a 500 MHz Digital Oscilloscope (OSC: LeCroy Wavejey 352A) and a 7.8 GHz radio frequency spectrum analyser (RFSA: Anritsu MS2683A), via a 7 GHz InGaAs photodetector (PD: EOT ET-5010 F) with rise and fall time of 28 ps. The spectral analysis was done using an optical spectrum analyser (OSA: Yokogawa AQ6375) with a resolution of 0.05 nm. A broadband power meter with thermal detector was used to observe the average output power.

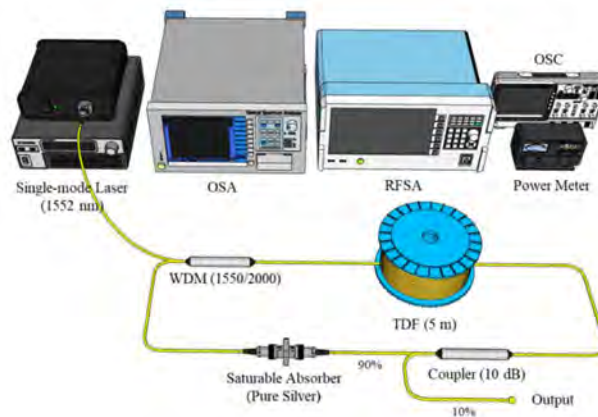


Figure 4.4: Configuration of the Q-switched TDFL with pure silver thin-film as SA

4.3.2 Q-switching Performance

The TDFL begins to produce a stable Q-switching pulse as it reaches the threshold pump power of 338 mW. The pulse can further observe up to pump power of 498 mW. At pump power beyond 500 mW, the silver thin-film reaches an over-saturated condition causing pulse to distort. The unstable pulse remains available until the pump power exceed 700 mW where it completely disappears. As soon as the pump power back at 498 mW, the pulse is recovered. The thin-film was left inside the cavity for 3 straight hours and the pulse remains, showing film capabilities to operates at long run. The thin-film was then removed from the cavity and the output shows no pulse generation, proving the pulse was induced by the introduction of silver thin-film.

The Q-switched phenomenon happens when the energy cumulated inside the cavity reaches a certain saturable stage, depending on SA. It can be achieved when all conduction state of the SA is occupied with electrons, excited by the photons. Figure 4.5 shows the temporal performance of Q-switched pulse taken at threshold (338 mW) and maximum (498 mW) pump powers. As shown, pulse become thinner at higher pump power with inclining of repetition rate, which is a fundamental of Q-switching characteristic. The downward spike can be observed due to high birefringence effect of silver towards 2-micron laser. At maximum applicable pump power, the pulse width recorded is 4.82 μs with repetition rate of 28.33 kHz. The pulse duration was measured to be around 35.30 μs , consistent with the value of repetition rate. The pulse was observed in frequency domain as illustrated in Figure 4.6. As seen, there are 16 dominant harmonics lining up over 600 kHz span. The fundamental peak is located at 28.33 kHz, with signal-to-noise ratio (SNR) of 32.51 dB. The fundamental peak location is based on the repetition rate of the pulse, while SNR is measured from the peak to pedestal to determine the stability of the pulse.

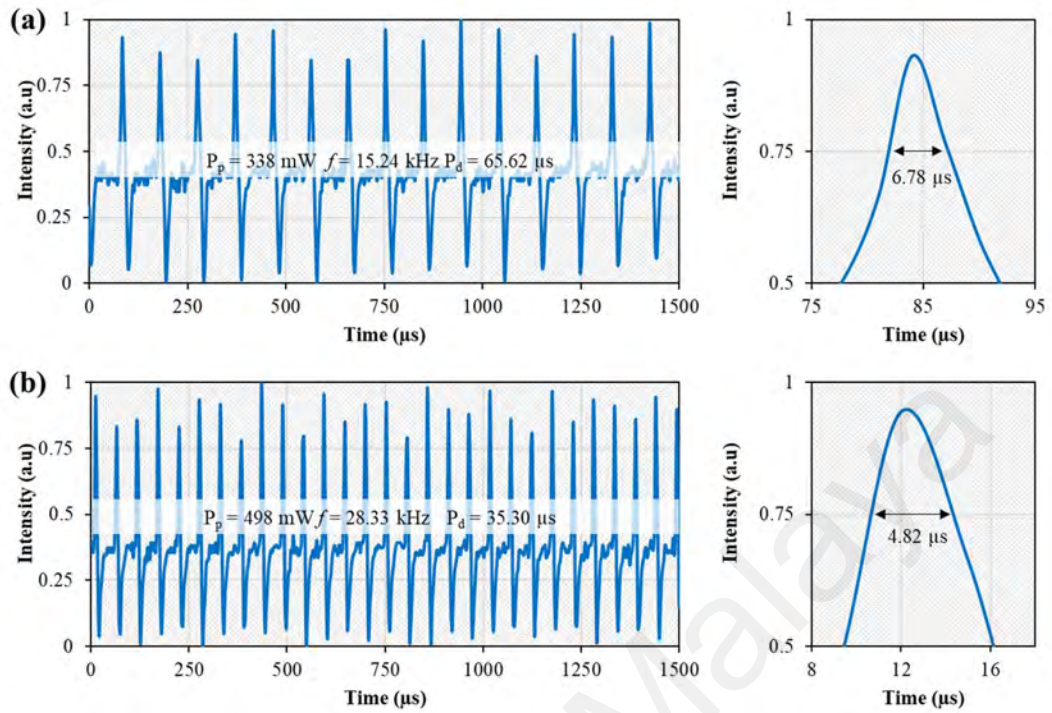


Figure 4.5: Temporal characteristics of a typical TDFL pulse train and single pulse envelope at (a) threshold and (b) maximum pump power.

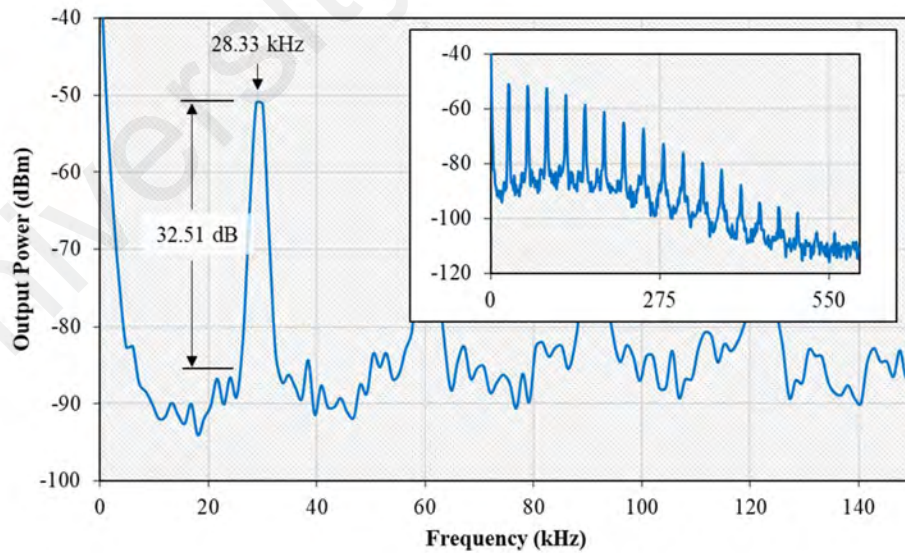


Figure 4.6: RF analysis of the pulse at maximum pump power

The optical spectrum of the Q-switched TDFL in comparison with continuous wave (CW) laser is shown in Figure 4.7. The spectral analysis was taken at threshold pump power of 338 mW. As shown, the CW laser was originated at 1971.51 nm and after thin-film was incorporated into the cavity, the loss generated force the peak to shift to the shorter wavelength of 1928.33 nm. The shifting happens to compensate the loss introduced by SA; thus, it moves to a region where more gain is accumulated. The optical SNR of the Q-switched laser spectrum is approximately 30.72 dB, with full-width at half-maximum (FWHM) of 3.2 nm taken from the width of the spectrum at 3 dB below the peak.

Other performances of the Q-switched TDFL are analysed under various pump power and plotted in Figure 4.8. As seen in Figure 4.8(a), the output power measured to increase linearly from 1.15 mW to 4.58 mW as the pump power increases, accommodating an efficiency of 2.05%. The efficiency can be further improved through cavity optimization. The peak power recorded to escalates from 11.1 mW to 32.2 mW, while the pulse shrinks from 6.78 μ s to 4.82 μ s. The peak inclines significantly compare to the output power due to the shrunken pulse width in Q-switching phenomenon. The pulse energy accumulated in a single pulse is measured to be 75.5 nJ at the threshold, increasing to 161.7 nJ at maximum pump power. The energy is affected by combination of either output power or pulse width. As seen in the beginning of pump increment in Figure 4.8(b), rapid shrunk on pulse width causing the pulse energy in Figure 4.8(a) to increase significantly at pump power 356 mW, proving the effect of pulse width to the energy. The saturable absorption characteristic of silver thin-film has wide potential in various laser applications. Plus, it offers simplicity and flexibility that assuredly will beneficial to users.

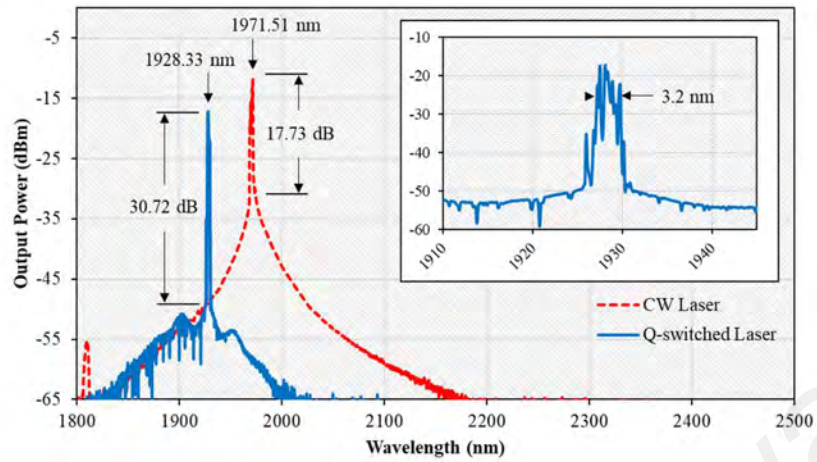


Figure 4.7: Laser spectrum for Q-switched and CW laser operation

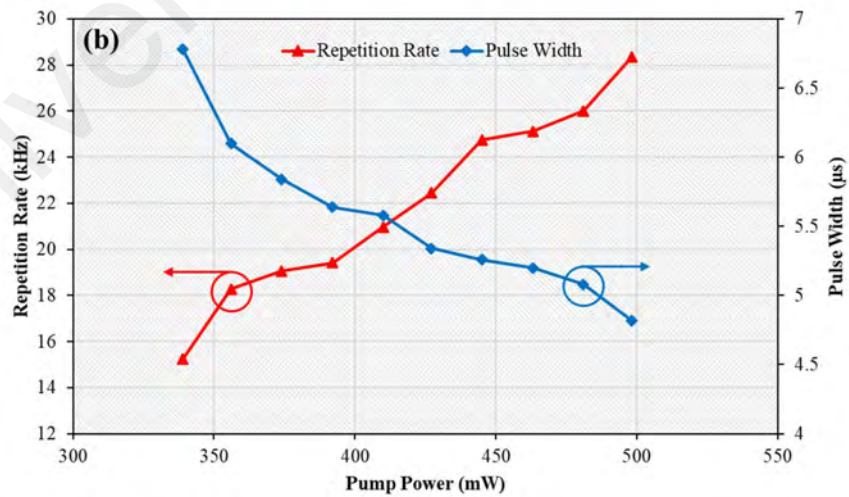
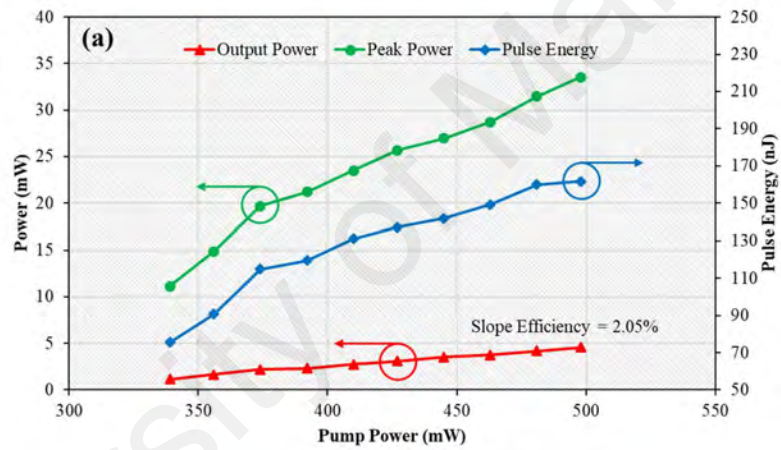


Figure 4.8: TDFL characteristics in variation of pump power (a) power and energy (b) Q-switching phenomenon on changing of pulse width and repetition rate

On the other hand, Table 4.1 compares the laser characteristics of proposed SA with another Q-switched laser operation in 2 μm region. As tabled, the silver SA exhibit decent outcome and comparable Q-switched performance in several attributes. The quality of the pulse can be enhanced by optimization of the laser cavity and the SA itself. The high scattering loss generates by metal-based SA such as silver is expected to decrease by reducing the thickness of both PVA thin-film and silver-coated layer.

Table 4.1: Comparison with recent reports on Q-switched laser at 2-micron wavelength

Ref.	Pump Power (mW)	Max. Output Power (mW)	Wave-length (nm)	Repetition Rate (kHz)	Pulse Width (μs)	Max. Pulse Energy (nJ)
<i>This work</i>	338 – 498	4.6	1928	15.24 – 28.33	4.8 – 6.8	161.7
(Li et al., 2019)	800 – 1500	18.2	1940	52.75 – 100.5	1.9 – 10.0	180.0
(Rusdi et al., 2019)	528 – 711	6.0	1929	6.71 – 19.58	4.2 – 9.2	310.0
(Koo et al., 2019)	95 – 210	1.1	1943	61.00 – 87.00	0.9 – 8.1	14.2

4.4 Q-switched Erbium-doped Fibre Laser operating at 1.55-micron Region

The fabricated silver thin-film was also incorporated into an erbium-doped fibre laser (EDFL) cavity as shown in Figure 4.9. For this setup, a 2.4 metre of erbium-doped fibre (EDF) was used as the gain medium. The erbium ion concentration and NA for the EDF are 2000 ppm and 0.24, respectively. The EDF was forward pumped by a laser source operating at 980 nm wavelength. It was channel into the EDF using a 980/1550 nm WDM. The small piece of the silver thin-film was sandwiched between two ferrules and integrated into the laser cavity. The insertion loss of the SA device was also measured to

be around 4.5 dB at 1.55-micron region. An additional optical isolator was inserted into the EDFL cavity to achieve a unidirectional formation of light propagation, suppress any detrimental effects inside the cavity. A 10-dB coupler was used to extract 10 % output while keeping the rest (90%) to oscillate inside the laser cavity. The temporal characteristic was realized by using a 350 MHz Digital Oscilloscope (OSC: GW Instek, GDS-3352) and a 7.8 GHz RF spectrum analyser (RFSA: Anritsu MS2683A), via a 1.2 GHz InGaAs photodetector (PD: Thorlabs DET101CFC). The spectral analysis was done using an optical spectrum analyser (OSA: Yokogawa AQ6370B) with a resolution of 0.02 nm. A broadband power meter with thermal detector was used to observe the average output power.

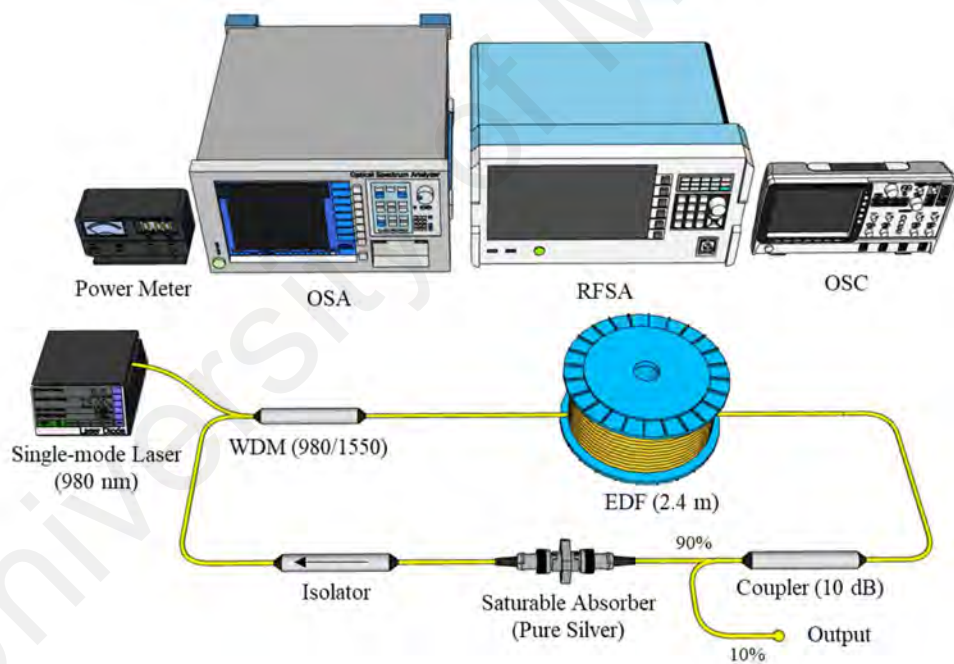


Figure 4.9: Configuration for Q-switched EDFL with silver thin-film

The continuous wave (CW) for EDFL was first generated at threshold pump power of 12.9 mW. Then the laser was transformed to stable Q-switched pulses at the pump power of 21.7 mW where the operation was sustained up to the maximum pump power 200 mW.

The spectral characteristics of the EDFL is shown in Figure 4.10. The optical spectrum of the EDFL indicated that the laser operated at centre wavelength of 1557.59 nm with optical signal-to-noise ratio (OSNR) of approximately 24 dB. The FWHM was about 0.025 nm. In absence of SA, the laser originally centred at 1565.34 nm. The laser was shifted due to compensation of the cavity loss introduced by the SA, as previously explained in section 4.3.

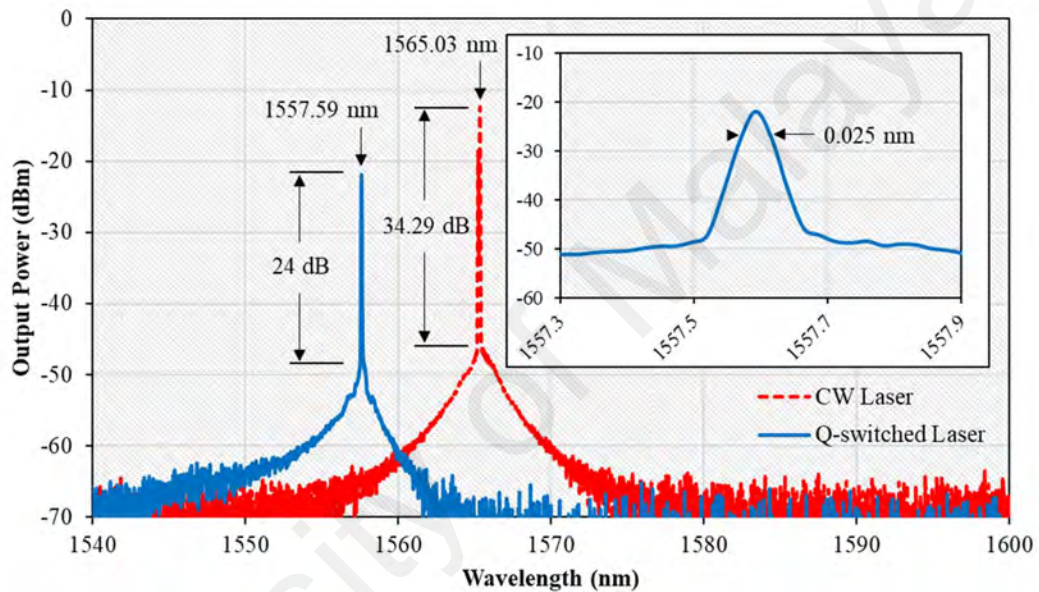


Figure 4.10: Output spectra of the EDFL configured with Q-switching and CW operation

Figure 4.11 shows two sets of pulse train obtained from the Q-switched EDFL at threshold and maximum pump powers of 21.7 mW and 201.4 mW, respectively. From the figures, the full-width half-maximum (FWHM) become narrower as the pump power was increased. This phenomenon demonstrates the typical characteristics of passive Q-switching output. The pulse width is reduced from 14.8 μ s at threshold power of 21.7 mW to 3.1 μ s at maximum pump power of 201.4 mW. Meanwhile, the repetition rate reacted inversely which increased from 27.32 kHz to 148.4 kHz for the same input pump

powers. The repetition rate and pulse width of the Q-switched EDFL changing with the variation of input pump power were investigated. The results are presented graphically in Figure 4.12, where the repetition rate of the Q-switched pulses was observed to monotonically escalate from 27.32 kHz to 148.80 kHz as the input pump power was varied from 21.7 mW to 201.4 mW. Simultaneously, the pulse width decreased from 14.8 μ s to 3.1 μ s. The pulse width is believed to be further reduced by either shortening the laser cavity or improving the film modulation depth characteristics.

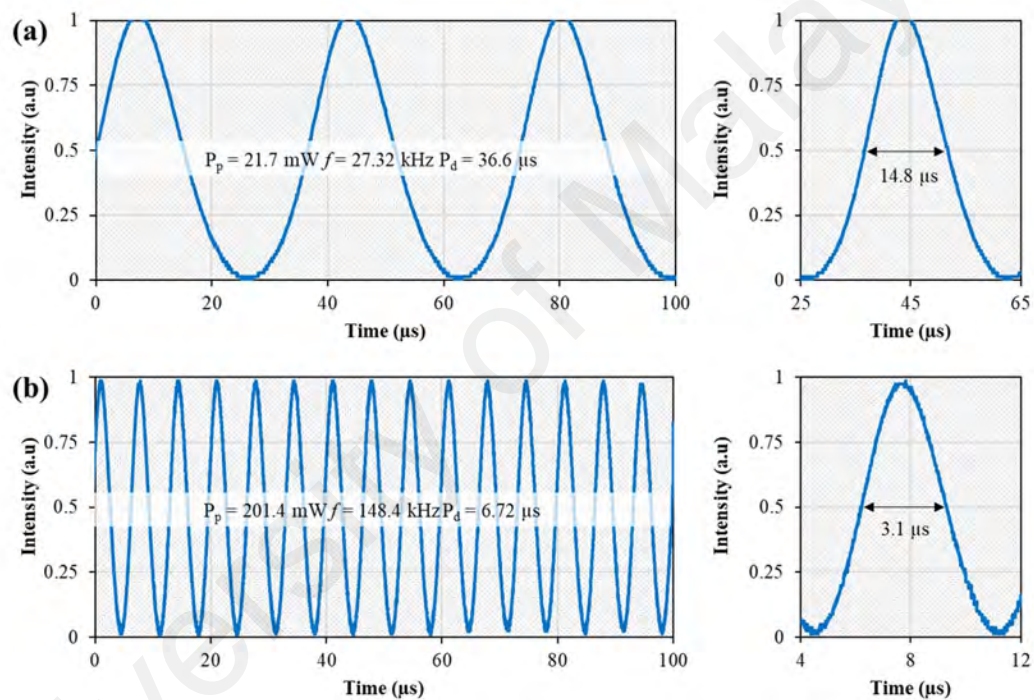


Figure 4.11: Typical pulse train and corresponding single pulse enveloped of the EDFL at (a) threshold and (b) maximum pump power

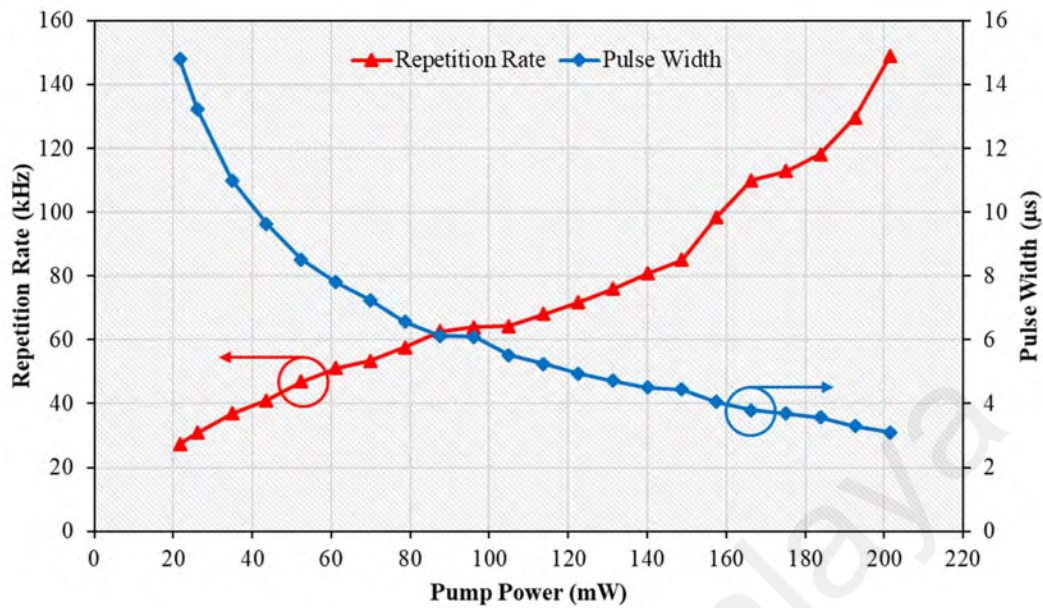


Figure 4.12: Repetition rate and pulse width analysis of the Q-switched laser at various pump power

The output power and single pulse energy varying with the pump power are shown in Figure 4.13. The output power increased from 0.220 mW to 3.821 mW as the input pump power was increased from 21.7 mW to 201.4 mW. The maximum average output power of 3.821 mW was resembled to single pulse energy of 25.68 nJ. Thus, the pulse energy and output power rose constantly due to accumulation of gain released from the increases of input pump power. Figure 4.14 shows the corresponding RF spectrum at input pump power of 201.4 mW, which was acquired within 160 kHz span. As presented in the figure, the fundamental repetition rate of the laser peaked at 148.80 kHz which proved with the pulse duration of 6.7 μs without noticeable timing jitter. The signal-to-noise ratio (SNR) of the RF spectrum was found at 41.57 dB and existence of harmonic peaks gradually decreased until 7th harmonic, and then disappeared. It is worth to mentioning that the Q-switching operation has a broad pulse width (micro-seconds) and the frequency domain transformation was corresponded to its time-domain. As the pump power was increased

above 201.4 mW, the Q-switched operation would vanish, proving that the damage threshold of silver thin-film is close to 201.4 mW.

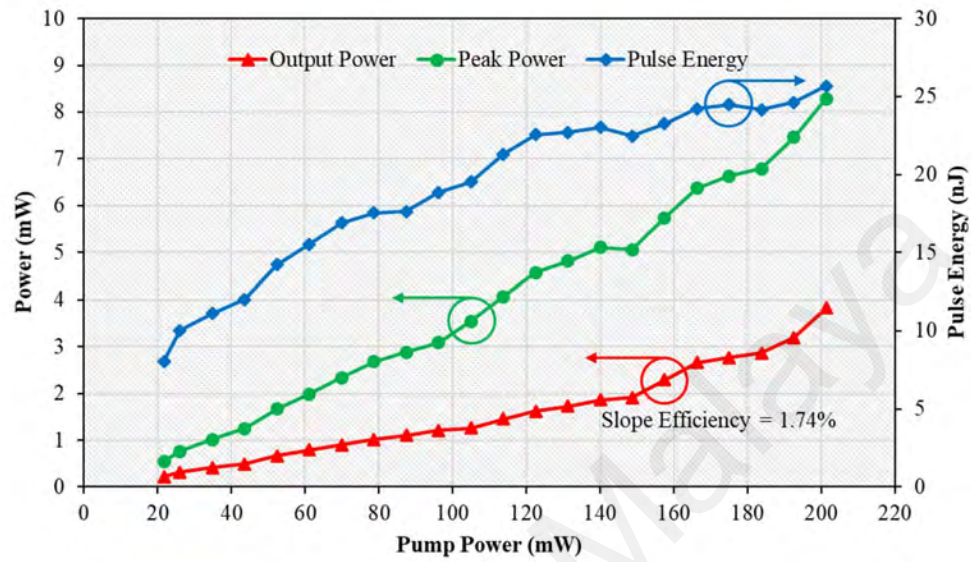


Figure 4.13: Output power and pulse energy analysis of the Q-switched laser at various pump power

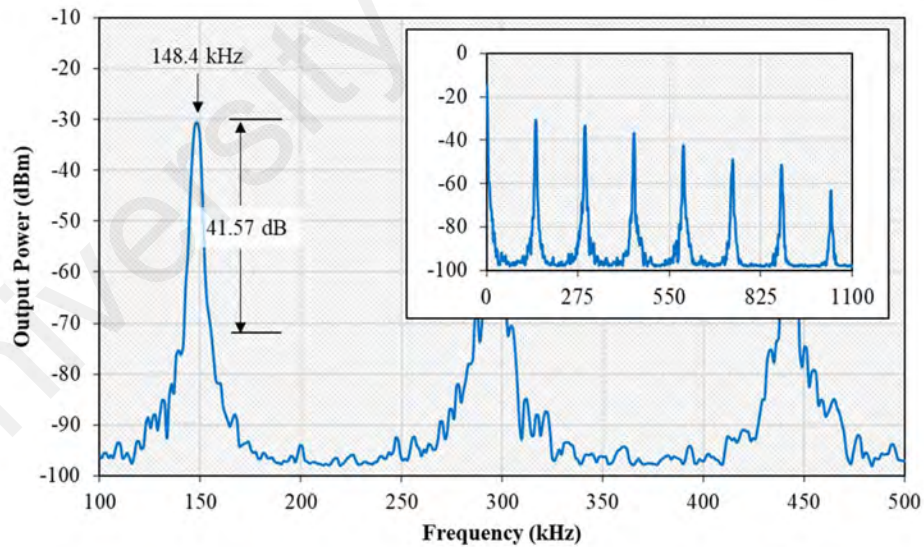


Figure 4.14: RF spectrum analysis of the Q-switched EDFL at maximum pump power

Table 4.2 compares the laser characteristics of proposed SA with another Q-switched laser operation in 1.55-micron region. As shown in the table, the silver SA exhibit decent outcome and comparable Q-switched performance in several attributes. The maximum pulse energy obtained is relatively lower compared to other works. This is most probably due to high SA loss.

Table 4.2: Comparison with recent reports on Q-switched laser at 1.55-micron wavelength

Ref.	Pump Power (mW)	Max. Output Power (mW)	Wave-length (nm)	Repetition Rate (kHz)	Pulse Width (μ s)	Max. Pulse Energy (nJ)
<i>1.5</i>	<i>22 – 201</i>	<i>3.8</i>	<i>1558</i>	<i>27.32 – 148.40</i>	<i>3.1 – 14.8</i>	<i>25.7</i>
(N. A. Siddiq et al., 2019)	32 – 94	2.9	1560	13.70 – 28.65	2.3 – 6.4	100.9
(Salam et al., 2019)	30 – 208	10.7	1560	39.22 – 87.40	3.4 – 9.5	122.6
(Prieto-Cortés et al., 2019)	475 - 1356	220.0	1552	70.00 – 161.30	1.1 – 4.2	1320.0

4.5 Q-switched Erbium-doped Fibre Laser with 1480 nm Pumping Regime

In this section, the passively Q-switched EDFL is demonstrated using the proposed silver thin-film as SA in conjunction with 1480 nm pumping. The experimental setup for the laser is shown in Figure 4.15. The setup is almost similar with the previous work as described in section 4.4 except for the use of 1480 nm laser diode and 95/5 coupler for the pump and output coupler, respectively.

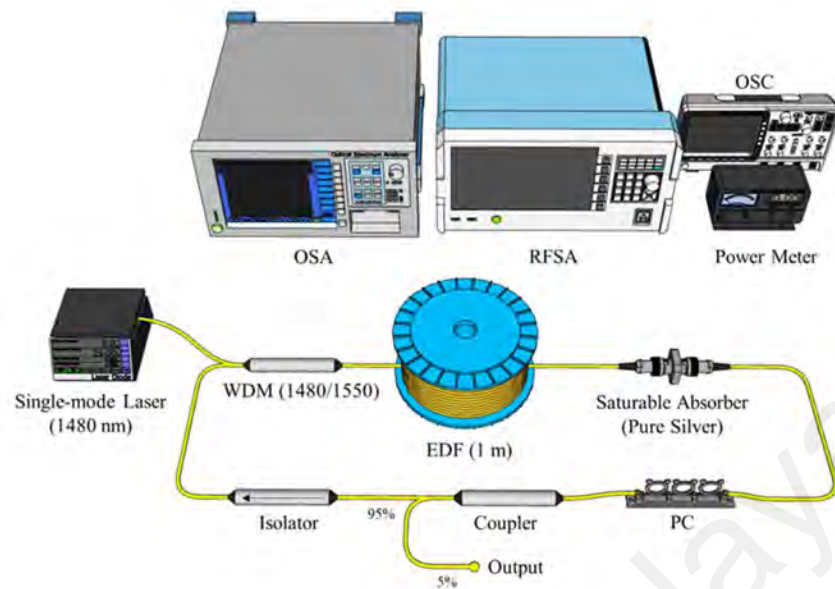


Figure 4.15: Configuration for the silver SA based Q-switched EDFL with 1480 nm pumping

The Q-switched EDFL induced by the silver thin-film was observed at pump power of 45.8 mW and its operation was maintained even when increasing the pump power of up to 133.5 mW. Between the pump power range, the Q-switched pulses appeared steadily, without showing any sign of fluctuation. Beyond this pump power range, the pulse train begins to become unstable and at certain point, diminished. Three pulse trains were analysed and presented in Figure 4.16. The figure compares the oscilloscope traces of Q-switched pulse trains for the proposed EDFL at three different pump powers of 45.8 mW, 89.6 mW, and 133.5 mW. As seen in the figure, the repetition rates of 19.14 kHz, 33.20 kHz and 47.71 kHz are obtained at the mentioned pump power. It is observed that at 45.8 mW, the proposed EDFL begins to lase in Q-switching mode and reaches the maximum repetition rate at 133.5 mW pump power before becoming unstable and disappear beyond this limit. An observation of pulse width indicates that it becomes narrower at higher pump power, while increasing the repetition rate. These characteristics reflect the fundamental operation of a passive Q-switched laser. The narrowest recorded pulse width

was $8.48 \mu\text{s}$ at maximum pump power of 133.5 mW , corresponding to pulse duration of $20.95 \mu\text{s}$ which is consistent with repetition rate.

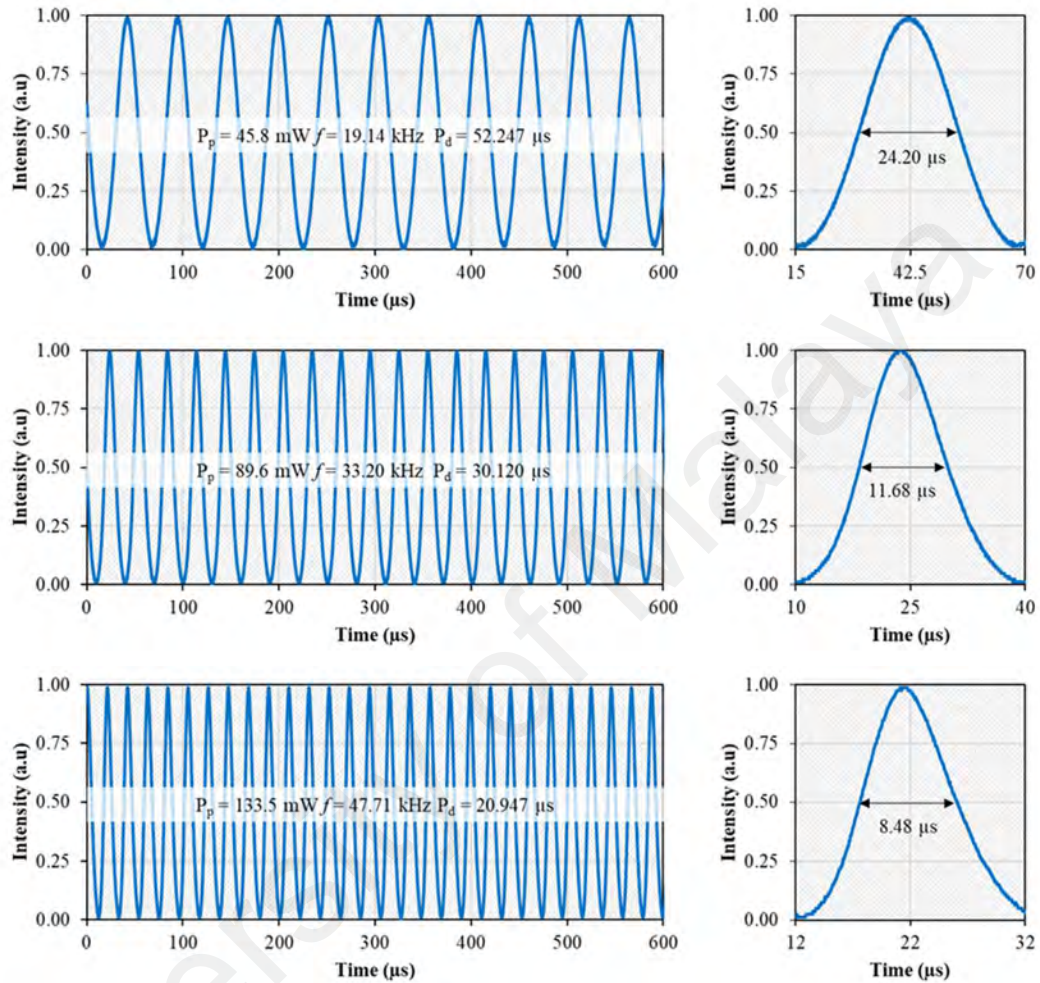


Figure 4.16: Typical pulse train at different pump powers (a) 45.8 mW (b) 89.6 mW , and (c) 133.5 mW

Figure 4.17 compares output spectrum of EDFL with and without the SA at the threshold pump power of 45.8 mW . The Q-switched laser was observed to operate at 1561.51 nm with FWHM and SNR measured are 0.119 nm and 28.48 dB respectively. The cavity only produces a typical CW laser in absence of silver thin-film which originated at 1572.8 nm as shown in Figure 4.17, showing that the ability to generate

pulses is from the silver thin-film. By incorporating silver thin-film into cavity, laser peak was shifted to shorter wavelength to compensate loss introduced by SA. This is attributed that laser peak is shifted to region where more gain is accumulated.

The ability of the silver SA in producing Q-switched pulse was further investigated by presenting the pulse in RF spectrum. Figure 4.18 shows the frequency spectrum at pump power of 133.5 mW, which was acquired within 220 kHz span. As given in figure, repetition rate of the laser peaked at 47.71 kHz without showing any noticeable timing jitter. The SNR of the fundamental frequency was obtained at 59.52 dB, which indicates the stability of the laser. The presence of harmonic frequencies until 12th harmonic further verifies the stability of the laser. As the pump power is increased above the maximum pump power of 133.5 mW, the Q-switched operation diminished completely.

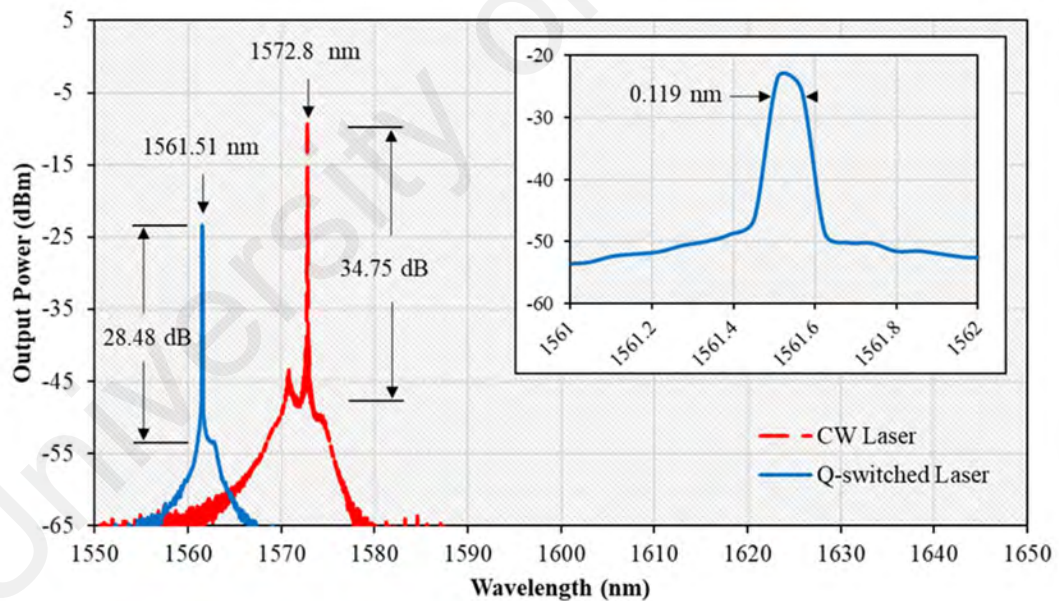


Figure 4.17: Output spectra of the Q-switched EDFL with and without SA device

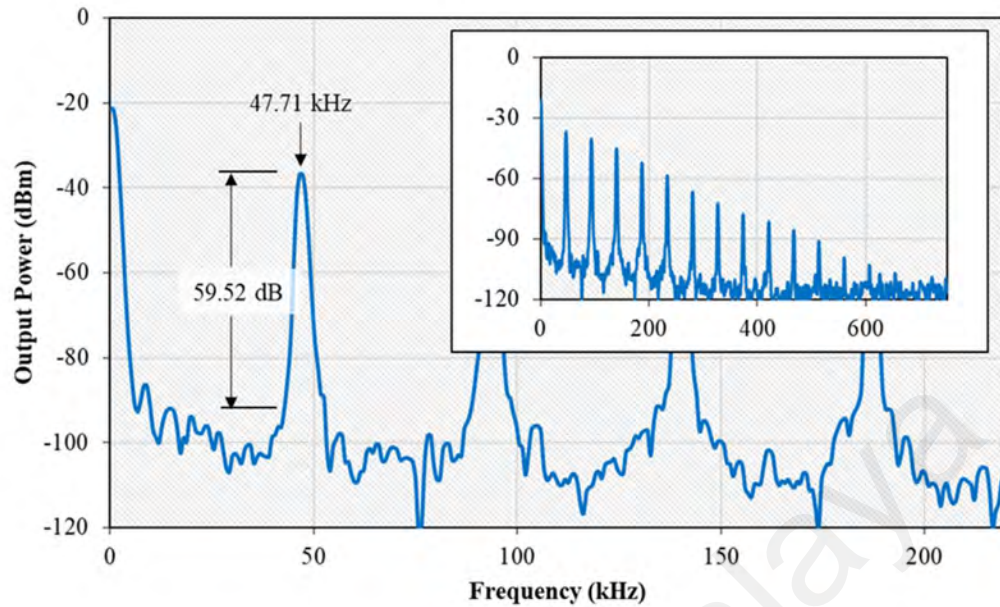


Figure 4.18: RF spectrum of the Q-switched laser

The Q-switching performances such as repetition rate, pulse width, pulse energy, output power, and peak power were investigated for the EDFL as the pump power was varied within 45.8 mW and 133.5 mW. The results were plotted appropriately into a scattering diagram as shown in Figures 4.19 and 4.20. Figure 4.19 highlighted the correlation between repetition rate and the pulse width against pump power. The repetition rate of the Q-switched EDFL is tuneable from 47.85 kHz to 119.28 kHz as the pump power is raised from 45.8 mW to 133.5 mW. In the meantime, the pulse width shows a decreasing trend from 24.20 μ s to 8.48 μ s within this range of pump power. This increased repetition rate and decreased pulse width is a typical phenomenon of Q-switched laser, which pulse characteristic is dependent to pump power. Figure 4.20 shows the relationship of energy and power with respect to pump power. Both energy and power show increasing pattern with inclining pump power. The pulse energy increases from 16.58 nJ to 50.49 nJ while the peak power increases from 6.85 mW to 59.54 mW for the increment of pump power of 45.8 mW to 133.5 mW. Analysis of average output power

showed an efficiency of 5.99%, increasing from 0.79 mW at 45.8 mW pump power to 6.02 mW at 133.5 mW. Compared to 980 nm pumping, the proposed 1480 nm pumping provides a higher pulse energy and output power. This is due to the use of inline pumping mechanism, which is more efficient.

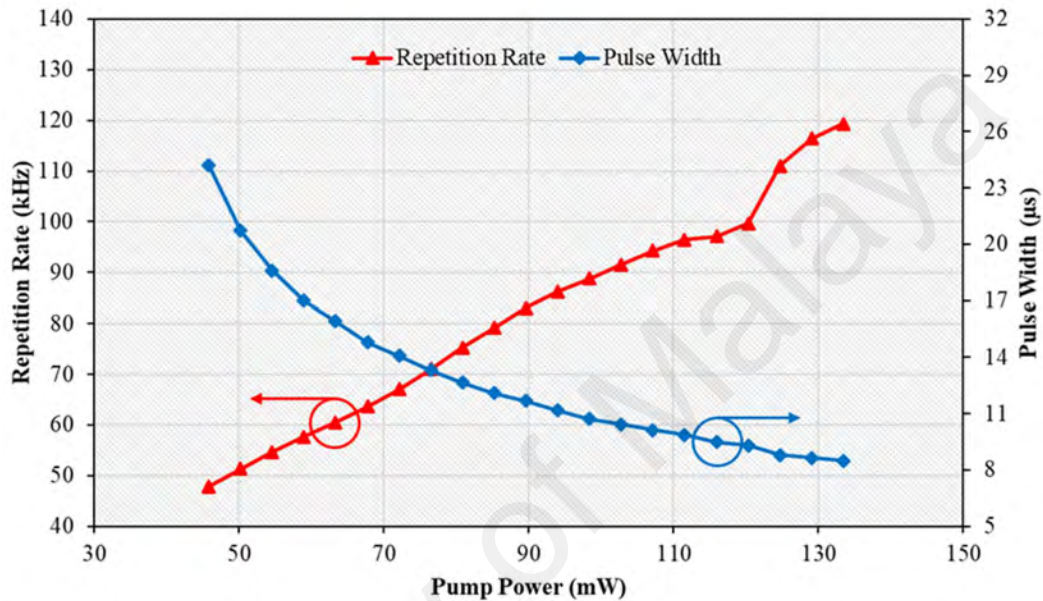


Figure 4.19: Pulse repetition rate and pulse width versus pump power

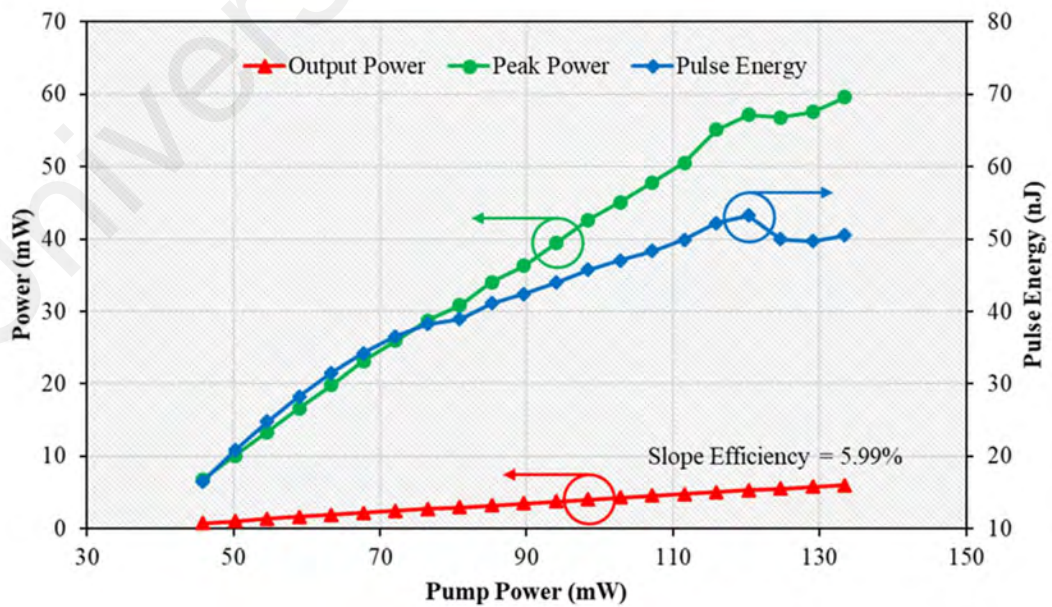


Figure 4.20: Average power, peak power and pulse energy versus pump power

4.6 Summary

Passively Q-switched TDFL and EDFL were successfully demonstrated using silver (Ag) as SA. The silver SA was fabricated using electron beam deposition technique onto a PVA thin-film and possessed a low modulation depth of 2% at 1.55-micron wavelength. The silver SA then was incorporated into TDFL and EDFL cavities for pulse generation. The Q-switched TDFL operating at 1928 nm was achieved at 338 mW pump power and its repetition rate can be tuned up to 28.33 kHz at pump power of 498 mW, without reducing the stability of the Q-switched pulse. The narrowest pulse width of 4.82 μs was recorded, with total energy accumulated at the pulse is 161.7 nJ. On the other hand, Q-switched EDFL operates at 1558 nm and able to produce pulses as the 980 nm pump power reaches the threshold of 21.7 mW. The repetition rates of laser are tuneable from 27.32 kHz to 148.8 kHz. The maximum average output power, the narrowest pulse width and the highest pulse energy produced was 3.8 mW, 3.1 μs and 25.7 nJ, respectively. The pulse energy can be improved to 50.49 nJ by implementing 1480 nm pumping. These results show that silver SA can be a good prospect in generating Q-switched pulse.

CHAPTER 5 : Q-SWITCHED AND MODE-LOCKED FIBRE LASERS USING SILVER DEPOSITED ONTO D-SHAPED FIBRE AS SATURABLE ABSORBER

5.1 Introduction

From the last decades, many studies on passively Q-switched and mode-locked fibre lasers have been carried out due to their advantages in terms of compactness, robustness, and simplicity (Daloz et al., 2019). Together with these advantages, the potential to be implemented into various end-user applications such as optical sensing, laser therapy, and high-speed internet attract more attention to this emerging technology. Up to date, combinations of diverse material and method have been reported, all aim to deliver the best saturable absorber (SA) for pulsed laser application. As discussed in the previous chapters, various SAs have been proposed on Q-switched and mode-locked pulse generation based on different 2D nanomaterials, ranging back from graphene, transition metal dichalcogenides (TMDs), a topological insulator (TIs), to black phosphorus (BP). Lately, MXene and Bismuthene come into the scene of ultrashort pulse application. All these 2D materials utilize the bandgap size of the material to determine the suitable operating wavelength based on their absorption profile.

On the other hand, metal-based have also gained interest in the recent years to take advantage of broad saturable absorption introduced by SPR effect at wide wavelength region, from visible to infrared. By this, the metal-based material able to operate alike 2D SAs with an additional function of operating in wider wavelength region. Adding to that, third-order nonlinearity of metal-based is much larger contrasted to other 2D materials, especially for gold and silver. The nonlinearity was projected to suppress the gain medium from any mode competition, which will improve the performance of both Q-switched and mode-locked lasers. These SPR and nonlinear characteristics play an important role in pulse generation, which influencing the absorption profile of the light propagation through the metal SA.

The usage of metal of gold (Au) and silver (Ag) were demonstrated as passive Q-switcher in Chapters 3 and 4, respectively to operate in various wavelength regions. The performances of the Q-switched lasers were impressive, thanks to their unique optical features. These features include their large third-order nonlinearity, fast response times of a few picoseconds, and broad absorption from localized surface plasmon resonance (SPR). In this chapter, stable Q-switched and mode-locked Erbium-doped fibre lasers (EDFLs) are proposed and demonstrated using pure silver, which were deposited onto a D-shaped silica fibre using an electron beam deposition method as a passive SA. The D-shaped fibre was fabricated using polishing wheel technique and the polishing depth was controlled by observing the insertion loss during the polishing process. Two-steps polishing technique was conducted with rough and fine abrasive paper pasted around a wheel in order to establish a smoother surface of D-shaped fibre for efficient light propagation.

Several works have been reported on the pulses generation in erbium-doped fibre laser (EDFL) cavity using silver as SA. For instance, Guo *et al.* demonstrated a self-started Q-switched laser operating at wavelength of 1564.5 nm. (Guo et al., 2015) The SA were prepared using solvothermal reduction method and the laser has produced Q-switched pulses with repetition rate of 58.5 kHz, pulse width of 2.4 μ s and pulse energy of 132 nJ at the pump power of 139 mW. The modulation depth of 18.5% was recorded, indicates the potentiality to perform as SA. Parallely, Ahmad *et. al* reported a tuneable Q-switched fibre laser using an silver-based SA with a deeper modulation depth of 31.6% (H Ahmad, NE Ruslan, ZA Ali, et al., 2016). The laser has 27.3 nm tuning capabilities. At 1558.4 nm wavelength operation, the laser generates pulses with 6.5 μ s pulse width and 24.4 kHz repetition rate.

In this chapter, a stable Q-switched Erbium-doped fibre laser (EDFL) is proposed and demonstrated using silver, which were deposited onto a D-shaped silica fibre using an electron beam deposition method as a passive SA. Recently, Zapata *et al.* had investigated the effect of different polishing length of D-shaped fibre on the mode-locked pulses generation using graphene material as a SA (Zapata et al., 2016). It was found that, D-shaped fibre with high polarization extinction ratio generates narrower pulse width. However, the relationship between polishing depth and lasing performance remains unclear. Therefore, in this work, a method of polishing D-shaped fibre that gives different polishing depth of D-shaped fibre is proposed and unveils the uniqueness of the polishing depth in producing efficient Q-switched pulses. Four samples of different polishing depth were used that produces pulse energy up to 139.08 nJ with the narrowest pulse recorded at 6.12 μ s, which is comparable to articles cited before. In authors' knowledge, this is the first work demonstrated a Q-switched EDFL utilizing the D-shaped fibre deposited by pure silver as SA. Compared to other materials, the use of silver is advantageous due to its mechanical strength. This may increase the maximum attainable energy and a damage threshold of the SA. Furthermore, it also has a large third-order nonlinearity, and broad absorption from localized surface plasmon resonance (SPR). This allows the SA to work in broader wavelength region

5.2 Fabrication and Characterization of SA Device Based on Silver Deposited onto D-shape Fibre

A side-polished D-shape fibre used in this study was fabricated using the wheel polishing technique setup as shown in Figure 5.1. A small part of a standard single mode optical fibre (Corning SMF-28) with the core and cladding diameter of 9 and 125 μ m, respectively that contain the buffer coating was stripped off in advance. The removal part

of the buffer then was clean using alcohol before placing the fibre on two fibre holders. The two types of abrasive paper which is 800-grid and 1000-grid was placed around the mechanical wheel to polish the fibre surface. The first polish used 800-grid sandpaper and after the certain insertion power losses in dB required, the 1000-grid sandpaper followed to obtain a smooth finish at the polished surface. The length of the polished area was measured to be around 1.5 mm. The side-view and cross-sectional view of the D-shape fibre was observed by a microscope, as shown in figure below. Figure 5.2 (a) shows the microscopic image of the standard SMF-28 fibre with the diameter of the fibre is $125.39\ \mu\text{m}$, while Figure 5.2 (b) shows the microscopic image of the side-polished D-shape fibre with diameter and length after the polishing process are $65.76\ \mu\text{m}$ and $1.49\ \text{mm}$, respectively. Inset image proves the polishing depth dimension of the D-shaped fibre through a cross-section microscopic view. Figure 5.3 shows the cross-section view of the side-polished fibre with the different losses. It is observed that the insertion power loss of the samples with the cross-section diameters of $69.48\ \mu\text{m}$, $66.18\ \mu\text{m}$, $64.43\ \mu\text{m}$ and $61.42\ \mu\text{m}$ are 1.2 dB, 2 dB, 3 dB and 3.5 dB, respectively. The characteristics of these samples are summarized in Table 5.1.

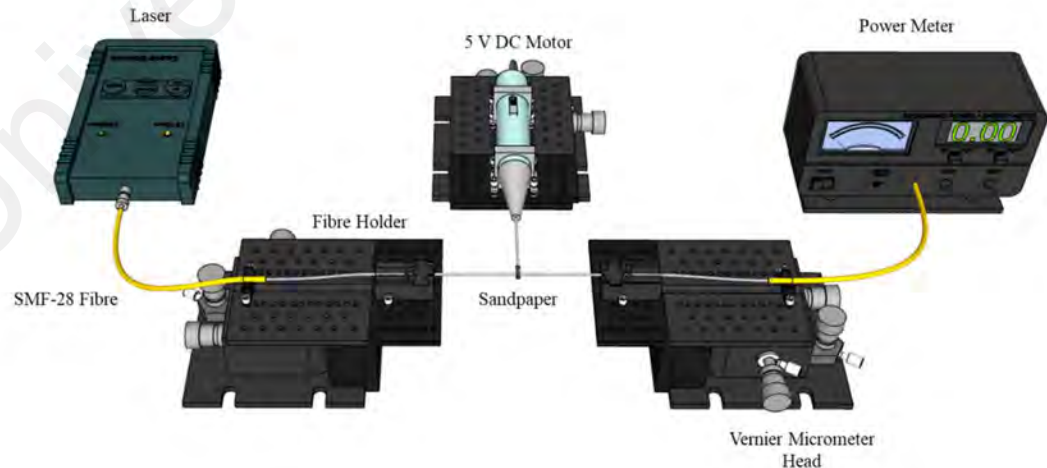


Figure 5.1: D-shaped fibre preparation setup

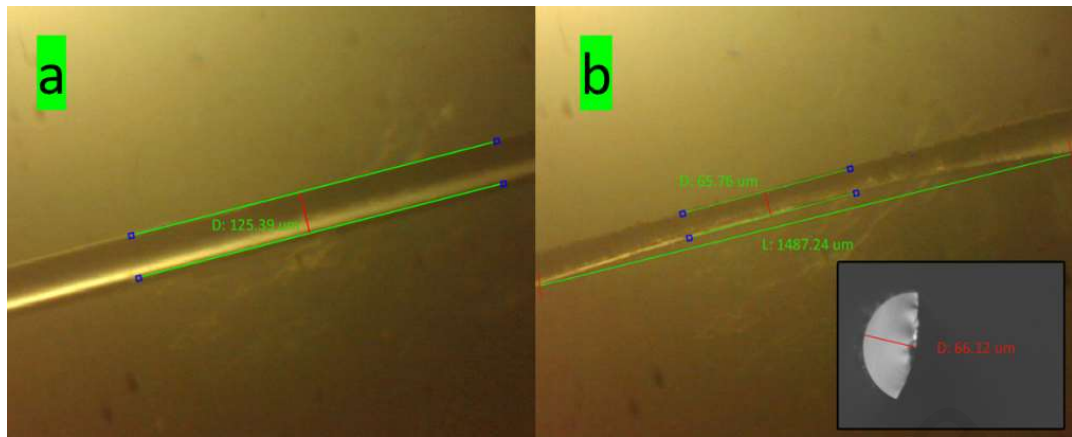


Figure 5.2: Comparison in dimension of a standard SMF to the polished fibre with loss of 2 dB. Inset shows a cross-section view of the fibre

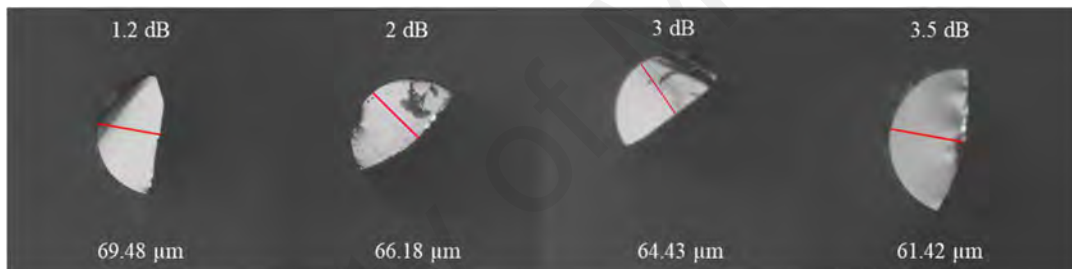


Figure 5.3: Cross-section microscopic view of the fibre at different insertion loss

Table 5.1: The D-shaped fibre characteristics of four samples with different polishing depth

Measured Insertion Loss (dB)	Remaining fibre radius (μm)	Amount of core removed (μm)
1.2	69.48	0.00
2.0	66.18	0.82
3.0	64.43	2.57
3.5	61.42	5.58

After the side-polished fibre was fabricated, the samples then placed on the electron beam machine (Model EB43-T) to apply the silver coating. The silver coating was applied

on the D-shaped using the electron beam deposition method. The thickness is homogeneously achieved by controlling the coating machine at full-vacuum condition of $10^{-5} \sim 10^{-7}$ Torr and current flowed to the tungsten filament inside the chamber, as illustrated in Figure 5.4. The thickness of the coated silver was set at 20 nm by controlling the exposure time through shutter. Meanwhile, Figure 5.5 shows the energy dispersive spectroscopy (EDS) of the silver on the surface of polished area. Figure 5.6 shows a linear absorption spectrum of the silver which indicates the absorption loss of about 4.7 dB at 1550 nm.

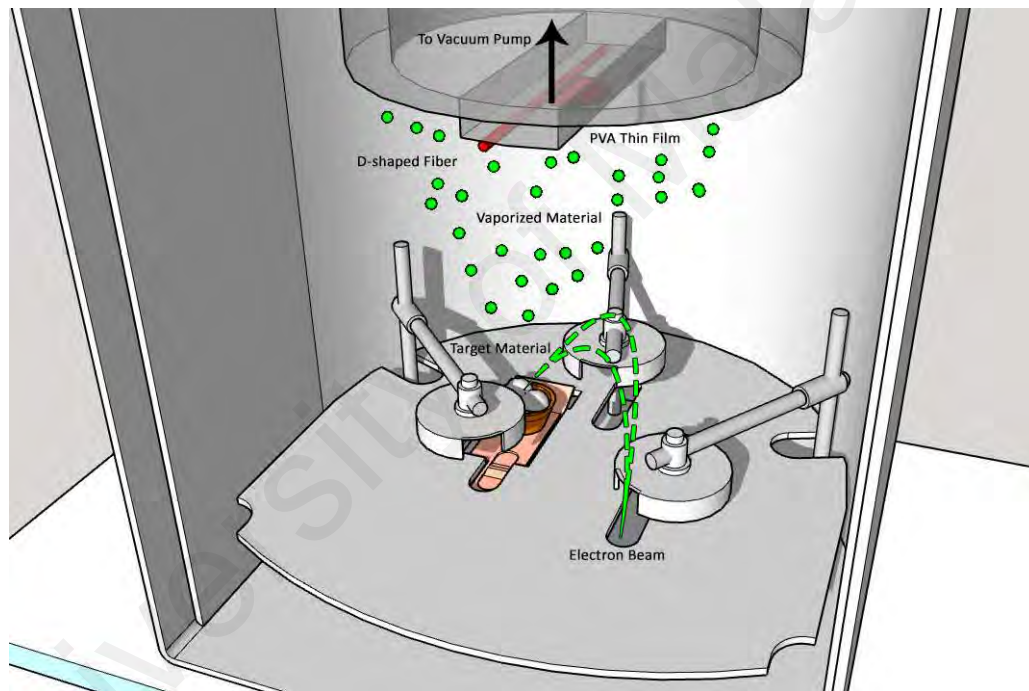


Figure 5.4: Coating process using E-beam evaporation method on substrates, such as D-shaped fibre

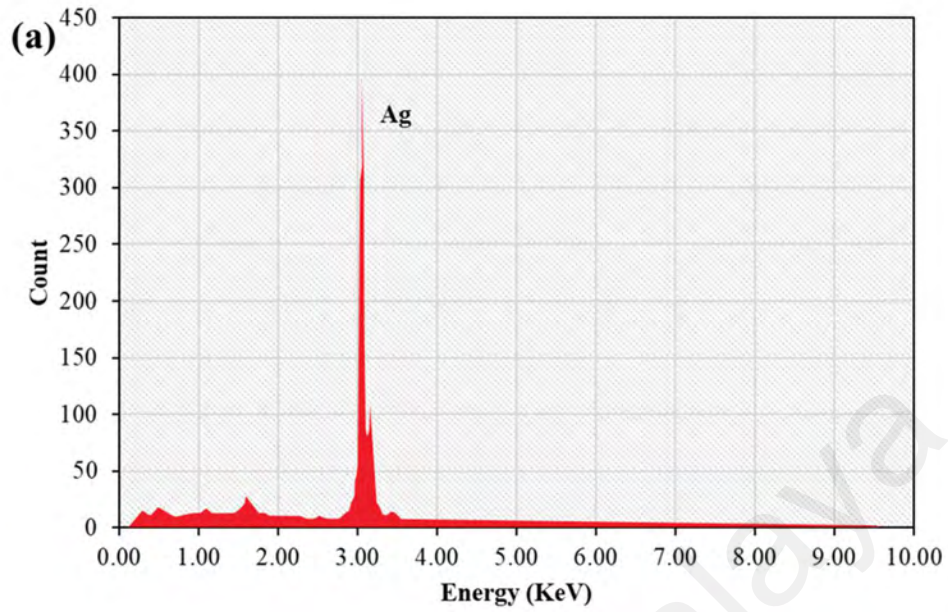


Figure 5.5: Energy dispersive spectroscopy (EDS) analysis on the surface of the D-shaped area

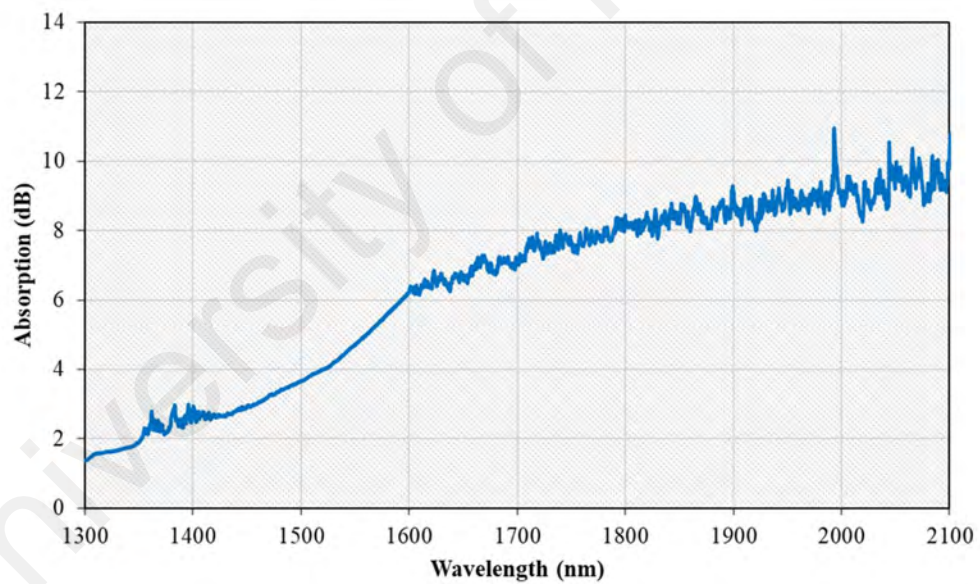


Figure 5.6: Linear absorption of the silver at different wavelength ranging from 1300 to 2100 nm

The non-linear optical absorption of the silver was measured based on the twin-balance detector method. The process starting with a mode-locked source with the wavelength of 1562 nm and pulse repetition rate of 1 MHz. The laser source then connected to the optical

attenuator and 3 dB coupler. The silver nonlinear absorption profile as given in Figure 5.7 shows that it has a saturable absorption of 2%, non-saturable absorption of 98% and saturable intensity of 0.7 MW/cm^2 . For this type of SA, the D-shaped structure introduced large radiation losses while the measured saturable absorption is relatively low because of indirect contact of photon to the silver layer which located on side of the core. However, this amount of the saturable absorption is sufficiently enough to modulate cavity loss and generate Q-switching pulses. The insertion loss of the SA device could be reduced by optimizing the D-shaped fibre fabrication and reducing the thickness of the silver layer.

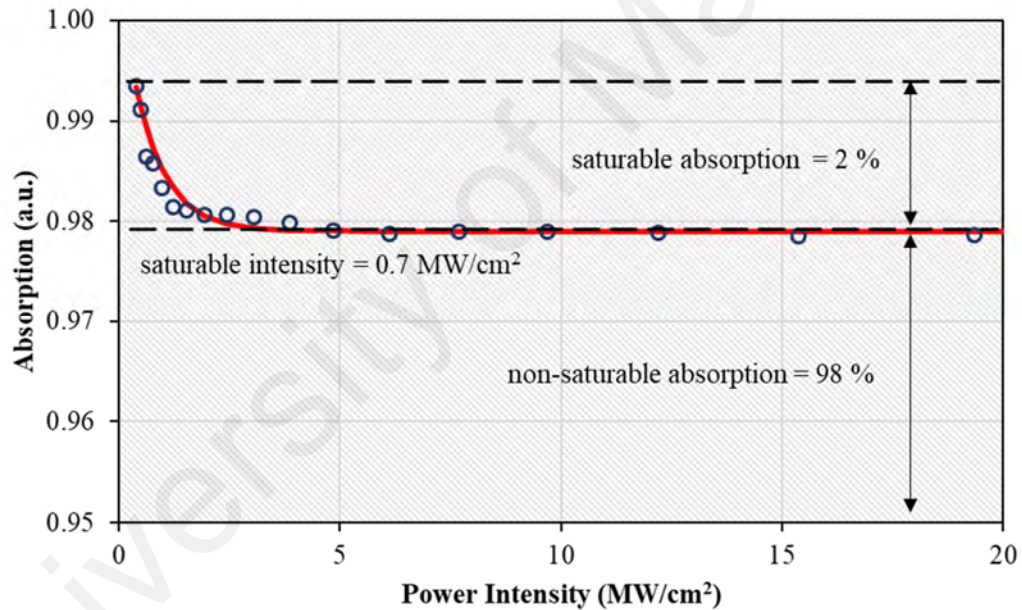


Figure 5.7 : Nonlinear absorption curve of the silver layer showing modulation depth of 2%.

5.3 Q-switched EDFL using Silver Deposited onto D-shaped Fibre as SA

The D-shaped fibre with silver was integrated into an EDFL cavity to realize the Q-switching operation. As shown in Figure 5.8, an active gain medium of 2.4-metre EDF was forward-pumped by a single-mode, 980 nm laser source via a 980/1550 nm

wavelength division multiplexer (WDM). The SA was employed by fusion splicing both end of the D-shaped fibre to the cavity. An optical isolator was used to prevent any possibilities of bidirectional light propagation inside the cavity, while the polarization controller (PC) was used to finely tune the birefringence property inside the cavity. To extract the laser for measurement, an optical coupler was used. The coupler taps 20% of the laser for analysis, while keeping the rest in the cavity for further oscillation. The tapped output was observed using multiple optical instruments, each to analyse a different aspect of the laser. For instance, optical spectrum analyser (OSA: Yokogawa AQ6370B) with a resolution of 0.02 nm was used for spectral analysis, while 350 MHz digital oscilloscope (OSC: GW Instek, GDS-3352) and radio frequency spectrum analyser (RFSA: Anritsu MS2683A) was used for temporal analysis on time and frequency domain. The output was fed into OSC and RFSA through a 1.2 GHz photodetector (PD: Thorlabs DET101CFC), with 60 picoseconds rise/fall time to interpret the pulsed laser. Aside, broadband optical power meter was used to measure the average output power of the lasers.

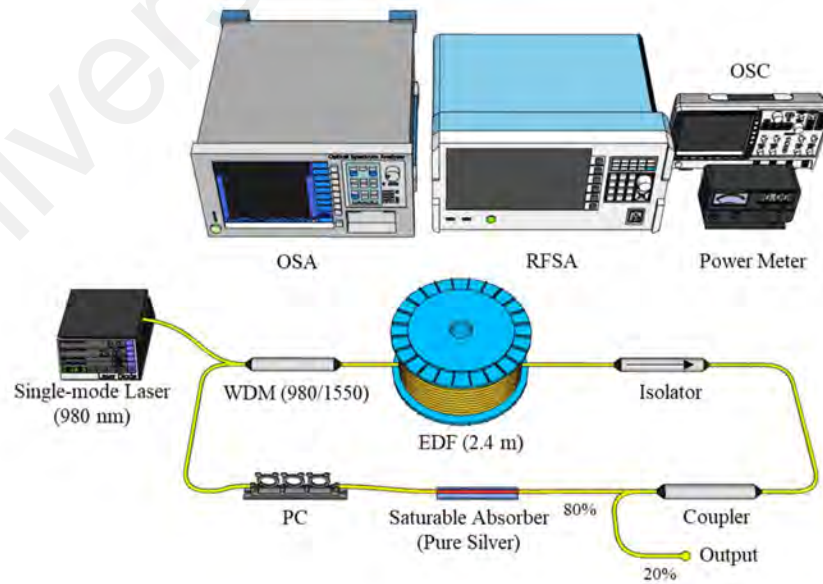


Figure 5.8: Experimental setup for Q-switched EDFL using D-shaped fibre with pure silver as SA

In this experiment, continuous wave (CW) starts to operate at the pump power of 27.5 mW, while self-started Q-switched appears by adjusting the pump power up to 35.2 mW. All four samples able to generate Q-switched at the same pump power of 35.2 mW towards 65.7 mW. This indicates the ability of those samples to generate Q-switched over a large variation of pump power with centre wavelength ranging from 1558 nm to 1560 nm as shown in Figure 5.9. In fact, the transfer method of silver onto D-shaped fibre using electron beam deposition are efficient as all the samples can generate Q-switched at the same pump power. To ensure that the lasing is induced by the silver, the D-shaped fibre is replaced with bare fibre connector and only CW is observed over wide pump power with no pulses generated. These results verified that the Q-switching operation was induced by the silver. We also increased the pump power up to the maximum of 200 mW, but the Q-switching pulses has been diminished. As we reduced back the pump power below 65.7 mW, the Q-switching pulses are recovered, thus the damage threshold was higher than that value (200 mW).

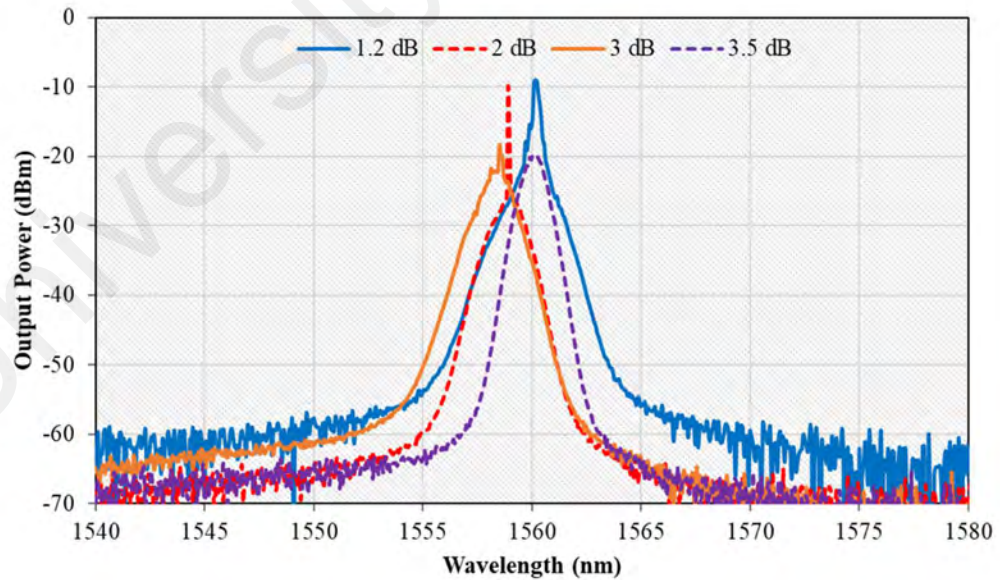


Figure 5.9: Spectral overview of the Q-switched EDFL at the threshold pump power of 35.2 mW

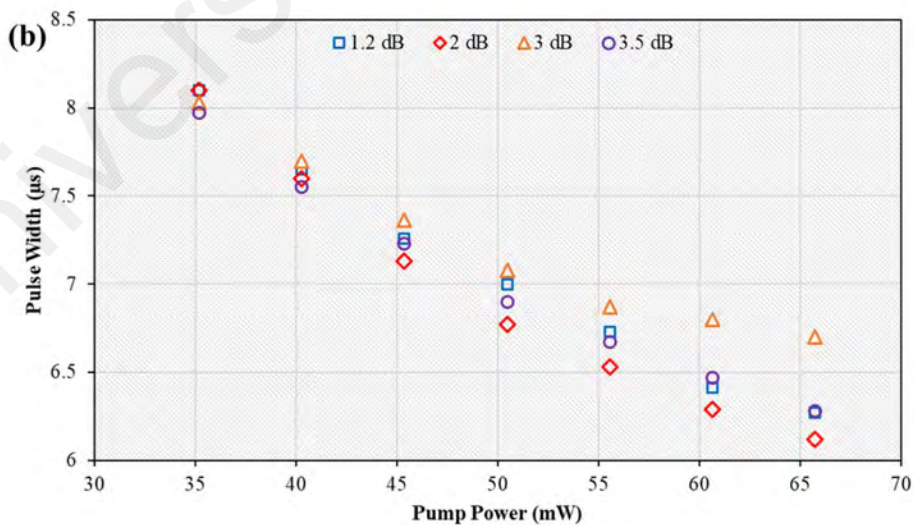
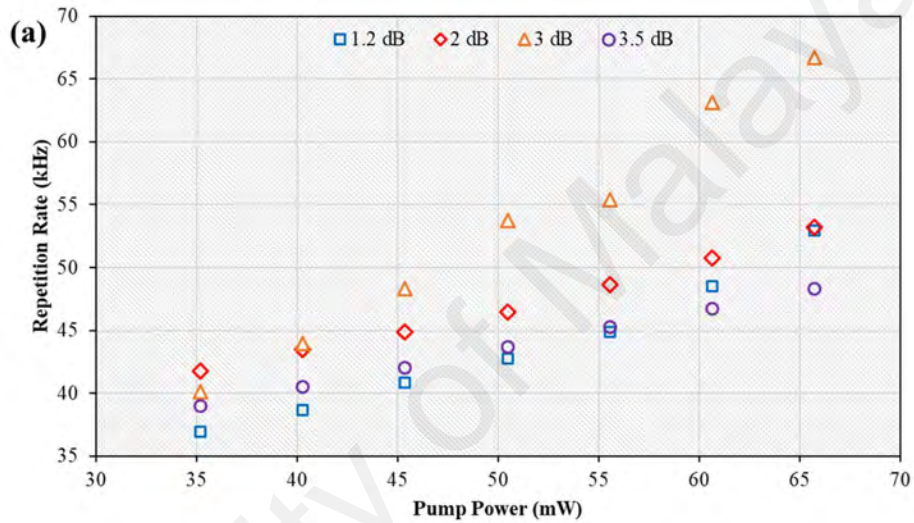
As shown in Table 5.2, different samples produce different 3 dB spectral bandwidth. The sample with 2 dB loss had produced the narrowest bandwidth of 0.13 nm and operates at centre wavelength of 1558.89 nm. Figure 5.10 shows the laser performance at various pump powers for all four fabricated samples. By supplying pump power of 35.2 mW to 65.7 mW, the repetition rate of the pulses increases from 36.9 kHz to 52.92 kHz with pulse width measured shrunken from 8.1 μ s to 6.27 μ s, for 1.2 dB sample. The same pattern appears for other fabricated samples which indicate that stable Q-switched is obtained. An increment of repetition rate together with the decrement of pulse width by varying the pump power indicates the typical Q-switched laser features.

Table 5.2 : Measured lasing performance of four different samples of D-shaped fibre with different insertion loss

Samples	Max. Output Power (dB)	3 dB Spectral Bandw. (nm)	Slope Effic. (%)	SNR (dB)	Min. Pulse Width (μs)	Max. Pulse Energy (nJ)	Max. Peak Power (mW)
1.2 dB	7.36	0.33	12.12	65.29	6.27	139.08	22.18
2 dB	6.67	0.13	11.10	67.82	6.12	125.40	20.49
3 dB	5.86	0.19	9.85	64.32	6.70	87.80	13.10
3.5 dB	6.48	0.92	10.80	65.04	6.28	134.13	21.36

Figure 5.10 (a) shows repetition rate as a function of pump power with 1.2 dB, 2 dB, 3 dB and 3.5 dB samples obtained the maximum repetition rate of 52.92 kHz, 53.19 kHz, 66.73 kHz, and 48.31 kHz, respectively. As captured in Figure 5.10 (b), the shortest pulse width is obtained using 2 dB sample which is 6.12 μ s whereas 1.2 dB sample, 3 dB sample and 3.5 dB sample obtain minimum pulse width of 6.27 μ s, 6.7 μ s and 6.28 μ s, respectively. It is shown in Figure 5.10 (c) that the maximum output power obtained by 1.2 dB, 2 dB, 3 dB and 3.5 dB samples are 7.36 mW, 6.67 mW, 5.86 mW, and 6.48 mW, respectively. By referring to Figure 5.10 (d), the highest pulse energy is consumed by 1.2 dB sample while other samples exhibit maximum pulse energy of 125.4 nJ, 87.8 nJ, and 134.13 nJ for 2 dB, 3 dB and 3.5 dB samples respectively. The high maximum pulse

energy observed, which is above 139 nJ, while maximum output power measured up to 5 mW for all samples ensured efficiency of generated Q-switched using D-shaped fibre with silver as SA. Finally, measured peak power was plotted in Figure 5.10 (e) with maximum peak power obtained are 22.18 mW, 20.49 mW, 13.10 mW and 21.36 mW by 1.2 dB, 2 dB, 3 dB and 3.5 dB samples respectively. Moreover, all silver samples prepared have high slope efficiency which is from 9% to 12%.



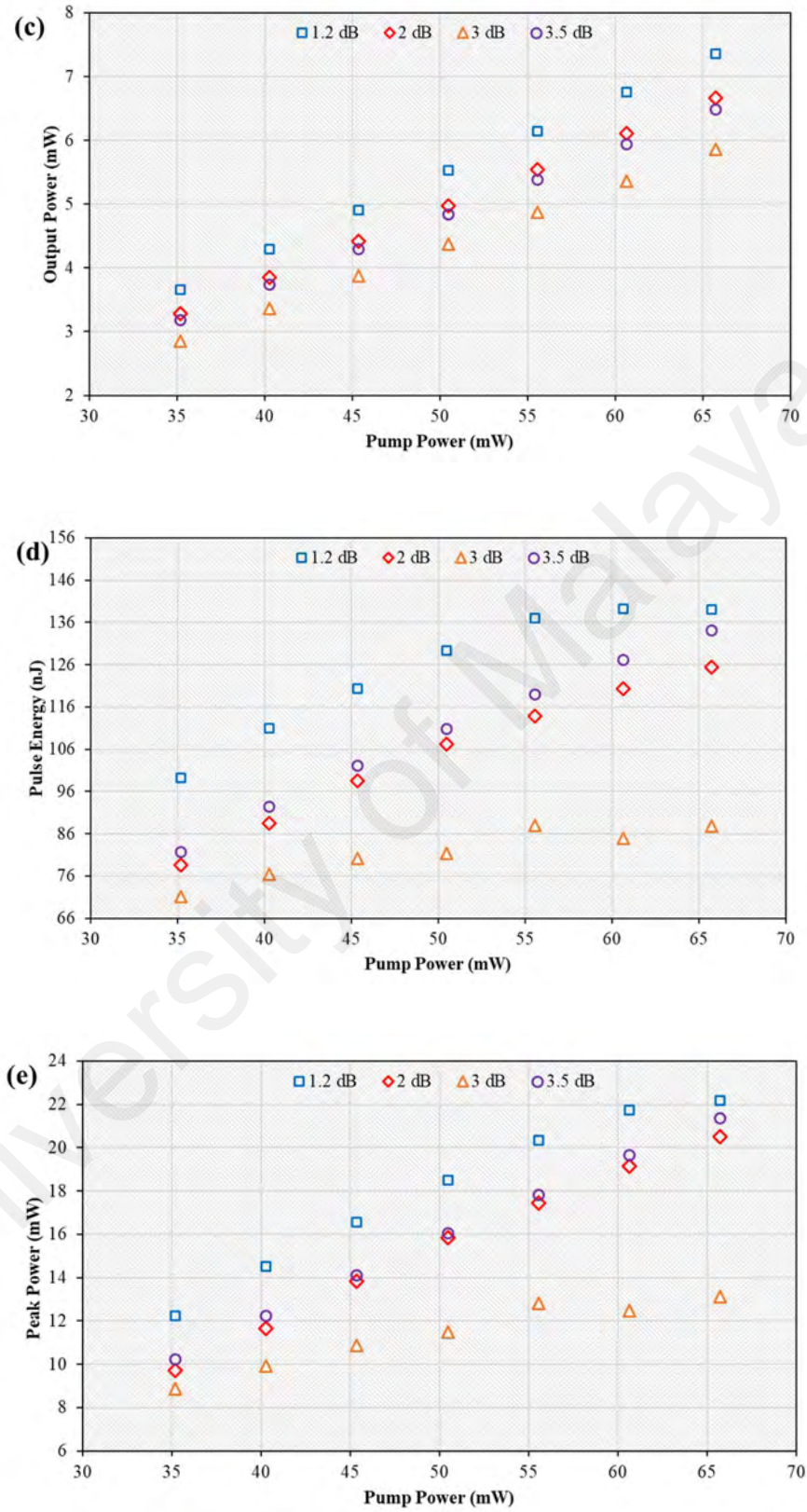


Figure 5.10: The performance of the Q-switched EDFL against pump power; (a) Repetition rate, (b) Pulse width, (c) Output power, (d) Pulse energy and (e) Peak power

Based on Table 5.2, all fabricated samples exhibit almost similar Q-switched parameters but samples of 1.2 dB and 2 dB generates Q-switched with excellent lasing performance with 1.2 dB obtained highest maximum output power, highest slope efficiency, highest maximum pulse energy and highest maximum peak power. Whereas, 2 dB sample exhibit narrowest spectral bandwidth, highest signal-to-noise ratio (SNR) and shortest pulse width. Therefore, an optimum polishing-depth for D-shaped fibre for the generation of Q-switched pulse to use insertion loss of 1.2 dB and 2 dB are proposed, with remaining fibre radius of 69.48 μm and 66.18 μm respectively. By polishing the D-shaped fibre using two steps polishing wheel technique, D-shaped fibre with 0 μm and 0.82 μm core removed are able to be produced while maintaining polishing length at 1.4 mm. Further increasing the polishing length and amount of core removed will suppressed the light-matter interaction inside D-shaped optical fibre thus disrupting signal propagation inside the laser cavity.

Figure 5.11 shows oscilloscope traces for all samples, with an additional figure of single envelope pulse for the corresponding trace. All these figures are taken at pump power of 65.7 mW. Figure 5.11(a) is the trace for 1.2 dB sample with 52.92 kHz repetition rate, corresponding to pulse duration of 18.896 μs . The pulse width was measured at half-maximum of the pulse, in this case is 6.27 μs . For 2 dB sample, repetition rate and pulse width are measured to be 53.10 kHz and 6.12 μs respectively, as shown in Figure 5.11(b). In Figure 5.11(c), 3 dB sample produced pulse at repetition rate of 66.60 kHz, with width measured to be 6.7 μs . The trace for 3.5 dB sample is illustrated in Figure 5.11(d), where the repetition rate and pulse width are measured to be 48.20 kHz and 6.28 μs respectively. Temporal characteristic was later explored in frequency domain, whereas the pulse trace is interpreted into frequency through the RFSA.

Figure 5.12 shows the frequency spectrum of all samples at the pump power of 65.7 mW, which was obtained within the span of 250 kHz. Inset figures show the spectrum at a wider span of 600 kHz. As shown in Figures 5.12 (a), (b), (c) and (d), the fundamental frequency of 1.2 dB, 2 dB, 3 dB and 3.5 dB samples are located at 52.92, 53.10, 66.6 and 48.2 kHz and exhibit a signal to noise ratio (SNR) of 65.29, 67.82, 64.34 and 65.5 dB, respectively. For all samples, SNR obtained is above 64 dB which indicate stability of Q-switched generated by all prepared silver SA. Highest SNR obtained by using 2 dB insertion loss D-shaped fibre which is 67.82 dB. So far, this is the highest SNR obtained in comparison to other work using silver-based SA. It is also worth to notice that the proposed laser operated stably in the laboratory condition for at least 48 hours without any noticeable degradation of performance.

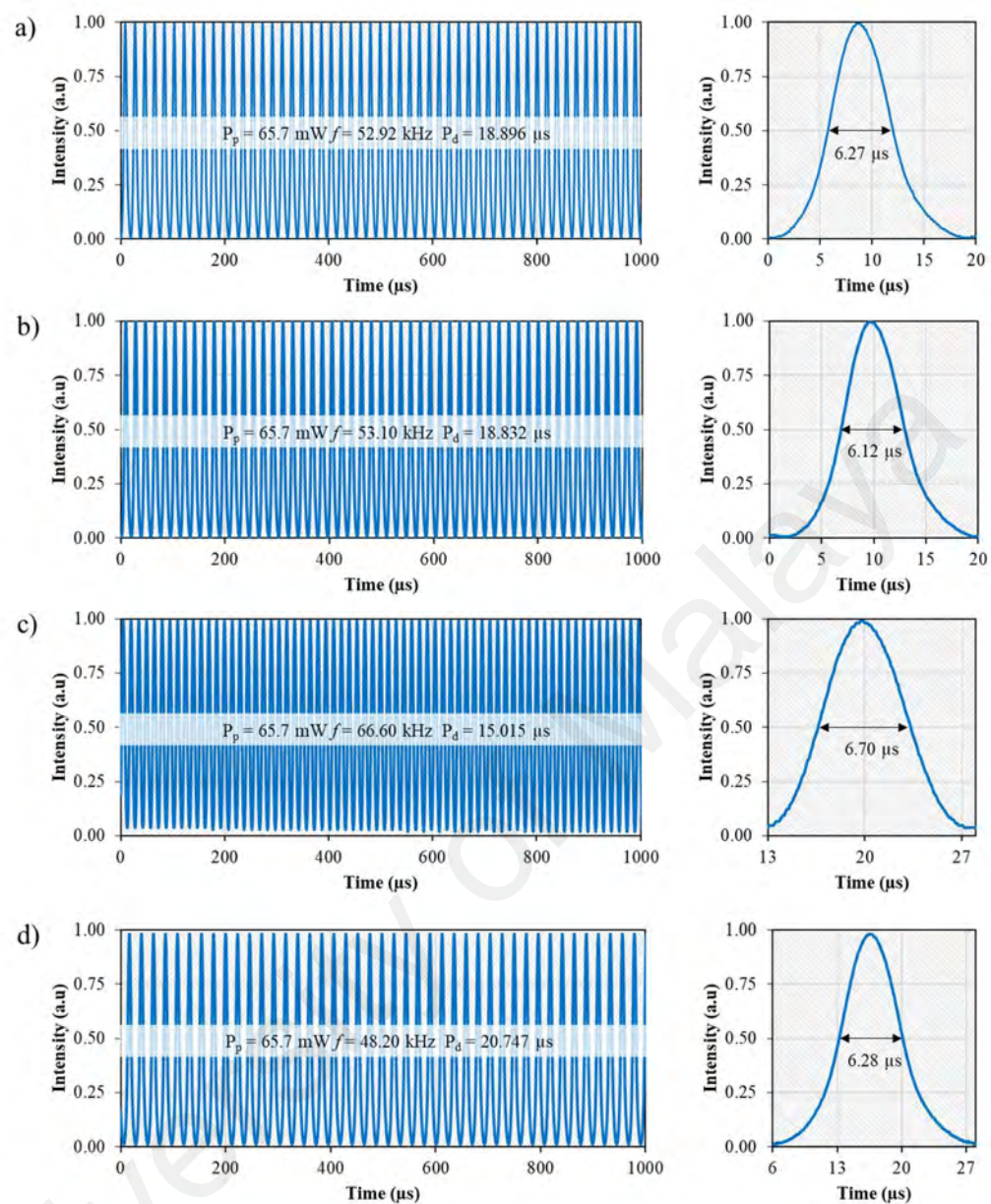
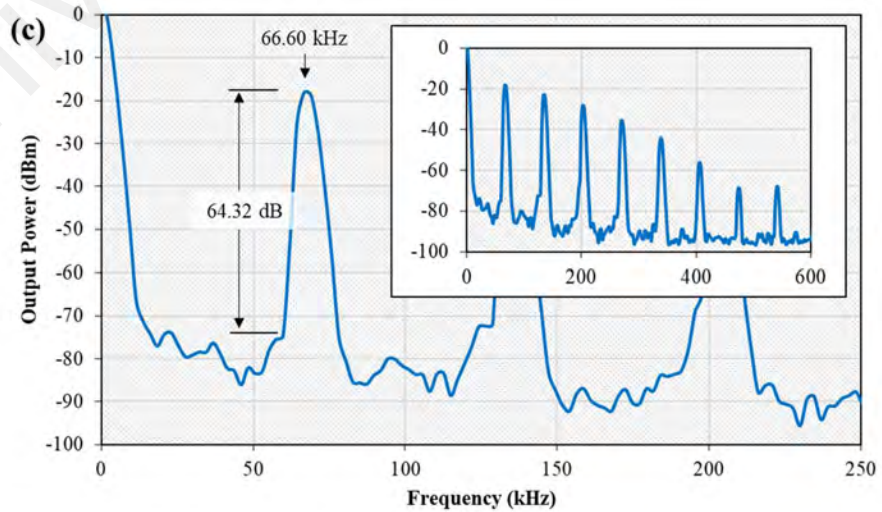
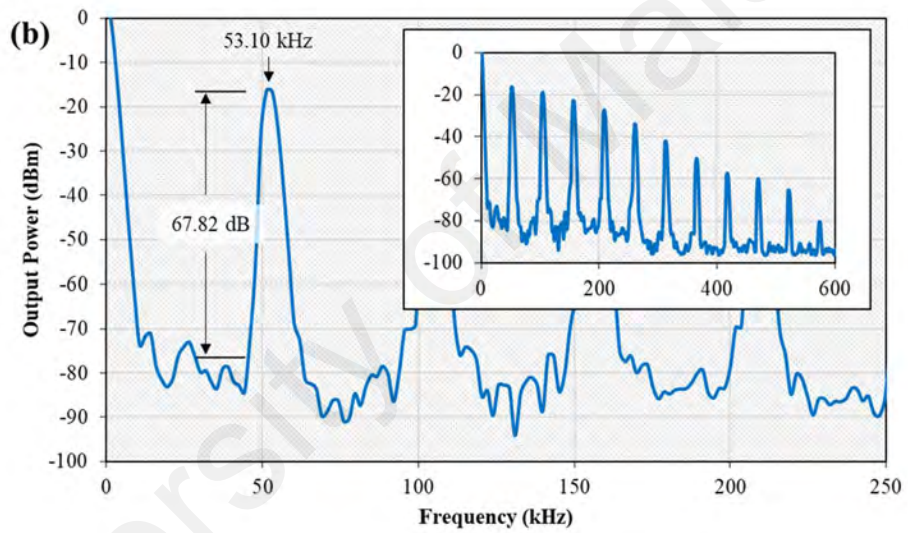
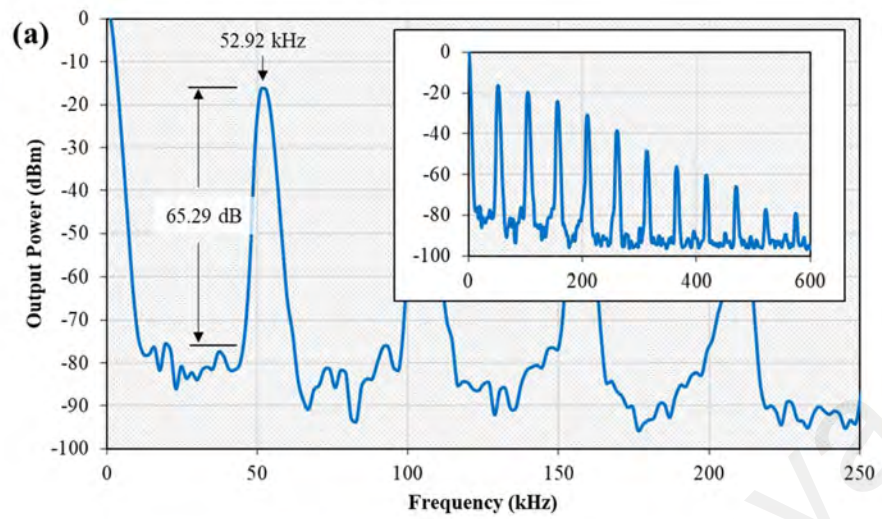


Figure 5.11: Oscilloscope trace for all samples at pump power of 65.7 mW



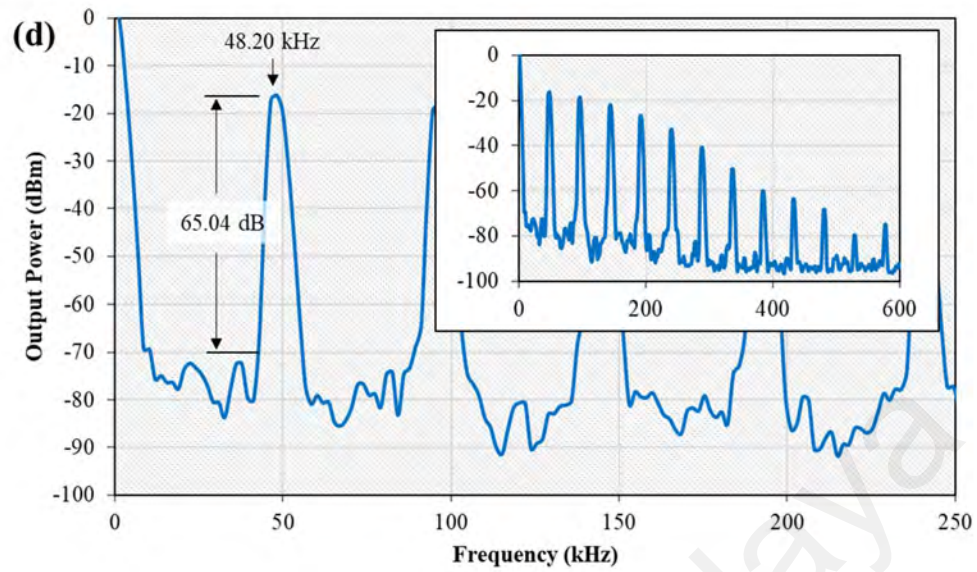


Figure 5.12: RF spectra for various samples at 65.7 mW pump power

By referring to Table 5.3, it is obtained that the performance of the proposed D-shaped fibre with silver-based SA is comparable to another silver-based SA device. For instance, maximum pulse energy obtained is 139.08 nJ which is comparable to previous work. In fact, maximum peak power observed for silver-based SA is 22.18 mW, higher than previous work by Lokman *et al.* which is 20.5 mW, highest maximum peak power recorded for Q-switched using silver as SA (Lokman et al., 2018). Based on the linear absorption range of the silver, the SA is also expected to work in other wavelengths such as 2-micron region.

Table 5.3: Comparison of silver-based saturable absorber lasing performance

Method	Mod. Depth (%)	Init. Pump Power (mW)	Max. Rep. Rate (kHz)	Min. Pulse Width (μs)	Max. Pulse Energy (nJ)	Max. Peak Power (mW)	SNR (dB)
MTMS (Jiang et al., 2018)	31.6	20.0	39.20	3.4	4.2	2.00	46.20
Optical Deposition (Feng et al., 2018)	18.5	19.9	58.50	4.2	132.0	-	-
MTMS (Lu et al., 2018)	31.6	20.0	74.07	3.2	8.2	2.55	35.00
PVA Film (Ma et al., 2015)	19.0	29.4	65.40	6.7	146.7	20.50	67.52
Proposed D-Shaped Fibre	2.0	35.2	66.74	6.1	139.1	22.18	67.82

5.4 Mode-locked EDFL using Silver Deposited onto D-shaped Fibre as SA

In contrast to Q-switching, mode-locking can be achieved by locking the phase of all oscillating modes in a cavity. Compared to the Q-switching, mode-locked pulses operate in a higher repetition rate which directly proportional to cavity length, but lower pulse energy, and shorter pulse duration. The mode-locked lasers are useful for nuclear fusion, non-linear optics and medical applications. They can be obtained by two common techniques; active and passive. An active technique is realized by using an external electrical device such as acousto-optic and mechanical modulator while passive technique is carried out by integrating a SA device into the laser resonator. Compared to active technique, the SA approach is preferable due to its simplicity, compact and cheaper fabrication costs.

In this section, a mode-locked pulse generation is demonstrated in EDFL cavity by using the silver, which were deposited onto D-shaped fibre as SA for the first time. A self-starting mode-locked laser is also obtained with slight modification of the previous

(Q-switched) laser cavity. The mode-locked laser operates at 1563.24 nm with a constant repetition frequency of 1 MHz and the pulse width of 455 ns within a pump power range from 70.8 to 101.3 mW.

In the experiment, a spool of 200-meter SMF was added in the previous cavity of Figure 5.8. The total cavity length is approximately 210 m. Q-switched pulses are no longer appeared in the output even at 68 mW pump power. The laser operates at CW mode at 68 mW pump power. A stable mode-locked laser operation was observed at pump power 70.8 mW after careful tuning of polarization controller. Figure 5.13 compared the output spectrum of the EDFL with CW and mode-locking operation, which was obtained at pump power of 68 mW and 70.8 mW, respectively. The mode-locked laser operates at 1563.24 nm wavelength, a couple nm shorter than that of CW laser. A typical shifting to lower wavelength was observed due to the mode-locked laser, which requires higher pump power to compensate for the cavity loss. The optical signal to noise ratio (OSNR) also increased from 42.93 dB to 47.62 dB as the laser operation is converted from CW to mode-locking. The full-width half-maximum (FWHM) of the mode-locked laser was measured to be 0.198 nm as shown in inset of Figure 5.13. Pump power was later increased while simultaneously observed the presence of mode-locked pulse. It was found that beyond 101.3 mW, mode-locked pulse begins to deteriorate, reaching maximum limit of its operation.

Figure 5.14 shows the temporal analysis of mode-locked laser at 101.3 mW. The analysis contains traces of pulse in continuous train and single envelope. It is worthy to mention that the mode-locked laser produced an identical shape and similar characteristic as the pump power was varied in a range from 70.8 to 101.3 mW. This constant pulse train output is common for mode-locking operation, where pulse generation is depending to cavity length. To prove that it is a genuine mode-locked laser, the cavity was measured

To investigate the stability of the mode-locked pulse, the radio frequency (RF) spectrum was recorded using an RF spectrum analyser. As shown in Figure 5.15, the fundamental frequency was obtained at 1.003 MHz, which aligned with the repetition rate of the pulse in the oscilloscope trace. Multiple peaks of harmonics were observed in the spectrum within 100 MHz span as shown in the inset figure. It is shown that the harmonic peaks become lower at larger frequency. This indicates the pulse width is relatively large and operates in nanosecond regime. The SNR value measured was 77.83 dB, taken from top to pedestal. This value suggests that the output pulse is stable. The result is in line with the small fluctuation of optical spectrum peak power.

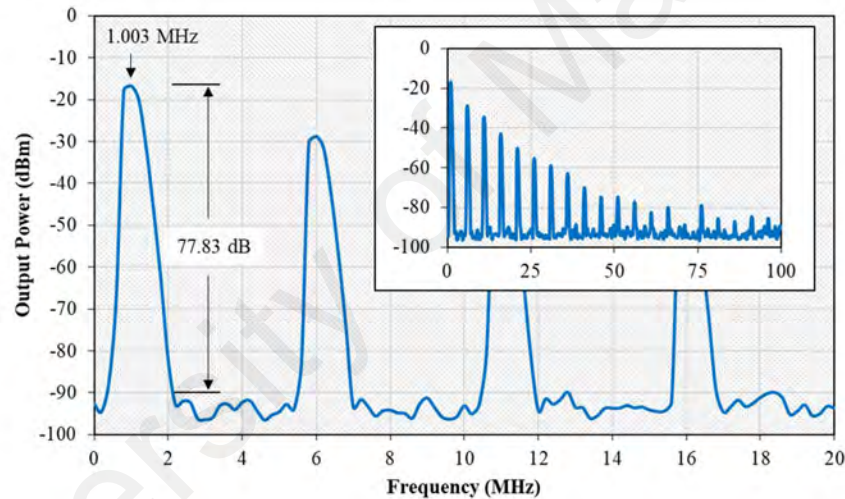


Figure 5.15: Frequency plot of the mode-locked laser at maximum pump power of 101.3 mW

Another important features that worth to underline is the efficiency. A scattering diagram was used to populate related data which consist of output power, peak power and pulse energy. All these data were taken at 7 different pump power in between 70.8 and 101.3 mW, as shown in Figure 5.16. The efficiency of laser at the output was measured using a trendline method, yielding a slope efficiency of 10.8%. The increasing pattern of

output power is almost identical to pulse energy, which represent an amount of power distributed among pulses. Peak power, on the other hand represent a value of FWHM power intensity in a single pulse. Both peak power Comparison of silver-based saturable absorber lasing performance and pulse energy rise linearly with pump power. For instance, the peak power increases from 14.83 to 23.58 mW as the pump power increases from 70.8 to 101.3 mW. The maximum pulse energy of 10.73 nJ was obtained at the maximum pump power of 101.3 mW.

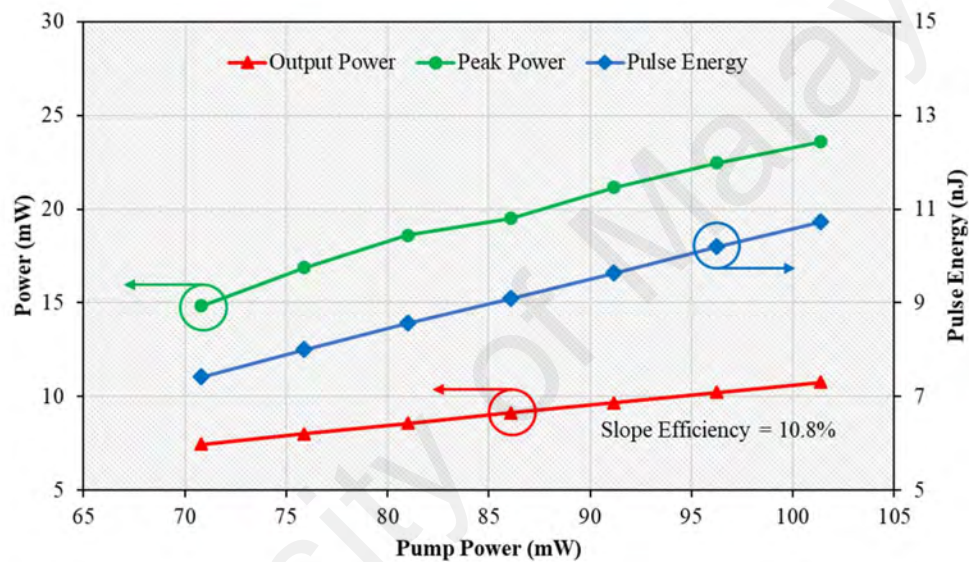


Figure 5.16: Average power, peak power and pulse energy analysis of the mode-locked laser at various pump power

5.5 Summary

Passively Q-switched and mode-locked EDFLs utilizing D-shaped fibre deposited silver using electron beam deposition were successfully proposed and demonstrated. The D-shaped fibre was polished using the polishing wheel technique with two steps polishing to ensure efficient light-matter interaction in D-shaped optical fibre. Variation of polishing depth is proposed resulting in better Q-switched performance using D-shaped fibre deposited silver. Proposed sample with 1.2 dB and 2 dB insertion losses obtained

the amount of core removed less than 1 μm generates Q-switched with shortest pulse width, highest pulse energy, highest output power and highest peak power in comparison to other polished samples. The generated pulses exhibit maximum repetition rate of 66.74 kHz, the minimum pulse width of 6.12 μs , maximum pulse energy of 139.08 nJ, the maximum peak power of 22.18 mW and SNR of 67.82 dB which is comparable to other passively Q-switched EDFL system. By inserting an additional 200-metre long SMF into the laser cavity, nanosecond mode-locked pulse was generated with a repetition rate of 1.0 MHz and a pulse width of 455 ns within the pump power range from 70.8 mW to 101.3 mW. The mode locked EDFL has the maximum output peak power and pulse energy of 23.58 mW and 10.73 nJ, respectively at 101.3 mW pump power. The SNR is around 77.83 dB, which indicates the excellent stability of the pulses. These experiments prove that the pure silver-based SA is suitable to be used as a Q-switcher and mode-locker at 1.55-micron region.

CHAPTER 6: CONCLUSION AND FUTURE WORKS

6.1 Conclusion

This thesis outlays a development and analysis works required to implement pure metal film into a fibre laser cavity as a passive Q-switcher and mode-locker. Vast experimental works was conducted and those successful experimental was reported in various scientific journals. The saturable absorber (SA) was tested into laser cavities at various operating wavelengths. Each of these laser cavities contain one gain media, of either thulium (Tm), erbium (Er), or ytterbium (Yt) to generates laser at 2-, 1.55- and 1-micron region, respectively. The SA material is based on two types of metallic material, noble metal to be exact; gold (Au) and silver (Ag). These two metals are coated using electron beam deposition technique, onto the surface of two host materials: polymer thin-film and silica fibre. The thin-film was prepared using polyvinyl alcohol (PVA), while the silica fibre was side-polished using mechanical polishing process. However, this deposition technique cannot be used to coat with gold onto the silica fibre due to inability to form a stable chemical binding of gold and silica.

In the first chapter, three main objectives were highlighted as a route map for this works. The first objective is related to the preparation and fabrication process of the silver and gold SAs. The gold SA was successfully fabricated using electron beam deposition technique onto a PVA thin-film as described in Chapter 3. Then, the thin-film was integrated into ytterbium-, erbium- and thulium-doped fibre laser cavities to generate Q-switched pulses in 1-, 1.55-, and 2-micron region respectively. The silver SA was also successfully fabricated using the similar approach and incorporated into TDFL and EDFL cavity for Q-switched pulse generation in 2- and 1.55-micron region, respectively, as described in Chapter 4. Another SA was also successfully developed utilizing D-shaped fibre deposited silver to demonstrate Q-switched and mode-locked EDFLs as described in Chapter 5.

The physical and optical properties of the silver and gold SAs were also successfully characterized based on various measurements to achieve the second objective of this work. A method such as energy-dispersive x-ray (EDX) was used to determine the chemical substance of the SA while the field emission scanning electron microscopy (FESEM) was used to observe the metallic distribution throughout the coating surface. A white-light source was used to measure the linear absorption characteristic while balance twin-detector technique was used to reveal the nonlinear absorption behaviour of the SA. The developed gold and silver SA have a modulation depth of around 4 and 2 % as reported in Chapter 3 and 4, respectively. The D-shape fibre coated silver-based SA also has a low modulation depth of 2% as mentioned in Chapter 5.

The final objective requires validation of these SAs to produce self-starting pulse inside various fibre laser cavities. Q-switched and mode-locked fibre lasers were successfully demonstrated at various region using the newly developed SAs. The performance of the SA in each of the cavity of 1-, 1.55- and 2-micron was reported, and the findings were summarized as in Table 6.1. However, the silver thin-film unable to produce pulse at 1-micron region due to high scattering of light interaction towards 16-nm thickness silver thin-film. Lower thickness of 8-nm was also tested to reduce the scattering loss but yet to produce any positive result. Plus, the D-shaped fibre of silver was tested only at 1.5-micron region due to the silver are well performed at that region compared to 2-micron region.

In summary, it can be concluded that these experimental works indicate the capabilities of the proposed metal-based SAs for pulse generation. These materials can be a great alternative to current SA material in producing Q-switching and mode-locking pulse.

Table 6.1: Summary of pulsed fibre laser generated by fabricated SAs

Gold (Au) Thin-film					
Pulse Operation	Wavelength (nm)	Repetition Rate (kHz)	Pulse Width (μs)	Output Power (mW)	Pulse Energy (nJ)
	1064	61.90	4.2	3.14	50.7
Q-switching	1561	88.10	4.3	2.90	32.9
	1949	21.95	2.6	1.97	89.8

Silver (Ag) Thin-film					
Pulse Operation	Wavelength (nm)	Repetition Rate (kHz)	Pulse Width (μs)	Output Power (mW)	Pulse Energy (nJ)
	1558	148.8	3.1	3.82	25.7
Q-switching	1928	49.7	4.4	4.83	159.9

Silver (Ag) D-shaped fibre					
Pulse Operation	Wavelength (nm)	Repetition Rate (kHz)	Pulse Width (μs)	Output Power (mW)	Pulse Energy (nJ)
	1561	52.9	6.2	7.36	139.1
Q-switching	1558	53.1	6.1	6.67	125.4
	1557	66.6	6.7	5.86	87.8
	1560	48.2	6.3	6.48	134.1
Mode-locking	1563	1006	0.5	10.76	10.73

6.2 Future Research Direction

The research finding shows that the proposed SA has a good prospect in generation of pulse in various fibre laser cavities. For the silver thin-film SA, implementation in 1-micron region is important especially in high-power laser application. By using the same electron beam machine, another method of thermal evaporation can be used in the future to deposit the silver onto the thin-film. With this method, the silver palette will be intensely heated until it turns into gaseous state. This may alter the particle size of the silver, hence may change the properties of the SA. The thickness if the coating is also

interesting to explore, whereas it may improve the performance. Optimization can be studied experimentally and theoretically.

For the side-polished fibre SA, another method can be used to adhere gold onto the silica fibre. It is suggested to put a preliminary coating of titanium or chromium layer below the gold layer. These two metals are stable to stick on the silica fibre, allowing gold to stick on top of them. It is important that the preliminary coating is very thin, thus it will not be affecting the operation of gold. These two metals are chosen due to high allowance of light transmission at high photon intensity. Other noble metal-based material is also possible to be implemented as SA such as platinum (Pt) and palladium (Pd). The SA has a great potential to be integrated in various applications such as micromachining, biomedical sensor, free-space optics and remote spectroscopy.

REFERENCES

- Ahmad, H., Reduan, S., Ruslan, N., Lee, C., Zulkifli, M., & Thambiratnam, K. (2018). Tunable Q-switched erbium-doped fiber laser in the C-band region using nanoparticles (TiO₂). *Optics communications*, 435, 283-288.
- Ahmad, H., Ruslan, N., Ali, Z., Reduan, S., Lee, C., Shaharuddin, R., Nayan, N., & Ismail, M. (2016). Ag-nanoparticle as a Q switched device for tunable C-band fiber laser. *Optics communications*, 381, 85-90.
- Ahmad, H., Ruslan, N., Ismail, M., Ali, Z., Reduan, S., Lee, C., & Harun, S. (2016). Silver nanoparticle-film based saturable absorber for passively Q-switched erbium-doped fiber laser (EDFL) in ring cavity configuration. *Laser Physics*, 26(9), 095103.
- Ahmad, H., Samion, M., Muhamad, A., Sharbirin, A., & Ismail, M. F. (2016). Passively Q-switched thulium-doped fiber laser with silver-nanoparticle film as the saturable absorber for operation at 2.0 μm . *Laser Physics Letters*, 13(12), 126201.
- Ahmad, H., Samion, M., & Yusoff, N. (2018). Soliton mode-locked thulium-doped fiber laser with cobalt oxide saturable absorber. *Optical Fiber Technology*, 45, 122-127.
- Al-Hayali, S., & Al-Janabi, A. (2018). Dual-wavelength passively Q-switched ytterbium-doped fiber laser using Fe₃O₄-nanoparticle saturable absorber and intracavity polarization. *Laser Physics*, 28(3), 035103.
- Alani, I., Ahmad, B. A., Ahmed, M., Latiff, A., Al-Masoodi, A., Lokman, M., & Harun, S. (2018). Nanosecond mode-locked erbium doped fiber laser based on zinc oxide thin film saturable absorber. *Indian Journal of Physics*, 1-7.
- Bao, Q., Zhang, H., Wang, Y., Ni, Z., Yan, Y., Shen, Z. X., Loh, K. P., & Tang, D. Y. (2009). Atomic-layer graphene as a saturable absorber for ultrafast pulsed lasers. *Advanced Functional Materials*, 19(19), 3077-3083.
- Bohren, C. F., & Huffman, D. R. (2008). *Absorption and scattering of light by small particles*: John Wiley & Sons.
- Brooks, R. R. (1992). *Noble metals and biological systems: their role in medicine, mineral exploration, and the environment*: CRC Press.
- Chen, Y., Tam, S., Chen, W., & Zheng, H. (1996). Application of the Taguchi method in the optimization of laser micro-engraving of photomasks. *International Journal of Materials*, 11(3-4), 333-344.
- Daloz, N., Robin, T., Cadier, B., Kieleck, C., Eichhorn, M., & Hildenbrand-Dhollande, A. (2019). 55 W actively Q-switched single oscillator Tm³⁺, Ho³⁺-codoped silica polarization maintaining 2.09 μm fiber laser. *Optics express*, 27(6), 8387-8394.

- Dausinger, F., & Lichtner, F. (2004). *Femtosecond technology for technical and medical applications* (Vol. 96): Springer Science & Business Media.
- Du, J., Wang, Q., Jiang, G., Xu, C., Zhao, C., Xiang, Y., Chen, Y., Wen, S., & Zhang, H. (2014). Ytterbium-doped fiber laser passively mode locked by few-layer Molybdenum Disulfide (MoS₂) saturable absorber functioned with evanescent field interaction. *Scientific reports*, 4, 6346.
- Dupriez, P., Piper, A., Malinowski, A., Sahu, J., Ibsen, M., Thomsen, B., Jeong, Y., Hickey, L., Zervas, M., & Nilsson, J. (2006). High average power, high repetition rate, picosecond pulsed fiber master oscillator power amplifier source seeded by a gain-switched laser diode at 1060 nm. *IEEE Photonics Technology Letters*, 18(9), 1013-1015.
- Elim, H. I., Yang, J., Lee, J.-Y., Mi, J., & Ji, W. (2006). Observation of saturable and reverse-saturable absorption at longitudinal surface plasmon resonance in gold nanorods. *Applied physics letters*, 88(8), 083107.
- Fan, D., Mou, C., Bai, X., Wang, S., Chen, N., & Zeng, X. (2014). Passively Q-switched erbium-doped fiber laser using evanescent field interaction with gold-nanosphere based saturable absorber. *Optics express*, 22(15), 18537-18542.
- Feng, X.-Y., Ding, B.-Y., Liang, W.-Y., Zhang, F., Ning, T.-Y., Liu, J., & Zhang, H. (2018). MXene Ti₃C₂T_x absorber for a 1.06 μm passively Q-switched ceramic laser. *Laser Physics Letters*, 15(8), 085805.
- Fernando, R., Semendy, F., & Wijewarnasuriya, P. (2012). *Altering Plasmonic Nanoparticle Size Through Thermal Annealing for Improved Photovoltaic Devices*. Retrieved from ARMY RESEARCH LAB ADELPHI MD SENSORS AND ELECTRON DEVICES DIRECTORATE:
- Fu, S.-G., Ouyang, X.-Y., Li, J.-J., & Liu, X.-J. (2017). Passively Q-switched Yb-doped fiber laser operating at 1.06 μm with two-dimensional silver nanoplate as saturable absorber. *Chinese Physics Letters*, 34(4), 044203.
- Gao, Y., Zhang, X., Li, Y., Liu, H., Wang, Y., Chang, Q., Jiao, W., & Song, Y. (2005). Saturable absorption and reverse saturable absorption in platinum nanoparticles. *Optics communications*, 251(4-6), 429-433.
- Grudin, A. (2013). Fibre laser directions. *Nature Photonics*, 7(11), 846-847.
- Guo, H., Feng, M., Song, F., Li, H., Ren, A., Wei, X., Li, Y., Xu, X., & Tian, J. (2015). Q-Switched Erbium-Doped Fiber Laser Based on Silver Nanoparticles as a Saturable Absorber. *IEEE Photonics Technology Letters*, 28(2), 135-138.
- Haris, H., Anyi, C., Ali, N., Arof, H., Ahmad, F., Nor, R., Zulkepely, N., & Harun, S. (2014). Passively Q-switched erbium-doped fiber laser at L-band region by employing multi-walled carbon nanotubes as saturable absorber. *Optoelectron. Adv. Mater.*, 8, 1025-1028.
- Herda, R., Kivistö, S., & Okhotnikov, O. G. (2008). Dynamic gain induced pulse shortening in Q-switched lasers. *Optics letters*, 33(9), 1011-1013.

- Huang, S.-L., Tsui, T.-Y., Wang, C.-H., & Kao, F.-J. (1999). Timing jitter reduction of a passively Q-switched laser. *Japanese journal of applied physics*, 38(3A), L239.
- Huang, S., Wang, Y., Yan, P., Zhao, J., Li, H., & Lin, R. (2014). Tunable and switchable multi-wavelength dissipative soliton generation in a graphene oxide mode-locked Yb-doped fiber laser. *Optics express*, 22(10), 11417-11426.
- Ichikawa, M., Araki, S., & Sakata, H. (2013). Wavelength control of a Tm-doped fiber laser using nonidentical mechanical long-period fiber gratings. *Laser Physics Letters*, 10(2), 025101.
- Ismail, M., Tan, S., Shahabuddin, N., Harun, S. W., Arof, H., & Ahmad, H. (2012). Performance comparison of mode-locked erbium-doped fiber laser with nonlinear polarization rotation and saturable absorber approaches. *Chinese Physics Letters*, 29(5), 054216.
- Jackson, S. D. (2007). Passively Q-switched Tm³⁺-doped silica fiber lasers. *Applied optics*, 46(16), 3311-3317.
- Jannifar, A., Baharom, M., Zulkipli, N., Bakri, J., & Harun, S. (2018). Q-switched Ytterbium-doped Fiber Laser with Nickel Oxide Nanoparticles Saturable Absorber. *Nonlinear Optics, Quantum Optics: Concepts in Modern Optics*, 49.
- Jiang, X., Liu, S., Liang, W., Luo, S., He, Z., Ge, Y., Wang, H., Cao, R., Zhang, F., & Wen, Q. (2018). Broadband Nonlinear Photonics in Few-Layer MXene Ti₃C₂T_x (T=F, O, or OH)(Laser Photonics Rev. 12 (2)/2018). *Laser & Photonics Reviews*, 12(2), 1870013.
- Keller, U. (2003). Recent developments in compact ultrafast lasers. *Nature*, 424(6950), 831.
- Koo, J., Jeong, K., Yu, B.-A., & Shin, W. (2019). Evanescent field interaction with Fe₃O₄ nano-particle for passively Q-switched thulium-doped fiber laser at 1.94 μ m. *Optics & Laser Technology*, 119, 105579.
- Koo, J., Lee, J., Kim, J., & Lee, J. H. (2018). A Q-switched, 1.89 μ m fiber laser using an Fe₃O₄-based saturable absorber. *Journal of Luminescence*, 195, 181-186.
- Langmuir, I. (1928). Oscillations in ionized gases. *Proceedings of the National Academy of Sciences of the United States of America*, 14(8), 627.
- Lecourt, J.-B., Martel, G., Guézo, M., Labbé, C., & Loualiche, S. (2006). Erbium-doped fiber laser passively Q-switched by an InGaAs/InP multiple quantum well saturable absorber. *Optics communications*, 263(1), 71-83.
- Lei, H., & Lijun, L. (1999). A study of laser cutting engineering ceramics. *Optics & Laser Technology*, 31(8), 531-538.
- Leone, C., Lopresto, V., & De Iorio, I. (2009). Wood engraving by Q-switched diode-pumped frequency-doubled Nd: YAG green laser. *Optics & Lasers in Engineering*, 47(1), 161-168.

- Li, S., Kang, Z., Li, N., Jia, H., Liu, M., Liu, J., Zhou, N., Qin, W., & Qin, G. (2019). Gold nanowires with surface plasmon resonance as saturable absorbers for passively Q-switched fiber lasers at 2 μm . *Optical Materials Express*, 9(5), 2406-2414.
- Liao, H., Xiao, R., Fu, J., Yu, P., Wong, G., & Sheng, P. (1997). Large third-order optical nonlinearity in Au: SiO₂ composite films near the percolation threshold. *Applied physics letters*, 70(1), 1-3.
- Lokman, M., Yusoff, S., Ahmad, F., Zakaria, R., Yahaya, H., Shafie, S., Rosnan, R., & Harun, S. (2018). Deposition of silver nanoparticles on polyvinyl alcohol film using electron beam evaporation and its application as a passive saturable absorber. *Results in Physics*, 11, 232-236.
- Lu, L., Liang, Z., Wu, L., Chen, Y., Song, Y., Dhanabalan, S. C., Ponraj, J. S., Dong, B., Xiang, Y., & Xing, F. (2018). Few-layer Bismuthene: Sonochemical Exfoliation, Nonlinear Optics and Applications for Ultrafast Photonics with Enhanced Stability (Laser Photonics Rev. 12 (1)/2018). *Laser & Photonics Reviews*, 12(1), 1870012.
- Ma, J., Lu, S., Guo, Z., Xu, X., Zhang, H., Tang, D., & Fan, D. (2015). Few-layer black phosphorus based saturable absorber mirror for pulsed solid-state lasers. *Optics express*, 23(17), 22643-22648.
- Maier, S. A. (2007). *Plasmonics: fundamentals and applications*: Springer Science & Business Media.
- Maiman, T. H. (1960). Stimulated optical radiation in ruby.
- Mao, D., Cui, X., He, Z., Lu, H., Zhang, W., Wang, L., Zhuang, Q., Hua, S., Mei, T., & Zhao, J. (2018). Broadband polarization-insensitive saturable absorption of Fe₂O₃ nanoparticles. *Nanoscale*, 10(45), 21219-21224.
- Muhammad, A., Yasin, M., Ahmad, M., Zakaria, R., Rahim, H., Jusoh, Z., Arof, H., & Harun, S. (2018). ALL-FIBER YTTERBIUM DOPED Q-SWITCHED FIBER LASER BASED ON COPPER NANOPARTICLES SATURABLE ABSORBER. *Digest Journal of Nanomaterials & Biostructures*, 13(1), 279-284.
- Murray, W. A., & Barnes, W. L. (2007). Plasmonic materials. *Advanced materials*, 19(22), 3771-3782.
- Nagayama, K., Kakui, M., Matsui, M., Saitoh, T., & Chigusa, Y. (2002). Ultra-low-loss (0.1484 dB/km) pure silica core fibre and extension of transmission distance. *Electronics Letters*, 38(20), 1.
- Nishizawa, N. (2014). Ultrashort pulse fiber lasers and their applications. *Japanese journal of applied physics*, 53(9), 090101.
- Novaro, O. (2005). Activity of closed d-shells in noble metal atoms. *Foundations of Chemistry*, 7(3), 241-268.

- Paschotta, R. (2008). *Encyclopedia of laser physics and technology* (Vol. 1): Wiley Online Library.
- Perry, M., Stuart, B., Banks, P., Feit, M., Yanovsky, V., & Rubenchik, A. (1999). Ultrashort-pulse laser machining of dielectric materials. *Applied Physics*, 85(9), 6803-6810.
- Prieto-Cortés, P., Álvarez-Tamayo, R., García-Méndez, M., Durán-Sánchez, M., Barcelata-Pinzón, A., & Ibarra-Escamilla, B. (2019). Magnetron sputtered Al-doped ZnO thin film as saturable absorber for passively Q-switched Er/Yb double clad fiber laser. *Laser Physics Letters*, 16(4), 045101.
- Qu, S., Zhang, Y., Li, H., Qiu, J., & Zhu, C. (2006). Nanosecond nonlinear absorption in Au and Ag nanoparticles precipitated glasses induced by a femtosecond laser. *Optical Materials*, 28(3), 259-265.
- Reardon, A. C. (2011). *Metallurgy for the Non-metallurgist*: ASM International.
- Rosdin, R., Ahmad, M., Jusoh, Z., Arof, H., & Harun, S. (2018). All-fiber Q-switched fiber laser based on silver nanoparticles saturable absorber. *Digest Journal of Nanomaterials and Biostructures*, 13, 1159-1164.
- Rundquist, A., Durfee, C. G., Chang, Z., Herne, C., Backus, S., Murnane, M. M., & Kapteyn, H. C. (1998). Phase-matched generation of coherent soft X-rays. *Science*, 280(5368), 1412-1415.
- Rusdi, M. F. M., Rosol, A. H. A., Rahman, M. F. A., Mahyuddin, M. B. H., Latiff, A. A., Ahmad, H., Harun, S. W., & Yasin, M. (2019). Q-switched and mode-locked thulium doped fiber lasers with nickel oxide film saturable absorber. *Optics communications*, 447, 6-12.
- Sakata, H., Araki, S., Toyama, R., & Tomiki, M. (2012). All-fiber Q-switched operation of thulium-doped silica fiber laser by piezoelectric microbending. *Applied optics*, 51(8), 1067-1070.
- Salam, S., Al-Masoodi, A., Al-Hiti, A. S., Al-Masoodi, A. H., Wang, P., Wong, W. R., & Harun, S. W. (2019). FIRpic thin film as saturable absorber for passively Q-switched and mode-locked erbium-doped fiber laser. *Optical Fiber Technology*, 50, 256-262.
- Siddiq, N., Chong, W., Yap, Y., Pramono, Y., & Ahmad, H. (2018). Tin (IV) oxide nanoparticles as a saturable absorber for a Q-switched erbium-doped fiber laser. *Laser Physics*, 28(12), 125104.
- Siddiq, N. A., Chong, W. Y., Pramono, Y. H., Muntini, M. S., & Ahmad, H. (2019). C-band tunable performance of passively Q-switched erbium-doped fiber laser using Tin (IV) oxide as a saturable absorber. *Optics communications*, 442, 1-7.
- Spühler, G., Paschotta, R., Fluck, R., Braun, B., Moser, M., Zhang, G., Gini, E., & Keller, U. (1999). Experimentally confirmed design guidelines for passively Q-switched microchip lasers using semiconductor saturable absorbers. *JOSA B*, 16(3), 376-388.

- Theodosiou, A., Aubrecht, J., Peterka, P., & Kalli, K. (2019). *Femtosecond laser plane-by-plane Bragg gratings for monolithic Thulium-doped fibre laser operating at 1970 nm*. Paper presented at the Micro-structured and Specialty Optical Fibres VI.
- Wu, D., Peng, J., Cai, Z., Weng, J., Luo, Z., Chen, N., & Xu, H. (2015). Gold nanoparticles as a saturable absorber for visible 635 nm Q-switched pulse generation. *Optics express*, 23(18), 24071-24076.
- Wu, Y., Zhang, C., Liu, J., Zhang, H., Yang, J., & Liu, J. (2017). Silver nanorods absorbers for Q-switched Nd: YAG ceramic laser. *Optics & Laser Technology*, 97, 268-271.
- Yao, T., Ji, J., & Nilsson, J. (2014). Ultra-low quantum-defect heating in ytterbium-doped aluminosilicate fibers. *Lightwave Technology*, 32(3), 429-434.
- Yu, Y., Bao, Y., Lin, L., Xu, H., Liu, R., & Zhou, Z. (2019). Large third-order optical nonlinearity and ultrafast optical response in thin Au nanodisks. *Optical Materials Express*, 9(7), 3021-3034.
- Zapata, J., Steinberg, D., Saito, L. A., De Oliveira, R., Cárdenas, A., & De Souza, E. T. (2016). Efficient graphene saturable absorbers on D-shaped optical fiber for ultrashort pulse generation. *Scientific reports*, 6(1), 1-8.
- Zayhowski, J. J., & Dill, C. (1994). Diode-pumped passively Q-switched picosecond microchip lasers. *Optics letters*, 19(18), 1427-1429.
- Zhang, H., Lu, S., Zheng, J., Du, J., Wen, S., Tang, D., & Loh, K. (2014). Molybdenum disulfide (MoS₂) as a broadband saturable absorber for ultra-fast photonics. *Optics express*, 22(6), 7249-7260.
- Zhang, X., Liu, X., Xu, X., Zhao, S., Li, T., Guo, L., & Yang, K. (2018). Self-assembled gold nanoparticles as saturable absorber for low-threshold all-solid-state pulsed 2 μm laser. *Optical Materials*, 83, 82-86.

LIST OF PUBLICATIONS AND PAPERS PRESENTED

ISI Journal Paper

1. **Ahmad, M. T.**, Muhammad, A. R., Zakaria, R., Rahim, H. R. A., Hamdan, K. S., Yusof, H. H. M., Arof, H & Harun, S. W. (2017). Gold nanoparticle based saturable absorber for Q-switching in 1.5 μm laser application. *Laser Physics*, 27(11), 115101.
2. **Ahmad, M. T.**, Muhammad, A. R., Haris, H., Rahim, H. R. A., Zakaria, R., Ahmad, H., & Harun, S. W. (2019). Q-switched Ytterbium doped fibre laser using gold nanoparticles saturable absorber fabricated by electron beam deposition. *Optik*, 182, 241-248.
3. **Ahmad, M. T.**, Rusdi, M. F. M., Jafry, A. A. A., Latiff, A. A., Zakaria, R., Zainuddin, N. A. M., Arof, H., Ahmad, H. & Harun, S. W. (2019). Q-switched erbium-doped fiber laser using silver nanoparticles deposited onto side-polished D-shaped fiber by electron beam deposition method. *Optical Fiber Technology*, 53, 101997.
4. **Ahmad, M. T.**, Muhammad, A. R., Zakaria, R., Ahmad, H., & Harun, S. W. (2020). Electron Beam Deposited Silver (Ag) Saturable Absorber as Passive Q-switcher in 1.5-and 2-micron Fiber Lasers. *Optik*, 164455.